Subversion of Host Genome Integrity by Human Herpesvirus 6

and *Chlamydia trachomatis*

Störung der Integrität des Wirts Genoms durch das Human Herpesvirus 6

und *Chlamydia trachomatis*

Doctoral thesis for a doctoral degree

at the Graduate School of Life Sciences,

Julius-Maximilians-Universität Würzburg,

submitted by

NITISH GULVE

from

Bhusawal (Maharashtra), INDIA

Würzburg **2018**

Members of the PhD Thesis Committee:

Chairperson: Prof. Dr. Alexander Buchberger

Primary Supervisor: Prof. Dr. Thomas Rudel

Supervisor (Second): Prof. Dr. Jörg Wischhusen

Supervisor (Third): Dr. Bhupesh Prusty

Date of Public Defence:

Date of Receipt of Certificates:

Affidavit

I hereby confirm that my thesis entitled **'Subversion of Host Genome Integrity by Human Herpesvirus 6 and** *Chlamydia trachomatis'* is the result of my own work. I did not receive any help or support from commercial consultants. All sources and / or materials applied are listed and specified in the thesis.

Furthermore, I confirm that this thesis has not yet been submitted as part of another examination process neither in identical nor in similar form.

Würzburg,

Eidesstattliche Erklärung

Hiermit erkläre ich an Eides statt, die Dissertation **'Störung der Integrität des Wirts Genoms durch das Human Herpesvirus 6 und** *Chlamydia trachomatis'* eigenständig, d.h. insbesondere selbständig und ohne Hilfe eines kommerziellen Promotionsberaters, angefertigt und keine anderen als die von mir angegebenen Quellen und Hilfsmittel verwendet zu haben.

Ich erkläre außerdem, dass die Dissertation weder in gleicher noch in ähnlicher Form bereits in einem anderen Prüfungsverfahren vorgelegen hat.

Würzburg,

Dedicated to My Parents,

Mr. Prithviraj Gulve and Mrs. Hemlata Gulve

ACKNOWLEDGEMENTS

<div align="right">**NITISH GULVE**</div>

TABLE OF CONTENTS

LIST OF FIGURES AND TABLES

FIGURES

TABLES

ABBREVIATIONS

%	Percentage
°C	Degree Celsius
μl	microliter
μM	micromolar
ADP	Adenosine diphosphate
AGGF1	angiogenic factor with G-patch and FHA domains 1
APE-1	Apurinic/apyrimidinic endonuclease
APS	Ammonium persulfate
ARF	Alternative reading frame
ATCC	American type culture collection
ATG12	Autophagy-related protein 12
ATM	Ataxia telangiectasia mutated
ATP	Adenosine triphosphate
BAD	Bcl2-associated death promoter
Bcl2	B-cell lymphoma 2
BECN1	Bcl-2 interacting coiled coil protein
BER	Base excision repair
BRCA	Breast cancer gene
C.tr	*Chlamydia trachomatis*
CA-125	Cancer antigen-125
CDK	Cyclin dependent kinases
CHIP	Chromatin immunoprecipitation
cIAP2	cellular Inhibitor of apoptosis protein 2
ciHHV-6	Chromosomally integrated human herpes virus 6
CPAF	*Chlamydia* protease like activity factor
DAPI	4',6-diamidino-2-phenylindole
DDR	DNA damage response
DGCR8	DiGeorge syndrome chromosomal region 8
DMSO	Dimethyl sulfoxide
DNA	Deoxyribonucleic acid
DR	Direct repeat
DR_L	Direct repeat left
DRP1	Dynamin related protein 1
DR_R	Direct repeat right
DSB	Double stranded break
DTT	Dithiothreitol
EB	Elementary bodies
EGFR	Epidermal growth factor receptor
EPHA2	Ephrin receptor A2
ERK	Extracellular signal regulated
EtBr	Ethidium Bromide
FGF2	Fibroblast growth factor 2
FGFR	Fibroblast growth factor receptor

FISH	Fluorescence *in situ* hybridization
G4	G-quadruplex
GAIP	G- alpha interacting protein isoform B
h	Hour(s)
H_2O_2	Hydrogen peroxide
HCMV	Human cytomegalovirus
HeLa	Henrietta Lacks
HER2	Human epidermal growth factor receptor 2
HFF	Human foreskin fibroblasts
HHV-6	Human herpesvirus 6
HIF-1α	Hypoxia activating factor-1 alpha
HOCl	Hypochlorous acid
HOSE	Human ovarian epithelial
hpi	Hours post-infection
HPV	Human papillomavirus
HR	Homologous recombination
HUVEC	Human umbilical vein endothelial cells
iciHHV-6	Inherited chromosomally integrated human herpes virus 6
IE	Immediate early
IgG	Immunoglobulin G
IL6	Interleukin 6
IL8	Interleukin 8
JAK	Janus kinase 2
kb	Kilo base pairs
KSHV	Kaposi's sarcoma-associated herpesvirus
LGV	Lymphogranuloma venereum
LPS	Lipopolysaccharide
MDM2	Mouse double minute 2 homolog
MCL1	Induced myeloid leukemia cell differentiation protein 1
min	Minute(s)
miRNA	MicroRNA
ml	milliliter
mM	millimole
MMP2	Matrix metalloproteinase 2
MMP9	Matrix metalloproteinase 9
MOI	Multiplicity of infection
MTOC	Microtubule organizing centre
NF-κβ	Nuclear factor -κβ
NHEJ	Non-homologous end joining
nM	nanomole
nm	nanometer
$^1O_2$	Singlet oxygen
O_3	Ozone
ORF	Open reading frame
P4	Progesterone
pac	Packaging sequence

PAZ	Piwi/Argonaute/Zwille
PBMC	Peripheral blood mononuclear cells
PCR	Polymerase chain reaction
PFGE	Pulsed field gel electrophoresis
PI3K	Phosphoinositide 3 kinase
PI3KA	Phosphoinositide 3 kinase catalytic subunit α
PID	Pelvic inflammatory disease
piRNA	piwi-interacting RNA
PNKP	Polynucleotide Kinase Phosphatase
Pol II	Polymerase II
Pol III	Polymerase III
Pol β	Polymerase beta
PTEN	Phosphatase and tensin homolog
PTM	Post-translational modification
PVDF	Polyvinylidene fluoride
RB	Reticulate bodies
RISC	RNA-induced silencing complex
RNA	Ribonucleic acid
ROS	Reactive oxygen species
RPA	Replicating protein A
RT	Room temperature
SAHF	Senescence-associated heterochromatin foci
SDS-PAGE	Sodium dodecyl sulfate polyacrylamide gel electrophoresis
sec	Seconds
siRNA	Small interfering RNA
SSA	Single strand annealing
SSB	Single stranded break
STAT3	Signal transducer and activator of transcription 3
STIC	Serous tubal intraepithelial carcinoma
T2SS	Type 2 secretion system
T3SS	Type 3 secretion system
TDP-1	Tyrosyl DNA phosphodiesterase 1
TEMED	Tetramethylethlenediamine
TFI	Tubal infertility
TFI	Tubal factor infertility
TGF-β	Transforming growth factor beta
TLS	Translesion DNA synthesis
TNF α	Tumor necrosis factor alpha
TNFR	Tumor necrosis factor receptor
TRS	Telomeric repeat sequences
UTR	Untranslated region

ABSTRACT

Ovarian cancer is one of the most common gynecological malignancies in the world. The prevalence of a microbial signature in ovarian cancer has been reported by several studies till date. In these microorganisms, Human herpesvirus 6 (HHV-6) and *Chlamydia trachomatis* (C.tr) are especially important as they have significantly high prevalence rate. Moreover, these pathogens are directly involved in causing DNA damage and thereby disrupting the integrity of host genome which is the underlying cause of any cancer.

This study focuses on how the two pathogens, HHV-6 and *C. trachomatis* can affect the genome integrity in their individual capacities and thereby may drive ovarian epithelial cells towards transformation. HHV-6 has unique tendency to integrate its genome into the host genome at sub-telomeric regions and achieve a state of latency. This latent virus may get reactivated during the course of life by stress, drugs such as steroids, during transplantation, pregnancy etc. The study presented here began with an interesting observation wherein the direct repeat (DR) sequences flanking the ends of double stranded viral genome were found in unusually high numbers in human blood samples as opposed to normal ratio of two DR copies per viral genome. This study was corroborated with *in vitro* data where cell lines were generated to mimic the HHV-6 status in human samples. The same observation of unusually high DR copies was found in these cell lines as well.

Interestingly, fluorescence *in situ* hybridization (FISH) and inverse polymerase chain reaction followed by southern blotting showed that DR sequences were found to be integrated in non-telomeric regions as opposed to the usual sub-telomeric integration sites in both human samples and in cell lines. Sanger sequencing confirmed the non-telomeric integration of viral DR sequences in the host genome.

Several studies have shown that *C. trachomatis* causes DNA damage and inhibits the signaling cascade of DNA damage response. However, the effect of *C. trachomatis* infection on process of DNA repair itself was not addressed. In this study, the effect of *C. trachomatis* infection on host base excision repair (BER) has been addressed. Base excision repair is a pathway which is responsible for replacing the oxidized bases with new undamaged ones. Interestingly, it was found that *C. trachomatis* infection downregulated polymerase β expression and attenuated polymerase β- mediated BER *in vitro*. The mechanism of the polymerase β downregulation was found to be associated with the changes in the host microRNAs and downregulation of tumor suppressor, p53. MicroRNA-499 which has a binding site in the polymerase β 3'UTR was shown to be upregulated during *C. trachomatis* infection. Inhibition of miR-499 using synthetic miR-499 inhibitor indeed improved the repair efficiency during *C. trachomatis* infection in the *in vitro* repair assay. Moreover, p53 transcriptionally regulates polymerase β and stabilizing p53 during *C. trachomatis* infection enhanced the repair efficiency.

Previous studies have shown that *C. trachomatis* can reactivate latent HHV-6. Therefore, genomic instability due to insertions of unstable 'transposon-like' HHV-6 DR followed by compromised BER during *C. trachomatis* infection cumulatively support the hypothesis of pathogenic infections as a probable cause of ovarian cancer.

ZUSAMMENFASSUNG

Eierstockkrebs ist eine der häufigsten gynäkologischen Bösartigkeiten weltweit. Bis heute haben verschiedene Studien gezeigt, dass bei Eierstockkrebs eine mikrobiologische Signatur vorherrschen kann. Unter diesen Mikroorganismen spielen das Humane Herpesvirus 6 (HHV-6) und *Chlamydia trachomatis* (C.tr) eine besonders wichtige Rolle, da sie mit einer hohen Signifikanz bei betroffenen Patienten vorkommen. Zudem können diese Pathogene DNA Schäden verursachen und damit die Integrität des Genoms zerstören, was die Grundlage jeder Krebsentstehung darstellt.

Diese Studie fokussiert sich darauf, wie die beiden Pathogene HHV-6 und *C. trachomatis* die Genom Integrität beeinflussen und dadurch die Transformation ovarialer Epithelzellen antreiben können. HHV-6 besitzt die einzigartige Neigung sich an der Subtelomer-Region in das Genom des Wirts zu integrieren und einen latenten Zustand zu erreichen. Dieser latente Virus kann während verschiedener Lebensphasen reaktiviert werden, wie durch Stress, Pharmaka (z.B. Steroide) und während Transplantationen oder Schwangerschaften. Die hier beschriebene Studie begann mit einer interessanten Beobachtung, bei der menschliche Blutproben eine ungewöhnlich hohe Anzahl an sogenannten *direct repeat* (DR) Sequenzen, die die Enden des doppelsträngigen Virus Genoms flankieren, aufwiesen, verglichen mit der normalen Rate der DR Kopien pro Virus Genom. Bestätigt wurde diese Beobachtung durch *in vitro* Daten, wofür Zelllinien generiert wurden, um den HHV-6 Wert in menschlichen Proben zu imitieren.

Interessanterweise konnten nachfolgende Experimente zeigen, dass die DR Sequenzen sowohl in menschlichen Proben als auch in Zelllinien-Proben, nicht in Subtelomer-Regionen integriert

waren. Durch Sanger Sequenzierung konnte die Integration der viralen DR Sequenzen außerhalb von Telomer Regionen in das Genom nachgewiesen werden.

Verschiedene Studien konnten zeigen, dass *C. trachomatis* DNA Schäden verursacht und die Signal Kaskade von Antworten auf DNA-Schädigungen inhibiert. Allerdings wurde die Auswirkung einer *C. trachomatis* Infektion auf den Prozess der DNA Reparatur selbst noch nicht behandelt. In dieser Studie wird die Auswirkung einer *C. trachomatis* Infektion auf Basen-Exzisionsreparatur (BER) thematisiert. Basen-Exzisionsreparatur ist ein Mechanismus, der dafür verantwortlich ist oxidierte Basen mit Unbeschädigten auszutauschen. Interessanterweise wurde herausgefunden, dass während einer *C. trachomatis* Infektion die Expression von Polymerase β herunterreguliert ist und dadurch die Polymerase β-vermittelte Basen-Exzisionsreparatur *in vitro* gestoppt wird. Der Mechanismus der Herunterregulierung von Polymerase β konnte mit Veränderungen in der microRNA des Wirts und mit einer Herunterregulierung des Tumorsuppressors p53 assoziiert werden. MicroRNA-499, die eine Bindungsstelle an der Polymerase β 3'UTR besitzt, wird während einer *C. trachomatis* Infektion hochreguliert. *In vitro* Reparatur-Assays haben gezeigt, dass die Reparatur-Effizienz während einer *C. trachomatis* Infektion durch die Inhibition von miR-499 tatsächlich verbessert wird. Darüber hinaus reguliert p53 auf transkriptioneller Ebene Polymerase β und eine Stabilisierung von p53 während einer *C. trachomatis* Infektion verbesserte die Reparatur-Effizienz.

Vorangegangene Studien haben gezeigt, dass *C. trachomatis* die latente Form von HHV-6 reaktiveren kann. Deshalb unterstützt die genomische Instabilität aufgrund einer Insertion von unstabilen `transposon-ähnlichen' HHV-6 DR, gefolgt von komprimierter BER während einer *C. trachomatis* Infektion, zunehmend die Hypothese, dass eine pathogene Infektion ein vermutlicher Auslöser von Eierstockkrebs ist.

1. INTRODUCTION

1.1 Ovarian Cancer

1.1.1 Overview of Ovarian Cancer

Ovarian cancer is one of the most lethal gynecological malignancies with an extremely poor 5-year survival expectancy worldwide. It is the fifth most common type of cancer occurring in the human population globally. Although 80% of the ovarian cancer cases are symptomatic when the cancer is still limited to the ovaries, these symptoms are often mistaken for gastrointestinal, genitourinary or other gynecological problems. Hence, ovarian cancer is often termed as a 'silent killer' (Goff et al., 2000). Another feature about ovarian cancer which makes it more formidable than other cancers is the anatomy of ovaries. The ovaries do not have an anatomical barrier to limit the metastasis in the near peritoneal cavity. Moreover, despite the medical advancements, only 20% of ovarian cancer cases are diagnosed when the cancer is limited to the ovaries (Berek et al., 2015). This makes it very important to identify biomarkers suggesting ovarian cancer.

Although ovarian cancer can develop from germ cells or granulosa cells, nearly 90% of the ovarian cancers are epithelial in origin and are believed to develop from ovarian surface epithelium or epithelial lining of the inclusion cyst (Feeley et al., 2001). The molecular and physiological underpinnings of ovarian cancer development are discussed in the following sections.

1.1.2 Molecular Pathogenesis of Ovarian Cancer

The hallmarks of any cancer are the capabilities acquired by normal cells in order to become immortal or metastatic and achieve continuous growth. These hallmarks form the organizing principle which differentiates normal cells from cancer cells. Briefly, these hallmarks are – proliferative signaling, evading apoptosis, evading growth suppressors, replicative immortality,

angiogenesis and finally, invasion and metastasis (Hanahan and Weinberg, 2011). These hallmarks stand true for ovarian cancer as well and are discussed in more detail in the following section.

Proliferative signaling- In rare cases of ovarian cancer there is overexpression of epidermal growth factor receptor (EGFR) or human epidermal growth factor receptor (HER2) due to mutations (Bookman et al., 2003; Gordon et al., 2005). However, in more than 70% of the cases phosphoinositide 3 kinase (PI3K) pathway is activated. The PI3K pathway is an important signal transduction system which has key regulatory roles in cell survival, proliferation and differentiation (Vivanco and Sawyers, 2002). The PI3K pathway is activated by activating mutations in the PI3K catalytic subunit α (PI3KA), or its overexpression. This pathway is also activated by inactivating mutations in the tumor suppressor phosphatase and tensin homolog (PTEN) which is its negative regulator (Vivanco and Sawyers, 2002). In many cancers, the pathway is also activated by signaling through protein tyrosine kinase growth receptors. In most ovarian cancers, interleukin IL-6 is also overexpressed which in turn activates Janus kinase 2 (JAK2) which induces phosphorylation and nuclear translocation of signal transducer and activator of transcription 3 (STAT3). STAT3 is a transcription factor and is translocated to the nucleus in more than 70% of ovarian cancer case (Bast et al., 2009).

Apoptosis- In more than 50% of ovarian cancer cases, mutation in the *TP53* gene causing a defective p53 protein have been reported (Berchuck et al., 1994; Havrilesky et al., 2003). Tumor suppressor, p53, is not only essential in apoptotic signaling but also plays an important role in several DNA repair pathways. Germline mutations in DNA repair proteins encoded by breast cancer genes BRCA1 and BRCA2 also account for 10-15% of ovarian cancers (Lancaster et al., 1996). Invasive epithelial ovarian cancers are resistant to pro-apoptotic receptor CD95-mediated signaling. These cancers also display high expression of anti-apoptotic proteins like Bcl-2 and Bcl-

X_L (Schuyer et al., 2001). Transforming growth factor β (TGF-β) mediates growth inhibition in normal ovarian epithelial cells which is lost in roughly 40% of ovarian epithelial cancers (Bast et al., 2009).

Replicative immortality, angiogenesis and invasion and metastasis- STAT3, which is upregulated in ovarian cancer, initiates proliferative signaling and inhibits apoptosis and induces angiogenesis. Upregulation of cyclins D1, E1 and E2F1, cyclin dependent kinases (CDK) and downregulation of CDK inhibitors like p16, p21 and p27 have been reported in several cases of ovarian cancer (Reimer et al., 2006). STAT3, stress hormones like adrenaline, noradrenaline, cortisol mediated upregulation of matrix metalloproteinase 2 (MMP2), MMP9 and transmembrane glycosylated protein CA-125 (cancer antigen 125) are highly overexpressed in ovarian cancer and contribute to invasion (Sood et al., 2006). Interleukins IL-6, IL-8 and fibroblast growth factor (FGF2) promote angiogenesis and are also upregulated in ovarian cancer (Davidson et al., 2001).

1.1.3 Physiological Origin of Ovarian Cancer

While early studies suggested incessant ovulation as the only contributing mechanism of ovarian cancer, recent studies have identified additional non-ovarian origins as well. The details of these hypotheses are summarized in the following section.

Incessant ovulation- The process of ovulation involves follicular rupture and release of the oocyte. This results in release of several proinflammatory cytokines, prostaglandins and potentially mutagenic oxidative stress and thereby may cause genomic instability. This led to the hypothesis of repetitive ovulation being the cause of ovarian cancer (Hunn J and Rodriguez GC., 2012). This hypothesis was also supported by several epidemiological studies (Fathalla, 2013).

Fimbria associated ovarian cancer- Initially, it was assumed that all ovarian cancers originated from the ovaries and hence the fallopian tubes were not carefully examined in cases with ovarian carcinoma. However, after careful *in situ* examination of fallopian tubes it was observed that small invasive tubal carcinomas were present in women with predisposition to ovarian cancer development (Kurman and Shih, 2010). This led to the belief that fallopian tube carcinoma was indeed associated with ovarian carcinoma and the hypothesis that ovarian carcinoma might develop because of implantation of malignant cells from the fallopian tubes into the ovaries. Moreover, subsequent follow-up studies demonstrated the association of serous tubal intraepithelial carcinoma (STIC) with nearly 70% of sporadic or non-hereditary cases of ovarian cancer. Since STIC is almost always detected in fimbria, these observations suggested fimbria as an origin of ovarian cancer (Kurman and Shih, 2011).
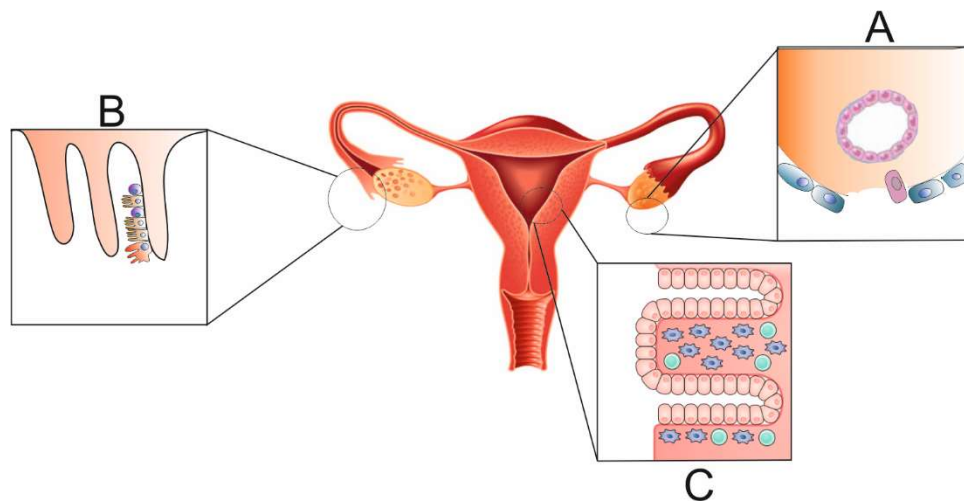
Figure 1.1. Hypotheses explaining the origin of ovarian cancer (A) Incessant ovulation- During normal ovulation epithelial cells are often damaged and subsequently repaired. Repeated ovulations make them more prone to acquire mutations. **(B)** The cells lining the fallopian tubes, especially the fimbrial cells become mutagenic because of oxidative stress and are implanted in the ovary due to their close proximity. **(C)** During endometriosis, the mutagenic cells travel in the opposite direction due to retrograde menstruation and are implanted in the ovary. Adapted from (Kurman and Shih, 2011).

Endometrium associated ovarian cancer- Endometriosis occurs when endometrium, the tissue lining the inside of the uterus grows outside the uterus. It occurs in roughly 10% of women worldwide and is associated risk factor of epithelial ovarian cancer (Anglesio et al., 2015). Endometriosis coexists with ovarian cancer and whole genome sequencing suggests a clonal relationship between multiple physically distinct endometrial lesions hinting at a common mobile precursor for these lesions (Anglesio et al., 2015). The clonal relationship between endometriosis and ovarian cancer also corroborates this finding (Anglesio et al., 2016).

Thus, several hypotheses, high throughput studies and epidemiological studies suggest a strong plausibility of extra ovarian tissue to be an origin of ovarian cancer alongside the well-established incessant ovulation hypothesis.

1.1.4 Microbial Signatures in Ovarian Cancer

Ovarian cancer is particularly lethal as most of the cases are diagnosed at a later stage and the symptoms are synonymous with those of other gynecological malignancies. Hence, finding a verified biomarker for the early onset as well the duration of the disease is of utmost importance. Epidemiological studies have shown association of sexually transmitted bacterial pathogens such as *Chlamydia trachomatis* and *Mycoplasma genitalium* but not of *Neisseria gonorrhoeae* in ovarian cancer (Idahl et al., 2010). However, there have been contradictory studies demonstrating the presence of IgG antibodies against *C. trachomatis* in ovarian cancer patients (Ness et al., 2008; Ness and Cottreau, 1999). Although, clear association of *C. trachomatis* in ovarian cancer is still debated, studies have shown association of *C. trachomatis* with pelvic inflammatory disease (PID) and tubal factor infertility (TFI) which are in turn linked with ovarian cancer (Risch and Howe, 1995; Weström and Wölner-Hanssen, 1993). A recent microarray based study by Banerjee *et al*

showed the presence of several bacterial and viral pathogens in ovarian cancer samples compared to matched (non-cancerous tissue adjacent to the tumor tissue) and unmatched controls (healthy control). This study shows the presence of *C. trachomatis* in 3% of the ovarian cancers. Several viral signatures were also identified in the same study including the herpesviruses HPV-16, HPV-18, HHV6A, HHV-6B, HHV-7 and KSHV (Banerjee et al., 2017). Presence of HHV-6A and HHV-6B in ovarian cancer was not reported before. In the same study, the genome sequences binding to the probes employed in the microarray were captured, amplified and subjected to next generation sequencing to identify the sites of viral insertions within the human chromosomes. Interestingly, HHV-6A and HHV-6B which is known to integrate in the telomeric regions of the human chromosomes was found in non-telomeric regions of different chromosomes in different samples. The coding sequence of U47 gene encoding the envelop glycoprotein O which is essential for morphogenesis of the virus was identified to be integrated in these regions. The details of these insertions are summarized in **Table 1.1**.

Gene	Chromosome	Location
SH3RF2	5	intronic
ZNF616	19	intronic
SYNDIG1	20	intronic
CPLX1	4	intronic
OR5I1	11	exonic
DPY19L1	7	downstream
LHX1*	7	intergenic-58 Kb upstream
IGFBP3	7	intergenic- 25 Kb upstream

Table 1.1. List of genes affected by HHV-6 integration in ovarian cancer samples including the site of integration. *All of the genes affected due to viral insertion, except LHX1 were associated significantly with various cancers (Banerjee et al., 2017).

1.2 Human herpesvirus 6

HHV-6 is a common betaherpesvirus infecting nearly every individual in early childhood. It causes a benign disease called 'exanthema subitum' which is characterized by a typical mild rash. It is genetically similar to human cytomegalovirus (HCMV) and can be sub-categorized into two species- HHV-6A and HHV-6B (Ablashi et al., 1993). This virus has a unique capability to integrate its DNA covalently in the sub-telomeric region of host chromosomes (ciHHV-6) and thereby maintain lifelong latency (Arbuckle et al., 2010). HHV-6 can integrate in the germ cells and can be transferred to the subsequent generations in a Mendelian fashion. The inherited viral DNA will be present in every nucleated cell of the individual and this condition is termed as inherited chromosomally integrated HHV-6 or iciHHV-6. It occurs in roughly 1% of the general population (Hall et al., 2017).

1.2.1 Discovery and Classification of HHV-6

HHV-6 was isolated from patients with lymphoproliferative disorders and AIDS in 1986 (Salahuddin et al., 2000). Electron microscopy studies revealed the structure of the virus to be icosahedral surrounded by tegument inside an enveloped particle of approximately 200 nm diameter. This was a characteristic morphology of herpesviruses (Biberfeld et al., 1987). In 1990, based on biological and genetic properties, this virus was classified in to *Herpesviridae* family, *Betaherpesvirinae* subfamily and *Roseolovirus* genus (Frenkel et al., 1990). After classification of HHV-6 many other strains were subsequently isolated from patients around the world. These strains were carefully studied and based on specific genetic and phenotypic properties these strains were further sub categorized into two variants HHV-6A and HHV-6B. HHV-6 is used as a general term and collectively refers to the two species (Agut et al., 2015).

1.2.2 Genome Organization of HHV-6

HHV-6 genome is a linear double stranded DNA consisting of a 143-145 kb long unique (U) region which is flanked by identical direct repeat sequences (DR_L and DR_R) on each end of the unique region. The direct repeat sequences are approximately 8 kb in length and thus the total length of the HHV-6 genome is about 160 kb-170 kb **(Figure 1.2)**.

DR (DR_L and DR_R) sequences have a unique cleavage packaging motif (pac-1 and pac-2) on each side and repeats of hexameric repeat sequences- GGGTTA. The sequences adjacent to the 'pac' sequences are related to human telomeric repeat sequences (TRS) (Braun et al., 1997). Pac-1 has TRS repeats which are separated by different nucleotide sequences and hence termed as heterogenous TRS repeats or het(GGGTTA) whereas the pac-2 has perfect hexameric GGGTTA repeats. These direct repeat sequences (DR) play an important role in the chromosomal integration of HHV-6 within the sub-telomeric regions of human chromosomes (ciHHV-6) (Arbuckle et al., 2010). It is believed that HHV-6 integrates by homologous recombination between pac-2 sequences of the DR_R and telomeric sequences of human chromosomes (Wallaschek et al., 2016).

HHV-6 ORFs

DR1-DR6   **U1-U100**

pac1   pac2   pac1   pac2

DR_L DR_R

het(GGGTTA)$_n$ (GGGTTA)$_n$ het(GGGTTA)$_n$ (GGGTTA)$_n$
T1   **T2**   **T1**   **T2**
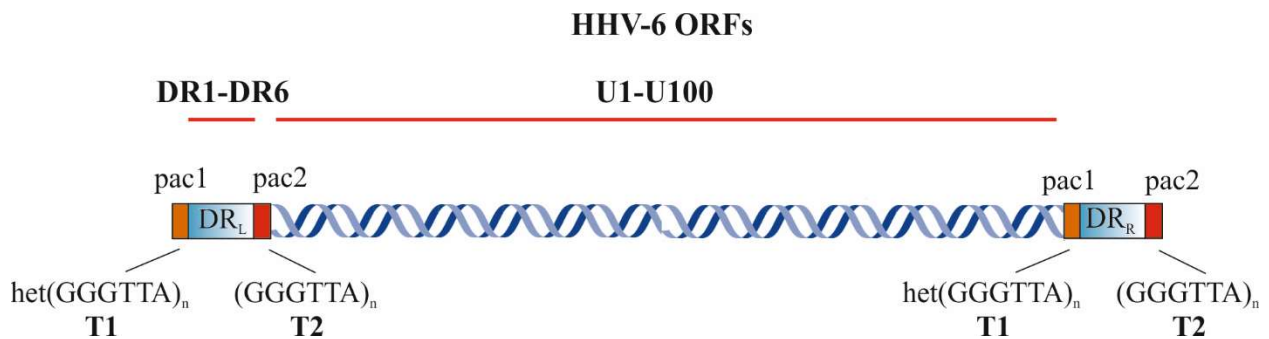
Figure 1.2. Schematic representation of HHV-6 genome. The double stranded viral genomic DNA is classified into different ORFS. It encodes for viral genes in the unique region (U1-U100) which is flanked by direct repeats to the right and left (DR_R and DR_L). The DR regions consist of perfect (pac2) and imperfect (pac1) hexameric repeats (GGGTTA)$_n$

HHV-6 encodes around 100 ORFs in the unique region, the genes are designated as U1, U2, U3 up to U100 and 7 ORFs in the DR region where the genes are designated as DR1 to DR7. Some of the genes are conserved between the *Roseolovirus* genus. Whereas some of the genes are specific to HHV-6. The unique region consists of genes encoding viral proteins such as immediate early proteins (IE-1 and IE-2), structural glycoproteins (gH, gB, gQ1) etc. involved in viral replication cycle. These genes are clustered systematically in two to eight ORFs and form the central part of the unique region (Gompels et al., 1995).

1.2.3 Replication Cycle of HHV-6

Although HHV-6 infects many different cell types *in vitro*, it prefers CD4+ T cells for active replication (De Bolle et al., 2005). HHV-6A uses the CD46 receptor which is ubiquitously present on all nucleated human cell membranes as a receptor whereas HHV-6B uses a more specific CD134, a member of tumor necrosis factor (TNF) superfamily which is present exclusively on activated T cells (Santoro et al., 1999; Tang et al., 2013). Apart from CD4+ lymphocytes, HHV-6A can infect CD8+ lymphocytes, natural killer cells, fibroblasts, epithelial cells, endothelial cells and astrocytes (Agut et al., 2015). Thus, HHV-6A more efficiently infects different cell types as compared to HHV-6B.

The first step in the replication cycle is marked by the binding of HHV-6 to its cellular receptor by means of a tetrameric protein complex composed of viral glycoproteins gH, gL, gQ1 and gQ2 (Tipples and Pellett, 2015). After attachment, the viral envelop is fused to the cell membrane and the nucleocapsid is released in the cytoplasm. It transverses to the nucleus via the microtubule network and releases the viral DNA in the nucleoplasm. After release of the DNA, the immediate early viral genes IE-1 and IE-2 are transcribed irrespective of the host cell protein synthesis. Following this, early (E) genes encoding enzymes such as those required for replication of the

virus like phosphotransferase, ribonucleotide reductase, uracil DNA glycosylase, DNA polymerase, polymerase processivity factor, origin binding protein, helicase and primase are transcribed (Tipples and Pellett, 2015). These enzymes favor the replication of viral DNA. Subsequently, the late genes encoding the packaging proteins and other structural proteins are transcribed (Tipples and Pellett, 2015). HHV-6 DNA replicates by the rolling circle mechanism (Agut et al., 2015). The replicated viral DNA is produced in the form of concatemers which are then cleaved and packaged according to the cleavage and packaging signals in the DR_L and DR_R regions. The capsid exits the nucleus and the final envelop made of viral glycoproteins is assembled in the Golgi apparatus followed by exocytosis. This entire process of infection and release of progeny virus takes up to 3 days (Agut et al., 2015).

1.2.4 Chromosomal Integration of HHV-6 (ciHHV-6)

The *Betaherpesvirinae* subfamily has four viruses including HHV-6A, HHV-6B, HHV-7 and HCMV. Out of these *Roseolovirus* genus viruses- HHV-6/B and HHV-7 are unique in their capability of maintaining a lifelong latency by integrating their DNA in the sub-telomeric regions of human chromosomes (Morissette and Flamand, 2010). This condition of chromosomally integrated HHV-6 (ciHHV-6) occurs in about 1% of the general population because of the covalent linking of viral and human DNA by homologous recombination between the telomeric repeat sequences present in the genomes of virus and human origin (Daibata et al., 1999). It is hypothesized that homologous recombination occurs between the perfect telomeric repeats present in the pac-2 signal in the DR_R and the telomeric sequences present in the human chromosomes. Most of the characterized ciHHV-6 genomes have a similar arrangement with the DR_R near the centromere end whereas the DR_L is positioned at the telomeric end of the chromosome. Integration of viral DNA via homologous recombination results in loss of DR_R-pac-2 signal. Studies have

shown that HHV-6 can integrate in the gametes both *in vitro* and *in vivo* and can result in inheritance of ciHHV-6 (Arbuckle et al., 2010; Hall et al., 2008). This inherited ciHHV-6 is passed on to the next generations in a Mendelian fashion and each of the new born harbors one copy of HHV-6 per nucleated cell (Pantry and Medveczky, 2017). This is most common mode of congenital transmission of HHV-6

Several hypotheses have been put forth till now explaining the mechanisms of viral integration. Studies have shown that the telomeric repeat sequences (T1 and T2) within the direct repeats (DR) are of utmost importance in process of viral integration (Wallaschek et al., 2016). One of the possible mechanism is during the break induced repair of host chromosomes caused by blockages such as G quadruplexes (G4) structure (Collin and Flamand, 2017). The open 3' end of the host chromosomes recruits Rad51 protein which searches for proximal homologous strands. Rad51 invades the direct repeat sequences in the HHV-6 genome if it is in the proximity thereby displacing one strand of the HHV-6 and allowing synthesis of the complementary strand (Collin and Flamand, 2017). The other mechanism is based on single stranded annealing (SSA) mechanism. SSA activation leads to alignment of the viral and human DNA in the direction of complementarity. This is followed by binding of the replication protein A (RPA) to the 3' end of both the genomes. RPA later recruits Rad52 which pairs the two genomes followed by synthesizing one of the viral strands (Collin and Flamand, 2017).

1.2.5 ciHHV-6 Reactivation and Disease

The first step in ciHHV-6 reactivation is excision of the viral genome from the host chromosomes followed by replication and transcription. The excision of viral genome from the human telomeric region is shown to occur by a telomeric circle or t-circle formation mechanism.

The telomeric circle formation can be explained by two models, the so-called single t-loop model and double t-loop model (Prusty et al., 2013a; Wood and Royle, 2017). In the double t-loop model, a short loop with one DR_L sequence and a long loop with unique region (U) and the other DR_R are formed resulting in excision of two circular genomes of viral origin **(Figure 1.3 I)**. The short loop formation begins when the 3' telomeric overhang invades the perfect (TTAGGG) repeats in the DR_R sequence. This results in excision of a double stranded circular molecule containing DR_L which is processed by the normal telomere processing assembly **(Figure 1.3 a)**. The formation of the long loop begins when the remaining truncated DR_L T2 is elongated and recombines with the perfect TTAGGG repeats in the DR_R T2 sequence resulting in excision of viral genome with DR_R **(Figure 1.3 b)** (Wood and Royle, 2017). In the single t-loop model **(Figure 1.3 II)**, homologous recombination between imperfect $(TTAGGG)_n$ sequences in the DR_L T1 and DR_R T1 occurs leading to excision of the viral genome with unique (U) region and only one DR (DR_L) region **(Figure 1.3 e)**. The DR_R remains in the host chromosome **(Figure 1.3 f)**.

ciHHV-6 is implicated as a causative agent in a wide range of diseases. Reactivation of ciHHV-6 was shown to be associated with angina pectoris (Gravel et al., 2015), heart failure (Kühl et al., 2015), adrenocorticoid tumors (Pinto et al., 2015), miscarriage in pregnant women (Drago et al., 2014; Ohashi et al., 2002), severe encephalitis (Ogata et al., 2017), Alzheimer's disease (Carbone et al., 2014) and abnormalities in transplant patients (Ogata et al., 2015). Das *et al* demonstrated that the female steroid hormone, progesterone, can cause reactivation of ciHHV-6 in pregnant women and the subsequent miscarriage due to reactivation can be avoided by avoiding progesterone from the prescribed therapy (Das et al., 2016).
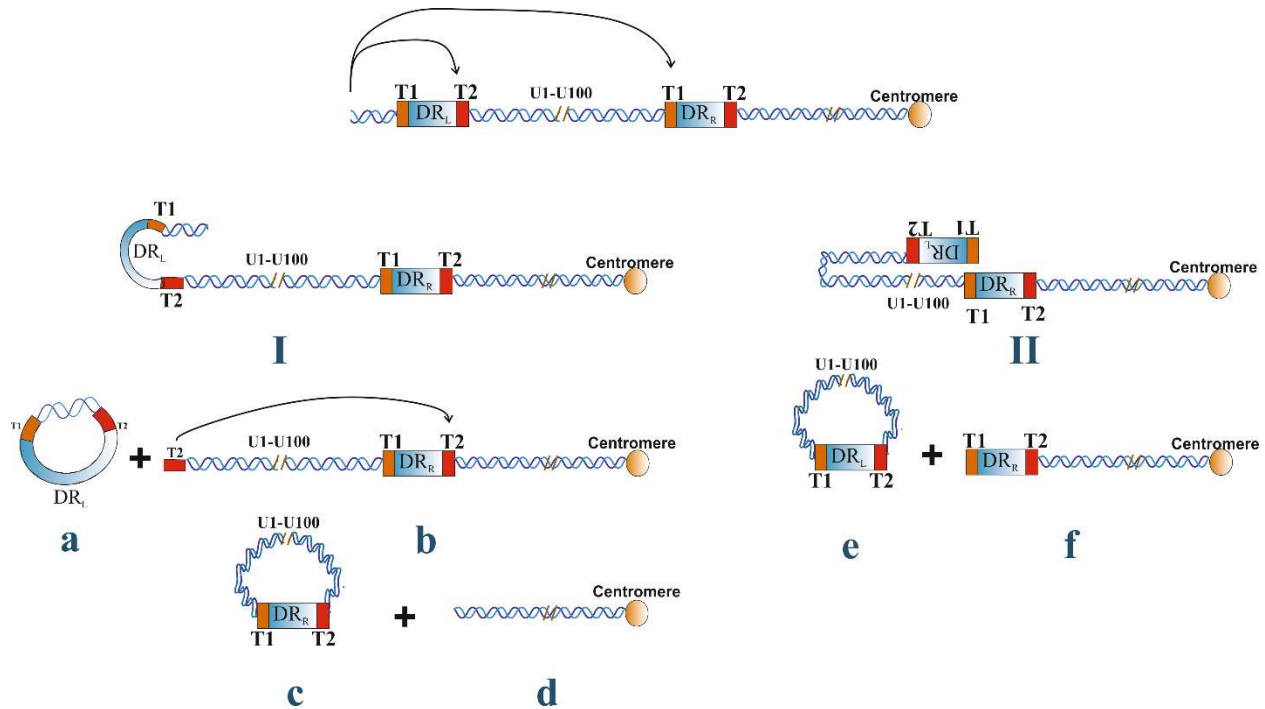
Figure 1.3. Schematic representation of different models of ciHHV-6 reactivation. On the left, in the double t-loop model, double t-loops are formed. First, a t-loop is formed between DR_L T1 and DR_L T2 giving rise to excision of circular DR_L (a). The DR_L T2 then forms the second t-loop with DR_R T2 leading to excision of HHV-6 genome containing DR_R (c). On the right, in the single t-loop model, a single t-loop forms between T1 repeats of DR_L and DR_R. This leads to excision of entire HHV-6 genome with a single DR- DR_L (e). DR_R, however, remains integrated in the host genome (f). Adapted from (Wood and Royle, 2017).

Prusty *et al* showed that *C. trachomatis* infection of the blood cells derived from ciHHV-6 patients can cause the formation of extra-chromosomal HHV-6 DNA followed by its replication (Prusty et al., 2013a). In a later study, it was shown that *C. trachomatis* causes this reactivation of ciHHV-6 by telomeric circle formation (Prusty et al., 2013b). Till date, only this telomeric circle model exists as a plausible explanation for the mechanism of excision of ciHHV-6 genome from human chromosomes.

1.3 Chlamydia trachomatis

The most common bacterial sexually transmitted infection worldwide is caused by *Chlamydia trachomatis*. Nearly 131 million new cases of *C. trachomatis* infection in adults and adolescents in the age range of 15-49 years are recorded annually (Reyburn, 2016). The prevalence rate of this infection is higher in women (4.2%) as compared to men (2.7%). It causes urethritis in men and cervicitis, endometritis and urethritis in women. Genital infections are asymptomatic in 70% of the infected women. It causes complications such as pelvic inflammatory disease (PID), increased risk for cervical carcinoma and infection related complications during pregnancy (Reyburn, 2016).

C. trachomatis is an obligatory intracellular, Gram-negative bacterium which belongs to the phylum Chlamydiae and family Chlamydiaceae. The family comprises of 11 different species, collectively called '*Chlamydiae*' which infects a wide range of organisms from amoeba to humans. *Chlamydia psittaci* is an avian pathogen which can infect humans, *Chlamydia muridarum* is a mouse pathogen whereas *Chlamydia trachomatis* and *Chlamydia pneumoniae* are major human pathogens (Tan and Bavoil, 2012). *C. trachomatis* is divided in to three biovars which cause genital infections, lymphogranuloma venereum (LGV) and trachoma (ocular infections). These biovars are further subdivided in different serovars. The trachoma biovar is sub-divided into serovars causing non-congenital blindness (A-C). The genital infection biovar causes sexually transmitted genital infections (serovars D-K) and is the most common sexually transmitted bacterial infection. The lymphogranuloma venereum biovar (serovars L1-L3) is more invasive and causes urogenital or rectal infections (Malhotra et al., 2013).

C. trachomatis has an extremely reduced genome of about 1.04 Mb with 895 open reading frames (Stephens et al., 1998). Its genome lacks genes essential for metabolism and hence is highly dependent on the host for metabolic enzymes. Although most of its genome is conserved between

the entire *Chlamydiae* family, 10% of the genome is specific to *C. trachomatis* and encodes virulence factors which are believed to aid the bacteria in host specificity and niche establishment (Bachmann et al., 2014).

Chlamydiae have a developmental cycle in which they alternate between two forms which are morphologically and functionally distinct- extracellular, infectious elementary bodies (EBs) and intracellular, non-infectious reticulate bodies (RBs).

1.3.1 Developmental cycle of *C. trachomatis*

Life cycle of *C. trachomatis* begins when the infectious EBs bind to the host cell **(Figure 1.4)**. EBs are protected by an outer membrane complex which is a network of proteins cross-linked by disulfide bonds making them resistant against physical stress and enabling them to survive the harsh extracellular environment. EBs are metabolically active and primarily use D-glucose-6-phosphate as a primary energy source (Omsland et al., 2014). They have the necessary proteins required for glucose catabolism which is possibly used immediately after infection to fulfill the energy requirements for differentiation into reticulate bodies (RBs) (Hackstadt, 2012). EBs bind to the host cell surface in a two-step fashion, first- low affinity binding to heparan sulfate proteoglycans and second- high affinity binding to a specific receptor (Hackstadt, 2012). The receptors for *C. trachomatis* EBs are many, including lipopolysaccharide (LPS), mannose-6-phosphate receptor, β-integrin, epidermal growth factor receptor (EGFR) and ephrin receptor A2 (EPHA2) (Mehlitz and Rudel, 2013).

After invasion, EBs induce actin remodeling which promotes efficient internalization of the bacteria. EBs then secrete an array of effector proteins through a specialized bacterial secretion system called type three secretion system (T3SS) in order to remodel the cytoskeleton and host cell signaling (Saka et al., 2011). The EBs are endocytosed by either clathrin-mediated, caveola-

mediated or independent mechanisms and are sequestered to a membrane bound compartment known as the inclusion (Hackstadt, 2012). Around 6-8 hours post infection (hpi), EBs differentiate into RBs and transcription of early genes take place which include inclusion membrane proteins (Inc) (Tan, 2012). The Inc proteins help in nutrient acquisition by redirecting the exocytic vesicles from the Golgi apparatus to the nascent inclusion. These inclusions are then transported to the microtubule organizing centre (MTOC) to promote access to nutrient rich compartments. *C. trachomatis* Inc proteins- IncB, CT101, CT222, CT850 are believed to participate in this process (Mital et al., 2015). They also play a role in inhibiting the fusion of inclusion with the lysosomes and thus avoiding the canonical endolysosomal pathway (Elwell et al., 2016). After differentiation to RBs (~16 hours post infection), mid-cycle proteins are expressed which function primarily to maintain the host cell viability (Tan, 2012). The bacteria divide by binary fission and the size of the inclusion increases gradually.

After about 24 hours post infection, RBs transition back to EBs and the late cycle genes are expressed (Tan, 2012). These include several DNA binding histone H1 and H2 like proteins Hc1 and Hc2 which condense the chromatin and switch off the transcription of many genes. The proteins that are synthesized in this phase are effectors which need to be packaged into the EBs to prepare them for further rounds of infection. Studies have shown that *C. trachomatis* secretes a protein called *Chlamydia* protease like activity factor (CPAF) through type 2 secretion system (T2SS) which is required to prepare the EBs for exit (Snavely et al., 2014). *C. trachomatis* exits the host cell by cell lysis which is characterized by rupture of the inclusion and the cell membrane thereby releasing the EBs and lysing the host cell (Hybiske and Stephens, 2007). Studies have also shown that *C. trachomatis* may exit the cell by extrusion mechanism where only a small portion

of the inclusion is released by membranous protrusion leaving the host cell intact (Elwell et al., 2016).
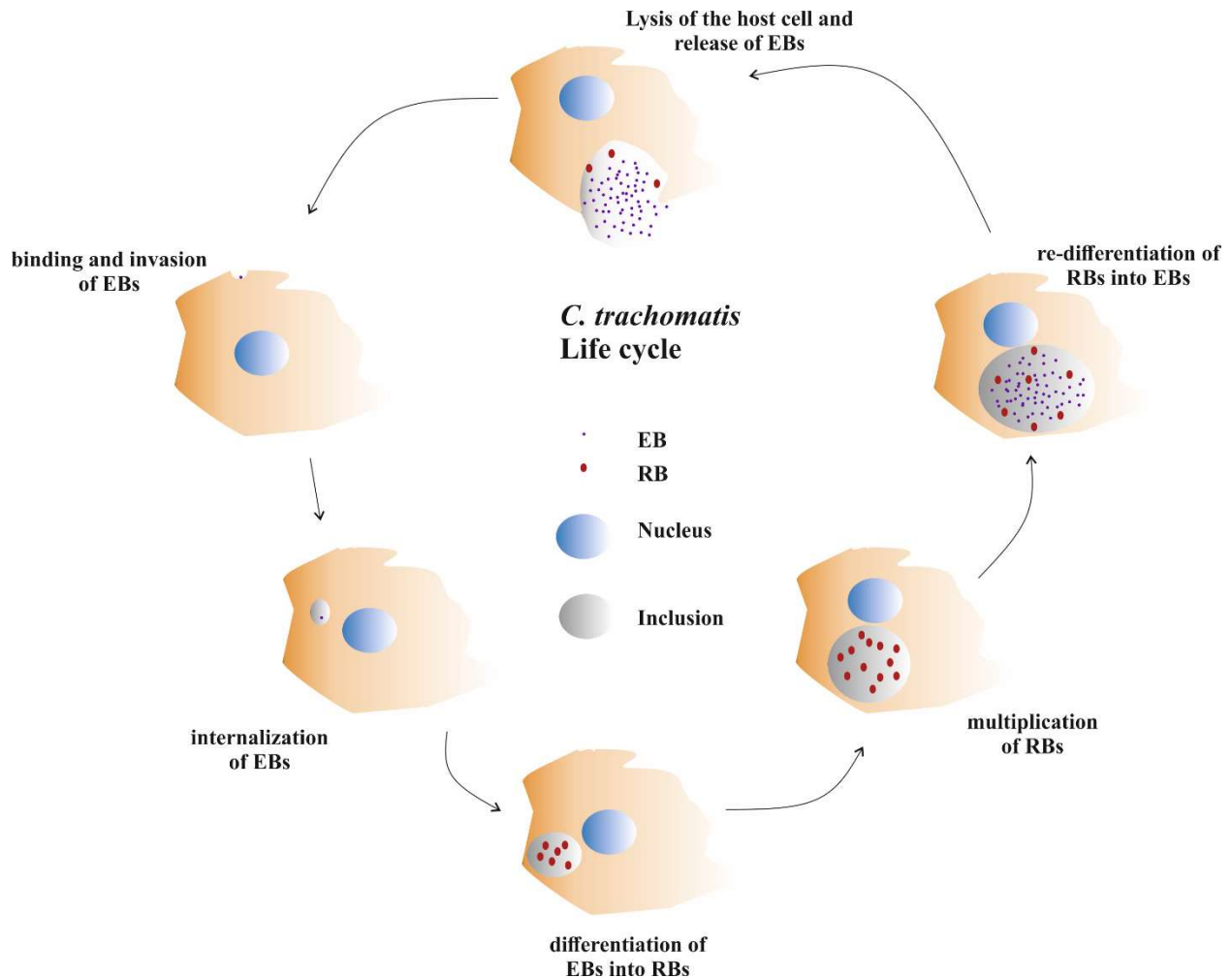
Figure 1.4. Developmental cycle of *C. trachomatis*. Life cycle of *C. trachomatis* starts by attachment of infectious EB on the cell membrane followed by its internalization and compartmentalization into an inclusion. The EBs then differentiate into RBs which are replicative form of the bacteria. After replication, the RBs re-differentiate into EBs and are released after lysis of the host cell to complete the cycle.

1.3.2 Modulation of host cell responses by *C. trachomatis*

As a result of its reduced genome, *C. trachomatis* lacks many of the genes which are indispensable in providing the bacteria with requirements such as glucose, lipids, amino acids, nucleotides and

other enzymes and co-factors. *C. trachomatis* acquires nutrients primarily by redirecting the exocytic vesicles towards the inclusion (Bastidas et al., 2013). They employ this strategy to acquire several lipid metabolites such as sphingomyelin, phosphatidylinositol, phosphatidylcholine and cholesterol (Elwell and Engel, 2012). Although *C. trachomatis* possess essential bacterial lipids which make up its membrane, it uses these acquired lipids for the purpose of replication and transition and re-transitions from different morphologies and maintenance of the inclusion. *C. trachomatis* is also known to fragment the Golgi apparatus during the mid-cycle of its infection, apparently to facilitate better acquisition of lipids (Elwell and Engel, 2012). *C. trachomatis* also inhibits the fragmentation of the mitochondria by downregulating dynamin related protein 1 (DRP1) (Chowdhury et al., 2017). By inhibiting mitochondrial fission and making them more elongated, *C. trachomatis* ensures a steady supply of ATP (Chowdhury et al., 2017).

Chlamydia, obligate intracellular bacteria, are often collectively termed as 'energy parasites'. Since an ATP-ADP translocase was found in the species, it was believed that they are completely dependent on the host for ATP supply. Later however, it was discovered that *Chlamydia* have complete functional pathways for glycolysis and the pentose phosphate pathways making them capable of producing ATP independently (Stephens et al., 1998). In spite of this, *C. trachomatis* upregulate the ATP synthesis in the host cell during the replicative phase of the RBs (Liang et al., 2018).

A recent study has shown that *C. trachomatis* infection changes the expression profile of the host cell microRNAs (Chowdhury et al., 2017). MicroRNAs or miRNAs are small, Pol II-dependent transcripts typically 20-22 nucleotides in length, non-coding RNAs encoded by the host genome (Bartel, 2004). They post-transcriptionally regulate the expression of nearly 60% of human protein coding genes (Friedman et al., 2009). Although not completely clear, it is believed that miRNAs

function by deadenylating and subsequently degrading host mRNAs. The details of the biogenesis and mechanism of action are explained in a separate chapter **(Introduction 1.4)**.

Bacteria	miRNA	Up/down-regulation
Helicobacter pylori	miR-1289, miR-30b, miR-584, miR-1290, miR-21, miR-222	upregulation
	miR-372, miR-373	downregulation
Salmonella spp.	miR-30c, miR-30b, miR-128	upregulation
	miR-15	downregulation
Mycobacterium tuberculosis	miR-132, miR-26a, miR-125b, miR-99b	upregulation
	miR-155, let-7f	downregulation

Table 1.2. List of microRNAs modulated by different bacteria. *H. pylori*, *Salmonella* spp. and *M. tuberculosis* modulate several host cell functions to promote their survival and proliferation by regulating host miRNAs (Duval et al., 2017).

Apart from *C. trachomatis* other bacteria like *Helicobacter pylori*, *Salmonella* spp. and *Mycobacterium tuberculosis* are also known to regulate the host cell miRNA profile. *Helicobacter pylori* upregulates the miRNA miR-30b which targets the host cell proteins BECN1 (Bcl-2 interacting coiled coil protein) and ATG12 (autophagy-related protein 12) involved in autophagy (Tang et al., 2012). *Salmonella* on the other hand, downregulates miR-15 which in turn de-represses cyclin D thereby promoting G1/S cell cycle transition (Maudet et al., 2014). *Mycobacterium tuberculosis* is known to upregulate miR-125b which binds to the 3'UTR of tumor

necrosis factor α (TNFα) mRNA and thereby downregulating its expression. This in turn decreases macrophage activation and mediated bacterial clearance (Rajaram et al., 2011). A list of bacterial pathogens modulating host miRNAs in summarized in **Table 1.2.**

1.3.3 *C. trachomatis*-induced DNA damage, DNA damage response and host cell survival

C. trachomatis being an intracellular pathogen actively modulates different host cell pathways in order to create conducive environment for the successful completion of its life cycle. During infection, however, *C. trachomatis* generates reactive oxygen species (ROS) which is shown to be essential for its growth and development (Abdul-Sater et al., 2010). ROS is comprised of superoxide ions, hydrogen peroxide and singlet oxygen and is known to cause oxidative DNA damage. A study shows that *C. trachomatis* causes ROS-mediated double stranded DNA breaks (DSBs) (Chumduri et al., 2013). The DSBs were identified by phosphorylated H2AX (Ser139), a specific marker for double strand breaks. Despite of the DNA damage, *C. trachomatis* infected cells showed a decreased colocalization of DNA damage response proteins ataxia telangiectasia mutated (ATM) and 53 binding protein 1(53BP1) at the damaged sites. *C. trachomatis* modulated the post translational modification (PTM) of various histones and thereby changing the epigenetic markup favorable for its survival. One of the prominent histone PTM was the trimethylation (lys9) of histone H3 (H3K9me3). H3K9me3 is another marker for DSBs and senescence-associated heterochromatin foci (SAHF) and is thought to be associated with heterochromatin formation during *C. trachomatis* infection (Chumduri et al., 2013). Increase in the SAHF also show marked increased activation of oncogenes. *C. trachomatis* is also shown to upregulate hTERT, a catalytic subunit of telomerase. hTERT helps in blocking apoptosis and contributes to cell proliferation and subsequent immortalization (Padberg *et al.,* 2013). *C. trachomatis* infected cells demonstrate a

decreased telomeric DNA damage signaling and increasing length of telomeres all of which point towards carcinogenesis.

Apart from modulating DNA damage response (DDR), *C. trachomatis* also actively inhibits apoptosis by other mechanisms. One of the mechanism is by mouse double minute 2 homolog (MDM)-mediated ubiquitylation and proteasomal degradation of tumor suppressor protein, p53 (Siegl et al., 2014). Other mechanisms include sequestering Bcl-2 associated agonist of cell death (BAD), or by upregulating anti- apoptotic proteins like MCL1 (Induced myeloid leukemia cell differentiation protein 1) or cIAP2 (cellular Inhibitor of apoptosis protein 2) (Bastidas et al., 2013; Verbeke et al., 2006). *C. trachomatis* also inhibits extrinsic apoptosis by inhibiting the activation of caspase 8. Extrinsic apoptosis functions by binding of the ligand to the death receptors such as Fas or tumor necrosis factor receptor (TNFR) on the cell membrane. These receptors activate caspase 8 which in turn activates the downstream signaling and finally activates the effector, caspase 3. Upon activation, caspase 3 is cleaved in its active subunits p17 and p13. *C. trachomatis* inhibits the cleavage of caspase 3 (Böhme et al., 2010).

C. trachomatis keeps the cell in a proliferating state by several mechanisms. It activates the extracellular signal regulated (ERK) cascade by binding to the fibroblast growth factor receptor (FGFR) (Kim et al., 2011). It also activates the PI3K pathway by binding to the ephrin receptor tyrosine kinase A2 (EPHA2) on the cell membrane (Subbarayal et al., 2015). These pathways in turn regulate host functions such as transcription, translation, cell cycle entry and proliferation.

1.4 MicroRNA- Biogenesis and Mechanisms

Mammals have mainly three classes of small RNAs- short interfering RNAs (siRNAs), microRNAs (miRNAs) and piwi-interacting RNAs (piRNAs) (Carthew and Sontheimer, 2009). MiRNAs are primarily generated by RNA polymerase II as capped and polyadenylated transcripts (Lee et al., 2004). However, there are reports showing that some preliminary or pre-miRNAs are transcribed by RNA polymerase III (Borchert et al., 2006). Typically, a transcript may encode a single miRNA and a protein or a cluster of different miRNAs. When a transcript encodes a single miRNA and a protein, the miRNA coding sequence is generally present within an intron. This resulting transcript is termed as primary miRNA or pri-miRNA. This pri-miRNA is ~33 nucleotide long and consists of an imperfect stem loop structure. The first step in towards generation of mature miRNA begins in the nucleus when Drosha, a nuclear RNase III, cleaves the imperfect stem loop of pri-miRNA to release a remainder transcript- preliminary or pre-miRNA (Kim, 2005). Drosha depends on a cofactor protein with a double strand RNA binding domains (dsRBD) called DGCR8. DGCR8 serves as a molecular anchor which is used by Drosha to position its catalytic site at the correct distance from the cleavage junction. Drosha and DGCR8 together form a microprocessor complex which is responsible for a successful cleavage (Denli et al., 2004). Pre-miRNA is then transported out of the nucleus and the second processing step occurs in the cytoplasm. The terminal loop region from pre-miRNA is cleaved by a canonical Dicer enzyme to create a mature ~22 bp miRNA duplex (Kim, 2005). Dicer enzyme has a so-called PAZ (Piwi/Argonaute/Zwille) domain and a RNase III domain (MacRae et al., 2006). PAZ domain specializes in binding to the dsRNA whereas RNase III domain specializes in cleavage. The double stranded products of the Dicer enzyme cleavage assemble in RNA-induced silencing complex (RISC). In this pathway, the duplex interacts with an Argonaute family protein, Ago effector protein (Meister and Tuschi, 2004). The

duplex is unwound and one of the two strands- the so-called 'guide strand' stably binds to the Ago protein. The other strand- the so-called 'passenger strand' is discarded. The RISC complex is directed to target by Watson-Crick base pairing by the guide strand.

Dicer, Ago and miRNA associate with a variety of mammalian proteins. A mammalian protein called GW182 is believed to associate itself with the Ago protein (Liu et al., 2005; Meister et al., 2005). This association is essential for the miRNA bound Ago to silence gene expression (Eulalio et al., 2008; Liu et al., 2005). Post-transcriptional repression by miRNA begins when miRNA acts as an adaptor to the miRISC complex and directs it to regulate specific mRNAs. Usually the miRNA-binding sites in mammalian mRNAs lie in the 3'UTR region and are generally present in multiple repeats. Most miRNAs bind to the respective mRNA through Watson-Crick base pairing through the miRNA nucleotides 2-8 which is termed as the 'seed region'. The degree of complementarity between miRNA-mRNA is an important determinant of regulatory mechanism. The mechanism by which miRISC regulates gene expression is a topic of on-going debate. One hypothesis suggests that the mechanism of repression acts upon the preinitiation of transcription i.e. before the recognition of mRNA 5' cap by transcriptional subunit eIF4E (Humphreys et al., 2005; Pillai et al., 2005). Whereas some believe that it happens postinitiation (Maroney et al., 2006). Another study suggests plausible mechanism by which miRISC regulates gene expression by causing premature ribosome dissociation during elongation of translation (Petersen et al., 2006).

Some studies on mammalian miRNA targeted gene regulation indicate that translational repression is not followed by mRNA degradation. However, in most miRNA-mediated gene regulation there is significant mRNA degradation (Bagga et al., 2005; Behm-Ansmant et al., 2006). mRNA is not degraded due to Ago-mediated cleavage, but rather due to deadenylation, decapping and exonuclease mediated digestion of mRNA (Behm-Ansmant et al., 2006). The abundance, type and

positions of mismatches within the miRNA/mRNA duplex can also play a crucial role in triggering degradation or translational repression (Aleman et al., 2007).

1.5 Base Excision Repair

Base excision repair (BER) is a key repair mechanism which is responsible for repairing thousands of DNA base lesions and thus maintaining genome integrity and thus prevent cancer and many other human diseases (Dianov and Hübscher, 2013). Mammalian genome is exposed to several endogenous and exogenous factors which have a potential to cause DNA lesions. DNA lesions arise due to intrinsic chemical instability of the DNA molecule in the cellular microenvironment which results in hydrolytic loss, base oxidations, mismatches and other chemical modifications of sugars and bases (Friedberg, 2003; Lindahl, 1993). The major source of endogenous DNA damage is the reactive oxygen species or ROS which is generated by normal cellular metabolism (Bohr, 2002). If this damage is left unrepaired, it encounters DNA replication and transcription giving rise to many mutations (Ensminger et al., 2014). Amongst several strategies to maintain the DNA blue print, BER forms the first line of defense which corrects the lesions caused by oxidative DNA damage and restores genomic stability. Deficiencies in BER is implicated in several human diseases including premature ageing, neurodegeneration and cancer (Bartkova et al., 2005; Lombard et al., 2005; Markkanen et al., 2015). It is estimated that a single human cell has to repair nearly 10,000 to 20,000 DNA lesions every day (Lindahl, 1993). Enzymes involved in the BER pathway recognize the damaged base, remove it and replace it with a new undamaged base. This process of BER is as fast as few minutes per BER reaction (Lan et al., 2004). Majority of BER is accomplished by a so-called 'short-patch' BER and results in removal and replacement of a single nucleotide (Dianov et al., 2000).

1.5.1 Mechanism of BER

The BER pathway is well studied and the entire BER process is reconstituted in cell-free assays using purified recombinant proteins (Dianov and Lindahl, 1994). The first step in BER is recognition of damaged DNA base by a damage specific DNA glycosylase followed by cleavage of the N-glycosylic bond between the base and the sugar moiety (Lindahl, 1979). The resulting abasic site, also called as apurinic/apyrimidinic site or AP site is further processed by an AP endonuclease- APE1. APE1 cleaves the phosphodiester bond at the 5' of AP site thereby generating a single strand break (SSB) or a nick or gap. This gap has a 3' hydroxyl group and a 5' deoxyribose phosphate. In this canonical pathway of BER, ligation of SSB is prevented by the 5' phosphate group which is eventually removed by AP-lyase activity of DNA polymerase β (Matsumoto and Kim, 1995). DNA polymerase β then fills the gap with an undamaged nucleotide and XRCC-1 and ligase III complex seals the ends.

However, the canonical short-patch BER pathway faces hindrances in the absence of 5' phosphate and 3' hydroxyl group. During the removal of damaged nucleotide, certain DNA glycosylases remove the base and also cleave the phosphodiester bond 3' to the gap to generate a gap with 3'-α,β-unsaturated aldehyde (Boiteux and Radicella, 2000) whereas another glycosylase called- Neil DNA glycosylase leaves a 3' phosphate end (Wiederhold et al., 2004). Sometimes there is direct damage to the sugar residues or endogenous oxidative metabolism may generate SSBs with modified 5' or 3' ends. Moreover, there are many other types of modified SSBs which are generated due to the abortive action of DNA ligase or DNA topoisomerase I or II (Ledesma et al., 2009). These non-canonical SSB blocks are cleaned up by specific enzymes and are prepared for DNA repair by short-patch BER. The five enzymes are – 1. Polymerase β, which removes the 5' phosphate group; 2. APE-1 which removes 3' phosphate groups; 3. Aprataxin cleans 5' termini

blocked by abortive action of DNA ligases; 4. tyrosyl DNA phosphodiesterase 1 (TDP1) which cleans SSBs generated by abortive DNA topoisomerase reactions; 5. Polynucleotide Kinase Phosphatase (PNKP) which dephosphorylates 3' ends and phosphorylates 5' ends (Dianov and Hübscher, 2013). These end processing enzymes convert the blocked ends to generate SSB or a gap with 5' phosphate and 3' hydroxyl group which is filled by DNA polymerase β and sealed by XRCC1-DNA Ligase III complex.

The entire process of BER is highly coordinated and occurs within a short span of time. Several co-immunoprecipitation experiments and studies on yeast two hybrid systems have lead the researchers to believe that BER process follows a *'passing the baton'* model (Wilson and Kunkel, 2000). In this model one enzyme performs its function and passes on the substrate to the next enzyme in a coordinated manner **(Figure 1.5)**. For instance, an oxidized base lesion would be passed from DNA glycosylase to APE1, followed by polymerase β and finally to XRCC1 and DNA ligase III. Several studies in the past indicated that the process of BER is accomplished by preassembled DNA repair protein complexes (Akbari et al., 2004; Caldecott, 2003). However, later it was clear that BER is a continuous process in which depending on the type of base lesion, different DNA glycosylases perform a high-speed scanning of the DNA and remove the damaged base resulting in an AP site. DNA glycosylases function independent of other BER enzymes and without the nucleation of BER complexes (Qi et al., 2012; Zharkov et al., 2010). Other end processing enzymes process this AP site followed by DNA polymerase β and XRCC1-Ligase III function. Polymerase β, XRCC1 and Ligase III form a complex at the DNA damage site. All the BER complexes recovered from the damage sites have polymerase β, XRCC1 and Ligase III along with damage specific proteins (Parsons et al., 2005).

Tumor suppressor p53 has an important function in coordination of BER (Offer et al., 1999). Both cell free extracts-based *in vitro* studies and *in vivo* studies suggest that p53 is indispensable for BER and its downregulation significantly impairs BER (Seo et al., 2002; Zhou et al., 2001). Recent studies have also shown that absence of p53 leads to accumulation of APE1 enzyme and ultimately lead to more DNA breaks (Poletto et al., 2016).
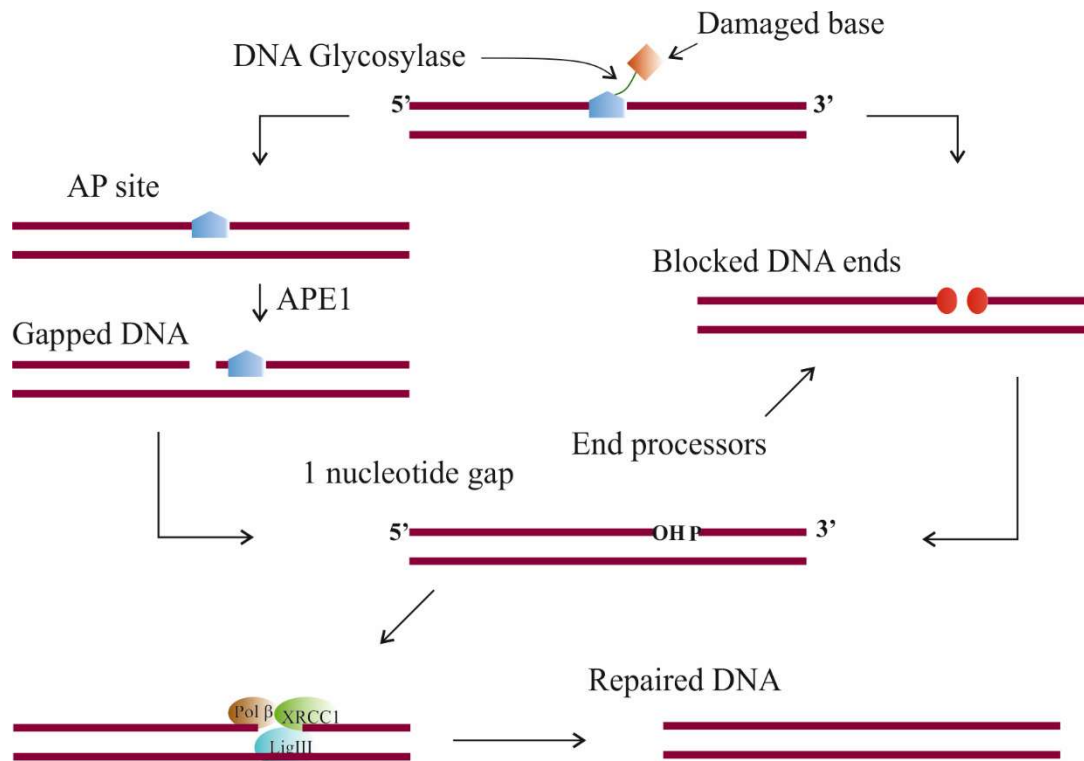
Figure 1.5. Scheme for major base excision repair pathway- short patch BER. Damaged base is removed by DNA glycosylase. Direct chemical modifications may lead to blocked DNA ends which are processed by end processing enzymes like Aprataxin and PNKP (on the right). APE1 processes the damaged site giving rise to a gapped DNA which is a substrate for Pol β (on the left). This gapped DNA is repaired by Pol β, XRCC1 and Lig III.

1.5.2 Regulation of BER

BER activity mainly takes place in G1 phase of the cell cycle where it maintains error-free transcription activity and prepares DNA for replication. However, if the DNA base damage is not

repaired during this time, then an independent backup mechanism called translesion DNA synthesis (TLS) assures genome integrity through different polymerases. Different polymerases involved in maintaining BER function in humans are polymerase β, polymerase λ which performs BER activity in mitochondrial DNA, polymerases δ and ε which are involved in long patch BER and polymerases ι and θ which have been reported to have AP lyase function (Dianov and Hübscher, 2013). These six polymerases have a potential BER function and maintain a reliable backup repair process to ensure genome integrity. However, if the SSBs are left unrepaired, they are encountered by the replication fork and are converted to double strand breaks (DSBs) (Kuzminov, 2001). These DSBs are then repaired by non-homologous end joining (NHEJ) and homologous recombination (HR) mechanisms. However, NHEJ and HR apparently do not have backup efficiency to maintain stable genome integrity as mice deficient in polymerase β, XRCC1 or DNA ligase III cannot survive and succumb to early embryonic lethality (Gao et al., 2011; Sobol et al., 1996; Tebbs et al., 2003). Moreover, even haploinsufficiency of polymerase β results in significant impairment of genome integrity and increase in DNA damage (Cabelof, 2012).

The function of BER process is controlled by steady-state levels of BER enzymes rather than switching the pathway on or off. This steady-state level depends upon the amount of endogenous DNA damage which in turn depend upon the cell type and physiological state of the cell like hypoxia, hypothermia or inflammation. Excess amount of BER proteins are subject to proteasomal degradation. This degradation of excess BER proteins is carried out by two E3 ubiquitin ligases-Mule and CHIP. Mule monoubiquitylates nonessential BER proteins followed by CHIP mediated extension of ubiquitin chain and proteasomal degradation (Parsons et al., 2008). Mule activity is in turn controlled by arthritis rheumatic fever (ARF) protein which accumulates in the cell upon

DNA damage (Khan et al., 2004). ARF binds to Mule and inhibits its activity thereby preventing the degradation of BER enzymes (Chen et al., 2005).

Recent studies have also shown that BER is regulated by microRNAs. Human uracil DNA glycosylase (UNG2) is a glycosylase which removes uracil residues from the DNA. Studies have shown that UNG2 is a direct target of miR-16, miR-34c and miR-199a (Hegre et al., 2013). A recent study has shown that DNA polymerase β, the prime gap filling polymerase is a direct target of miR-499 (Wang et al., 2015). miR-499 has a single binding site in the 3'UTR of polymerase β mRNA. This study has shown that miR-499 facilitates polymerase β degradation by binding to the 3'UTR region of polymerase β mRNA and thereby sensitizes esophageal carcinoma cells to cisplatin treatment (Wang et al., 2015).

1.6 AIM OF THIS WORK

Ovarian cancer is associated with many different microbial signatures, HHV-6 and *Chlamydia* being the two important of the few. HHV-6 was thought to be a benign virus which caused rash-like symptoms in early life. Recent studies have shown the detrimental effects of reactivation of chromosomally integrated HHV-6 (ciHHV-6). However, the mechanism by which ciHHV-6 reactivation may lead to oncogenesis is not yet clearly studied. Many different mechanisms have been proposed for *Chlamydia* mediated transformation of the cell. These are mainly focused on signaling pathway mediated malfunctioning. Previous research from our department has shown that *C. trachomatis* can reactivate ciHHV-6. Therefore, it was of prime importance to understand how *C. trachomatis*, HHV-6 or reactivation of ciHHV-6 can play a role in transformation of cell.

The present study aims to understand the molecular mechanism through which the two pathogens would bring about transformation by modulating the host genome integrity. In the first part of the study, integration of ciHHV-6 has been investigated by focusing on the nature of direct repeat (DR) sequences in the HHV-6 genome. The DR sequences were analyzed for their copy number and their integration sites within human chromosomes. Sequencing of the integration sites revealed unstable and unusual characteristic of DR repeat sequences implicating their plausible role in oncogenesis.

C. trachomatis causes ROS mediated DNA damage and DNA double strand breaks (DSBs). However, ROS also primarily causes single strand breaks (SSBs) which when left unrepaired cause DSBs. The mechanism which repairs SSBs is base excision repair (BER). Hence, in the second part of the study, the effect of *C. trachomatis* on BER capacity of host cell was investigated. A mechanism is suggested through which *Chlamydia* may bring about this effect on BER. This

mechanism is further empirically addressed. Effect of *C. trachomatis* on epigenetic makeup and telomere length has also been briefly investigated.

Based on these two studies, this present work has put forth a hypothesis to understand how *C. trachomatis* and HHV-6 independently or inter-dependently play a role in ovarian cell transformation and may initiate the onset of ovarian cancer.

2. MATERIALS

2.1 Cell lines

Cell line	Origin/Characteristic	Growth medium
HOSE (Human ovarian surface epithelial)	Primary Human ovarian surface epithelial cells	Ovarian surface epithelial (OSE) cell culture medium + 10% growth supplement
HeLa 229	Human cervical carcinoma epithelial cells	RPMI 1640 + 10% Fetal bovine serum (FBS)
SKOV-3	Human ovarian carcinoma epithelial cells	DMEM F12 + 10% Fetal bovine serum (FBS)
HUVECs (Human umbilical vein endothelial)	Primary Human umbilical vein endothelial cells	Medium 200 + 10% Low serum growth supplement
H1299	Human lung carcinoma cell with homozygous partial deletion in *TP53* gene	RPMI 1640 + 10% Fetal bovine serum (FBS)

2.2 Cell Culture Medium and Buffers

Medium/Buffer	Source
Primary OSE medium	ScienCell Research Laboratories, California, US
RPMI 1640	GIBCO Brl, Germany
Medium 200	GIBCO Brl, Germany
DMEM F12	GIBCO Brl, Germany
OPTIMEM (for transfection)	GIBCO Brl, Germany
Freezing media	90% heat inactivated FBS + 10% DMSO
SPG buffer (for C. trachomatis stock preparation)	0.22 M sucrose, 10 mM Na_2HPO_4, 3.8 KH_2PO_4, 5 mM glutamate

Polyethyleneimine (PEI) stock solution for transfection	Dissolve PEI powder to a concentration of 2 mg/ml in deionized water. Heat at 80°C for 10 min. Allow solution to cool to room temperature (RT). Adjust pH to 7.0 with 5 M HCl. Sterilize through 0.2 µ filters. Freeze aliquots at -20°C

2.3 Bacterial Strains

E. coli DH5α	Hanahan, 1983
C. trachomatis L2	ATCC

2.4 Antibodies

Antibody	Host	Dilution	Company
Primary antibodies			
anti-polymerase β	polyclonal rabbit	1:1000	Abcam
anti-APE1	polyclonal rabbit	1:1000	Novus Biologicals
anti-p53	monoclonal mouse	1:1000	Santa Cruz
anti-actin	monoclonal mouse	1:2000	Santa Cruz
anti-CPAF	monoclonal mouse	1:500	Generous gift from Guangming Zhong
anti-HSP60 (*C. trachomatis*)	monoclonal mouse	1:1000	Santa Cruz
anti-cytokeratin8	monoclonal mouse	1:1000	Santa Cruz
Secondary antibodies			
Anti-rabbit IgG HRP-linked	Goat	1:5000	Santa Cruz
Anti-mouse IgG HRP-linked	Goat	1:5000	Santa Cruz

2.5 Buffers for SDS-PAGE and Western Blot

Buffers	Ingredients
10 x SDS buffer (/L)	30.275 g Tris, 144 g glycine, 10 g SDS
10x TBS (/L)	60.5 g Tris, 87.6 g NaCl, adjust to pH 7.5 with HCl
TBST20	1 x TBS + 0.5% (v/v) Tween20
Blocking solution	TBST20 + 5% (w/v) dry milk powder
Stripping buffer (500 ml)	Catalog no#46430 Thermo Scientific
2x Laemmli buffer	100 mM Tris/HCl [pH 6.8], 20% (v/v) glycerol, 4% (w/v) SDS, 1.5% (v/v) 2-mercaptoethanol, bromophenol blue
10% SDS Resolving gel solution	For 10 ml: 4.15 ml H2O, 3.38 ml 30% (v/v) acrylamide: bisacrylamide mix (37.5:1), 2.5 ml 10% (w/v) SDS, 2.5 ml, 1.5 M Tris/HCl [pH 8.8], 0.1 ml 10% APS, 4 µl TEMED
SDS Stacking gel solution	For 5 ml: 3.4 ml H2O, 0.83 ml 30% (v/v) acrylamide: bisacrylamide mix (37.5:1), 0.63 ml 1.0 M Tris/HCl [pH 6.8], 0.1 ml 10% (w/v) SDS, 0.05 ml 10% APS, 5 µl TEMED
10x Semi-Dry Transfer buffer (/L)	24 g Tris, 113 g glycine, 2 g SDS in 1 L deionized H_2O [pH 7.4]
1x Semi-Dry Transfer buffer	1x semi dry buffer [800 ml] + 20% (v/v) methanol [200 ml]
ECL solution 1	100 mM Tris HCl pH 8.5, 2.5 mM Luminol, 0.4 mM p-coumaric acid
ECL solution 2	100 mM Tris HCl pH 8.5, 0.02 % H2O2

2.6 Buffers for Comet Assay

Buffers	Ingredients
Lysing Solution	2.5 M NaCl, 100 mM EDTA, 10 mM Tris base [pH 10] Freshly add 1% Triton-X 100 and 10% DMSO. Refrigerate 30 min before use.
Electrophoresis Buffer	300 mM NaOH, 1 mM EDTA
Neutralization Buffer	0.4 M Tris [pH 7.5]
Staining Solution	Ethidium Bromide (EtBr; 10X Stock - 20 µg/mL)

2.7 Buffers for Nuclear extract preparation

Buffers	Ingredients
Buffer A	20 mM HEPES [pH 7.6], 20% [v/v] glycerol, 10 mM NaCl, 1.5 mM MgCl$_2$, 0.2 mM EDTA, 1 mM DTT, 0.1% Triton X-100, 100 mM phenyl methyl sulfonyl fluoride (PMSF), 2 µg/ml leupeptin and 10 µg/ml Aproteinin
Buffer B	20 mM HEPES [pH 7.6], 25% [v/v] glycerol, 500 mM NaCl, 1.5 mM MgCl$_2$, 0.2 mM EDTA, 1 mM DTT, 0.1% Triton X-100, 100 mM PMSF, 2 µg/ml leupeptin and 10 µg/ml Aproteinin

2.8 Buffers for Fluorescence *in situ* hybridization (FISH)

Buffers	Ingredients
20X SSC Buffer	3 M NaCl, 0.3 M Trisodium citrate (Na$_3$C$_6$H$_5$O$_7$), 1 L H$_2$O [pH 7.0] Autoclaved and stored at RT.
2X SSC Buffer + T20	100 ml 20X SSC + 900 ml H$_2$O + 1 ml Tween 20
0.5 X SSC Buffer + T20	25 ml 20X SSC + 900 ml H$_2$O + 1 ml Tween 20
Hybridization Buffer	70 µl formamide + 0.5 µl 1 M Tris [pH 7.5] + 5 µl 10% Blocking solution (Roche) +4.5 µl H$_2$O + 20 µl labelled probe
10X PBS	NaCl 1.37 M, KCl 27 mM, Na$_2$HPO$_4$ 100 mM, KH$_2$PO$_4$ 18 mM H$_2$O add 1 L

2.9 Buffers for Southern Blotting

Buffers	Ingredients
2.5X DNA Denaturing Buffer	1.5 M NaCl, 0.5 M NaOH
1X DNA Neutralizing Buffer	3 M NaCl, 0.5 M Tris, 0.3 M Trisodium citrate (Na$_3$C$_6$H$_5$O$_7$) [pH 7.0]
20X SSC Solution	3M NaCl, 0.3M Trisodium citrate [pH 7.0]
Hybridization Buffer	ULTRAhyb™ Ultrasensitive Hybridization Buffer- Thermo Scientific

2.10 Buffers for Repair Assay

Buffers	Ingredients
10X Annealing Buffer	100 mM Tris-Cl [pH 7.5], 500 mM NaCl, 10 mM EDTA, Sterilize through 0.22 μ filter
10X Repair Assay Buffer	500 mM HEPES [pH 7.5], 200 mM KCl, 10 mM EDTA, 20 mM DTT, Sterilize through 0.22 μ filter
2X Urea Stop buffer	8 M Urea, 0.5 M EDTA, 1M Tris-Cl [pH 7.5], 0.2% xylene cynol and 0.2% bromophenol blue
5X TBE	0.5 M Tris, 0.5 M Boric acid, 0.01 M EDTA

2.11 Oligonucleotides

Oligonucleotides	Sequence (5'-3')
Parent Y (P2)	TACTAGGTAGCACGAGGCACTATATCAGGTAACTTCGATTCACGACTGCAGTCTA
Oligo A (A)	TAGACTGCAGTCGTGAATCGAAGTTACCTG
Oligo B (B)	[Phos] TATAGTGCCTCGTGCTACCTAGTA
Parent X (P1)	TCGAGTCCATAAAGTAGTATACGCTACGCTGACCAAGCACGAGGCACTATAGATTCACGACTGC
Oligo 1 (X1)	GCAGTCGTGAAT
Oligo 2 (X2)	[Phos] TATAGTGCCTCGTGCT
Oligo 3 (X3)	[Phos] GGTCAGCGTAGCGTATACT
Oligo 4 (X4)	[Phos] CTTTATGGACTCGA

2.12 Primers for Polymerase β study

Oligonucleotides	Sequence (5'-3')
miR-499 Forward + Reverse	Custom synthesized (Exiqon)
5S rRNA Forward + Reverse	Custom synthesized (Exiqon)
U6 snRNA Forward + Reverse	Custom synthesized (Exiqon)
Polymerase β 3'UTR Forward	ATATCTCGAGTGTATCCTCCCT
Polymerase β 3'UTR Reverse	ACGTCGCCGGCGTAATAGTACATGAGGTT

2.13 Oligonucleotides for Polymerase β study

Polymerase β siRNA	ON-TARGETplus SMARTpool POLB siRNA	Dharmacon L-005164-00-0005
p53 siRNA	ON-TARGETplus Human TP53 siRNA	Dharmacon L-003329-00-0005
miR-499 Inhibitor	Anti-hsa-miR-499a-5p miScript miRNA Inhibitor MIMAT0002870: 5'UUAAGACUUGCAGUGAUGUUU	Qiagen MIN0002870
miR-499 Mimic	Syn-hsa-miR-499a-5p miScript miRNA Mimic MIMAT0002870: 5'UUAAGACUUGCAGUGAUGUUU	Qiagen MSY0002870

2.14 Primers for HHV-6 study

Oligonucleotides	Sequence (5'-3')
Primer pair 1 (DR6)	For- CCGGCGATTCCCGGAGATGC Rev- CCGCGTGATTGAAGGGTGA
Primer pair 2 (DR7)	For- ATGTAACCAACTCCCAGCTCGAC Rev- GTTGGTACGTTTCCCACAGTCGT
Primer pair 3 (U22)	For- GGATCCAAAGCAAACCAGCAAGA Rev- TGGCGGATGGCTAGTGTGCC
Primer pair 4 (U42)	For- AGTTAGTTTCACAGGTGTCAGC Rev- ACCGAAATCTTTCTTTTACTTGTC
Primer pair 5 (U79)	For- AATGGGTTCTCTAACGGTGGAT Rev- ATTCATCATGTTGTTGATCTTCGTG
Primer pair 6 (U91)	For- CGTTAAAGATACTGGCATGTCT Rev- TAAAGTCTCTACTGAAGAAGCA
Primer pair 7 (U94)	For- ACGGGGACGTGCTAATCCAT Rev- TCCGGGTGGACCGATAAAAC
Primer pair 8 (U83)	For- TATGTAGTTCCCCCGATGCG Rev- TCTGTTTTCCCAGGTACGGC
Primer pair 9 (DR$_L$ junction)	For- GCACAACCCACCCATGTGGTAGTCGCGG Rev- TTCCATCGGTTCTTCGCGCTCAC
Primer pair 10 (DR$_R$ junction)	For- CTACTCACCTCTGAGGCACT Rev- GGATTTGACGTAATTTTTAAAACGC
DR$_L$ Inverse PCR Forward	TTGGTTTCCCTCAGGGTTCG
DR$_L$ Inverse PCR Reverse 1	CCGTTAGCGGCATCCTAGAG
DR$_L$ Inverse PCR Reverse 2	TGCCCGGCACGCACCGTTAG
DR$_R$ Inverse PCR Forward	GCACAACCCACCCATGTGGTAGTCGCGG

DR$_R$ Inverse PCR Reverse	CGTGTGTACGCGTCCGTGGTAGAAACGCG
DR$_R$ Inverse PCR Nested Forward	TGGGTACGTAGATGGGGCAT
DR$_R$ Inverse PCR Nested Reverse	GTGACAACGGATTACGGAGGT
Viral DR Forward (for FISH probe)	For- AGGAACAGACAGACGGCCAC
Viral DR Reverse (for FISH probe)	Rev- CTCTGCGGGGATTCACGGAT
HHV-6A DR	For- CCGGCGATTCCCGGAGATGC
	Rev- CCGCGTGATTGAAGGGTGA
HHV-6B DR	For- AAACCCTACCATCCTTCGGC
	Rev- GGGACGATCCCGTTAACCAA
PI15	For GGCGGAAGCGCTACATTCGCA
	Rev TATTCCATATTTGCTGCCGGTGGGA

2.15 Commercial kits

RNA Isolation	miRNeasy micro kit	Qiagen
cDNA synthesis	Revertaid First strand cDNA synthesis kit	Thermo Scientific
miRNA cDNA synthesis and qPCR	miRCURY LNA™ Universal RT microRNA PCR	Exiqon
Plasmid Mini-prep	NucleoSpin® Plasmid QuickPure	Macherey Nagel
Plasmid Midi-prep	NucleoBond® PC 100	Macherey Nagel
Pulsed Field Gel Electrophoresis	CHEF Genomic DNA Plug Kits	Bio-Rad
FISH probe labelling kit	PromoFluor-550 Nick Translation Labeling Kit	Promokine
Luciferase assay	Dual-Glo® Luciferase Assay System (E2920)	Promega
TA Cloning	TOPO PCR 2.1 cloning kit	Life technologies

2.16 Fine Chemicals

Hydrogen Peroxide	Sigma Aldrich (H1009-100ml)
Progesterone	Sigma Aldrich (P8783-1G)
Clasto-lactacystin	Sigma Aldrich (L7035-.1MG)
DAPI	Sigma Aldrich (D9542-5MG)
Hiperfect (Transfection reagent)	Qiagen (301705)
Complete Protease Inhibitor	Roche
Histopaque 1077	Sigma Aldrich (10771)

2.17 Consumables

Culture plates, disposable pipettes, pipette tips, cryotubes and reaction tubes	Sarstedt (Nümbrecht)
Culture dishes, flasks, 15 ml and 50 ml reaction tubes, well plates, medium bottles and filters for sterile filtration	Corning, USA
PVDF membrane for immunoblotting	GE Healthcare
Nylon membrane for southern blotting- Amersham Hybond-XL	GE Healthcare
Blotting paper	Hartenstein (Würzburg)
All other consumables	Sigma (St. Louis, USA), VWR (Radnor, USA) and Hartenstein (Würzburg)

2.18 Technical Equipment

1000/500 Constant Voltage Power Supply	Bio-Rad
Table top Centrifuge 5417R	Eppendorf
BD FACSAria™ III Cell Sorter	BD Biosciences
DMIRB Inverted Fluorescence Microscope	Leica

Electronic balance ABS 80-4	Kern
Heracell™ 240i incubator	Thermo Fisher Scientific
Heraeus Megafuge 1.0R	Thermo Fisher Scientific
HERAsafe® sterile hood	Thermo Fisher Scientific
Infinite® M200 Multimode microplate reader	Tecan
NanoDrop 1000 spectrophotometer	Peqlab Biotechnology
OptimaTM L-80 XP ultracentrifuge	Beckman Coulter
Owl™ Separation HEP-1 Semi Dry Electroblotting System	Thermo Fisher Scientific
Invitrogen™ Mini Gel Tank (for SDS-PAGE)	Invitrogen
Thermal cycler GS1	G-Storm
Typhoon 9200 Imager	GE Healthcare
Ultrapure Water Systems	Merck Millipore
DRII Pulsed field apparatus	Bio-Rad

3. METHODS

3.1 Cell Biology techniques

3.1.1 Cell culture methods

Maintenance of adherent cell lines- All cell lines were cultivated at a humid micro-environment at 37 °C with 5% CO_2. HeLa 229 and H1299 were maintained in RPMI 1640 medium (GIBCO) with 10% FCS (GIBCO). SKOV-3 cells were maintained in DMEM F12 medium (GIBCO) with 10% FCS. U2OS cells were maintained in McCoy's 5A medium with 10% FCS. Primary human umbilical cord endothelial cells (HUVEC) were maintained in Medium 200 (GIBCO) with low serum growth supplement (LSGS) provided by the manufacturer (GIBCO). Primary human foreskin fibroblasts (HFF) were maintained in primary cell culture medium (ATCC) with the supplied growth supplements (ATCC). Primary human ovarian surface epithelial (HOSE) cells were maintained in ovarian epithelial cell culture medium -OEpiCM (ScienCell) with the supplied serum growth supplement.

All the media and buffers used to maintain cell lines were sterile and handled only in sterile conditions. The monolayer of adherent cells in a cell culture flask was washed with 1X PBS pre-warmed at 37 °C. 1-2 ml of Trypsin/EDTA (GIBCO) was added on the washed monolayer and the flask was incubated at 37 °C for 2-5 min to detach the cells. The detached cells were flushed with medium containing FCS (as FCS stops trypsin activity) and required number of cells were seeded back in the flask and supplied with fresh medium. For seeding in well plates, the cells were diluted accordingly in a falcon tube before seeding.

Freezing cell lines- For freezing, the cells were trypsinized as described earlier. Complete medium was used to detach the cells and collect them in a falcon tube. The cells were centrifuged at 800 g

for 10 min at room temperature. The supernatant was discarded and the resultant pellet was resuspended in (1ml/10^6 cells) freezing medium (90% FCS + 10% DMSO). The cells were immediately aliquoted in labelled cryotubes and placed in freezing containers filled with isopropanol to ensure a slow and gentle cooling process (-1 °C/min) and frozen at -80 °C for 24 h after which they were transferred in liquid nitrogen.

3.1.2 Fluorescence *in situ* hybridization (FISH)

Cell preparation- The adherent cells were arrested in metaphase by treating them with Colcemid (Sigma-Aldrich). Colcemid was added in the concentration of 1 μg per 10 ml of medium to cell monolayer in a standard T-75 flask (10 μl per 10 ml medium) for 4 h at 37 °C. The cells were mildly trypsinized. The trypsinized cells were collected in a falcon in fresh medium and the centrifuged at 180 g for 10 min at room temperature. The supernatant was discarded and the pellet was gently washed with 1X PBS by centrifuging at 180 g for 10 min followed by discarding the supernatant. The pellet was then dislodged by gentle flicking and was resuspended in 1 ml of 0.075 M KCl (pre-warmed at 37 °C). To this, 9 ml of warm 0.075 M KCl was added dropwise and the tube was incubated at room temperature for 15 min. The tube was centrifuged at 180 g for 10 min at room temperature. The supernatant was removed using a pipette and the pellet was dislodged by gentle flicking. The cells were resuspended in 1 ml of fixative (methanol: glacial acetic acid - 3:1) precooled at -20°C. To this, 9 ml of cold fixative was added dropwise and care was taken that the cells do not form clumps. The cells were incubated at -20 °C for at least 1 h. The cells were then centrifuged at 180 g for 10 min and the supernatant was removed using pipette. The pellet was dislodged by gentle flicking and 10 ml of cold fixative was added dropwise so as to not form any clumps. The cells were centrifuged again at 180 g for 10 min at room temperature and this

washing step was repeated 2 more times. Finally, the pellet was resuspended in 1 ml of fresh cold fixative and the cells were stored in a screw cap tube at 4 °C until further use.

Metaphase chromosome slide preparation- For slide preparation, the slides were cleaned on both the sides with a clean tissue paper and incubated in cold fixative in Coplin jars and incubated at -20 °C until further use. The slides were then removed from the jar and kept on a flat surface. Roughly 50 to 100 µl of cells were dropped from a height of about 1-2 feet on these slides. The slides were immediately incubated at 37 °C on a heat block with wet tissue paper stacks on it. Heat aids in bursting open the cells and humidity prevents the cells from drying prior to bursting. Later, the slides were carefully dried and used immediately or stored in a closed box until required.

Fluorescent probe preparation- The HHV-6 fluorescent probe was prepared using PCR amplified fragments of different HHV-6 ORFs. The primer sequences used to amplify these regions are mentioned in the materials section. The amplified products were purified using the MN PCR purification kit and were pooled together to a final concentration of 1 µg. The amplified products were labelled with the fluorophore by nick translation using the PromoFluor-500 Nick Translation Labeling Kit (PromoCell GmBH). The following reaction components were added in an Eppendorf tube and incubated at 15 °C for 90 min.

10x NT labeling buffer	2 µl
PromoFluor-500 NT labeling mix	2 µl
Template DNA	1-1.5 µg
10x Enzyme mix	2 µl
PCR-grade water	Fill up to 20 µl

The reaction was stopped by adding 5 µl of stop buffer incubating for 5 min at room temperature. The fluorescent probe was then stored at -20 °C or used directly by diluting the probe to a final volume of 50 µl.

The fluorescent probe was then denatured before using in the hybridization reaction. The denaturation reaction was carried out as follows:

Formamide	70 µl
1 M Tris-Cl pH= 7.5	0.5 µl
Fluorescently Labelled Probe	20 µl
10% Blocking solution (Roche)	5 µl
PCR-grade water	Fill up to 100 µl

The reaction components were boiled at 95 °C for 5 min. After boiling, 20 µl of the probe was directly used on one slide for *in situ* hybridization.

In situ hybridization- All the hybridization steps were carried out in Coplin jars unless otherwise specified. The slides were washed with 1X PBS for 5 min to remove any dust on the surface. Further, the slides were fixed in 3.7% formaldehyde for 10 min at room temperature. They were washed thrice with 1X PBS at room temperature for 10 min each. The chromosomes were dehydrated by treating them with 70%, 85% and 100% ethanol in a sequential manner. The slides were taken out of the jars and air-dried. The slides were treated with Pepsin prewarmed at 45 °C for 30 min and incubated at 37 °C in a moist chamber. After incubation, the slides with washed again in a Coplin jar with 1X PBS for 5 min. The washing step was repeated twice. After washing, the slides were again fixed with 3.7% formaldehyde similar to the previous step followed by sequential dehydration in 70%, 85% and 100% ethanol. After dehydration, the slides were air dried and 20 µl of hybridization probe (after denaturing at 95 °C) was added and a coverslip was gently

placed on the top and sealed with rubber cement (Fixogum- Marabu). The slides were further incubated at 80 °C for 5 min and then incubated at 37 °C overnight in a moist chamber.

The rubber cement was removed the following day and the slides were gently placed in 1X PBS. The slides were then washed with 2X SSC buffer at room temperature for 5 min. Next, the slides were incubated in 2X SSC with 1 μg/ml DAPI at room temperature to stain the DNA. Following this, the slides were washed with 2X SSC with 0.1% Tween 20 at 65 °C with gentle shaking for 10 min. The slides were further washed with 0.5X SSC with 0.1% Tween 20 at room temperature. The slides were dipped in de-ionized water shortly and then air dried. Later the slides were mounted using a mounting medium (X) and a coverslip was gently placed on the top. The coverslip was sealed using a nail polish. The slides were stored at 4 °C for 16-24 h and then analyzed on an epifluorescence microscope.

3.1.3 Peripheral Blood Mononuclear Cells (PBMC) Isolation

Fresh PBMC were isolated from blood samples using Histopaque 1077 (Sigma Aldrich) solution. The blood was diluted 2 times with sterile 1X PBS. It was layered carefully on 1 volume of Histopaque 1077 solution in a falcon tube. It was centrifuged at 600 g for 30 min at room temperature. The banded PBMC layer were separated and washed twice with sterile 1X PBS. The PBMC pellet was then resuspended in RPMI with 10 % FCS and cultured in the same medium at 37 °C with 5 % CO_2. PBMC were cultured in tissue culture flasks (Corning) for 48 h after which monocytes were separated as they adhered to the flask.

3.1.4 Luciferase Assay

Luciferase assay was performed using the Dual-Glo® Luciferase Assay System kit(Promega) according to manufacturer's instructions. For the assay, cells were lysed in a 6-well plate using Lysis buffer provided in the kit. 500 μl Lysis buffer per well was used for lysis. In a 96-well plate

100 µl dual luciferase reagent (LAR II) per well was pipetted. Later, 20 µl of the lysate was used per well in the 96-well plate. After mixing the samples by pipetting up and down, the luminescence from Firefly luciferase was measured in a microplate reader (Tecan). Later, 100 µl of Stop&Glo reagent was added which quenched Firefly luciferase signal and served as a substrate for Renilla luciferase. After mixing the samples by pipetting up and down, the luminescence from Renilla luciferase was measured in the microplate reader. Firefly luciferase was used as a control for transfection and was normalized in each sample.

3.2 Molecular Biology techniques

3.2.1 Cloning of polymerase β 3'UTR

For cloning, plasmid and amplified fragment of pol β 3'UTR were digested with restriction enzymes from Thermo Scientific. The digestion was carried out at 37 °C overnight. On the next day, the reaction was terminated by diluting in nuclease free water and purifying using Macherey-Nagel purification kits as described in **3.2.2.** Subsequently, the purified plasmid and insert was ligated using T4 DNA ligase at 16 °C overnight and then transformed in competent *E. Coli.* A detailed chart of restriction enzymes and plasmids used in the study is as follows

| PsiCheck 2.0 | NotI | XhoI |
| Polymerase β 3'UTR | NotI | XhoI |

3.2.2 Purification of the DNA fragments from gel blocks or PCR reactions

The DNA fragment excised from the agarose gel or product of a PCR reaction was further purified using Gel-PCR clean up kit (Macherey Nagel). For gel clean up, the gel piece was dissolved in a binding buffer provided in the kit and incubated at 50 °C for 10 min. For PCR clean up, the PCR product (minimum volume of 100 µl) was diluted in twice the volumes of binding buffer. After

dissolving, it (maximum volume 700 µl) was loaded on the purification columns and centrifuged at 11000 g for 30 sec. The flow through was discarded and the columns were washed with the wash buffer (700 µl) provided in the kit. The flow through was discarded again and the washing step was repeated. The columns were dried by centrifuging the them at 11000 g for 1 min and discarding the remaining flow through. The DNA was further eluted by adding 25 µl of nuclease free water on the columns and incubating them at room temperature for 5 min followed by centrifuging them at 11000g for 1 min. The purified fragment was collected and stored at -20 °C until further use.

3.2.3 Agarose gel separation of nucleic acids

Agarose gel electrophoresis is an old technique used to separate nucleic acids DNA and RNA based on their size. DNA is negatively charged owing to the phosphate groups in the sugar-phosphate backbone. This negatively charged DNA migrates according to its size towards anode under an electric field. Shorter DNA fragments migrate faster than the larger fragments. Agarose matrix is used to separate the nucleic acids. Agarose solution (0.8-1 %) was made by boiling the agar powder in 1X TBE buffer in a microwave. After cooling the agarose solution to about 50 °C, an intercalating agent like ethidium bromide (EtBr) was added at a final concentration of 0.5 µg/ml which intercalates the DNA and makes it visible under ultra violet light (λ =300 nm). The DNA was visualized in a gel documentation system. For cutting out the desired bands, the gel was visualized in a preparatory mode and the desired band was excised using a clean scalpel in an Eppendorf tube.

3.2.4 Alkaline Comet Assay

Alkaline comet assay was performed on the nuclei isolated from uninfected and infected cells. Nuclei were isolated at resting condition, in 200 µM H_2O_2 stress and 16 h post stress in order to study repair.

Slide preparation- Slides for the assay were prepared by coating 1% normal melting agarose (NMA) on glass slides. Briefly, 500 µl of NMA maintained at 45 $^{\circ}$C was gently added on the slide followed by placing a coverslip gently to obtain an even flat surface. The slides were incubated at 4 $^{\circ}$C for 15 min to allow the agar to set and the coverslip was removed. Subsequently, the nuclei, resuspended in 25 µl 1X PBS, were diluted with 75 µl of 0.5% low melting agarose (LMA) and immediately added on the coated glass slide followed by placing a coverslip to obtain a flat surface. The slides were incubated in 4 $^{\circ}$C for 15 min and further were processed for comet assay.

Comet assay- The slides were gently dipped in freshly prepared precooled lysing solution for at least 2 hrs at 4 $^{\circ}$C. Subsequently, the slides were immersed in alkaline electrophoresis buffer pH>13 in the electrophoresis chamber for 20 min at 4 $^{\circ}$C to allow unwinding of DNA. Finally, the electrophoresis was carried out at 0.6 V/cm for 30 min. After electrophoresis, the slides were rinsed in neutralization buffer three times for 5 min each. The slides were stained in DAPI and later scored in an epifluorescence microscope.

Analysis- The percentage tail DNA was calculated using an ImageJ macro 'OpenComet' (Gyori et al., 2014) using the default settings. At least 30 nuclei were scored for each type of treatment and 3 independent experiments were performed similarly.

3.2.5 Nuclear Extract Preparation

Nuclei were isolated using a modified protocol published by Riol *et al* (Riol et al., 1999). The cells were trypsinized and washed once with cold 1X PBS. The cell pellet was resuspended in Nuclear Buffer A, gently mixed by pipetting for 2-5 times and incubated on ice for 15 min. After incubation, the lysates were centrifuged at 850 g for 15 min in a precooled centrifuge at 4 °C. The supernatant was labelled as cytoplasmic fraction and stored separately at -80 °C. The nuclear pellet was washed once more with Nuclear Buffer A. The resultant pellet was resuspended in Nuclear Buffer B and mixed thoroughly by tapping the tube. The tubes were incubated on ice for 1 h and gently tap mixed every 10 min. The nuclear extract was centrifuged in a precooled centrifuge at 18000 g for 15 min and the supernatant was labelled as nuclear extract and stored at -80 °C.

3.2.6 *In vitro* Base Excision Repair Assay

Substrate Preparation- Two different substrates, S1 and S2 were utilized for the repair assay. S1 was prepared by annealing parent oligonucleotide P1 with short complimentary oligonucleotides X1, X2, X3 and X4. X1 was end labelled with radioactive P^{32} at 5' end using T4 Polynucleotide Kinase with forward reaction buffer A. Subsequently, the labelled oligonucleotide was separated on a denaturing urea polyacrylamide gel and was cut and purified using phenol and chloroform. The short oligonucleotides were designed in such a way that they produced 3 single nucleotide gaps after annealing. For annealing, P1, X1, X2, X3 and X4 were added in a tube each at a final concentration of 5 µM in 1X annealing buffer and boiled at 95 °C in a water bath for 5 min. The tube was allowed to cool at room temperature overnight. The annealed substrate was purified subsequently using G-25 sepharose columns. For substrate S2, parent oligo P2 was annealed with shorter oligos A and B where oligo A was labelled with radioactive P^{32}. Further steps were similar to substrate S1 preparation.

Base Excision Repair Assay- Base excision repair assay was performed by incubating the annealed substrates with native nuclear lysates at 30 °C for 20 min to 1 h. Post incubation, the reaction was stopped by adding 2 X urea stop buffer and boiling at 95 °C for 5 min. The products were finally separated on a 10 % polyacrylamide 8 M urea denaturing gel. The gel was pre-run for 1 h and the samples were loaded after cleaning the wells. The gel was run at 10 mA for 1 to 2 h till the dye reached 2/3ʳᵈ of the gel. After separation, the gel was wrapped in a plastic saran wrap and exposed overnight to autoradiography phosphor imager film. Subsequently, the film was analyzed using Typhoon phosphor imager (GE Healthcare).

3.2.7 Transfections

siRNA, microRNA inhibitor and mimic- HOSE cells were grown in a monolayer with complete growth medium, OEpiCM (ScienCell). The monolayer was washed once with 1X PBS and supplied with transfection medium, Opti-MEM (Thermo scientific) (400 µl per 1 well of 12 well plate) at least 1 h before transfection. Then, 5 nM stocks of Polymerase β and p53 siRNA and miR-499 inhibitor and mimics were diluted 1:100 in 100 µl of Opti-MEM. To this, 3 µl of transfection reagent Hiperfect (Qiagen) was added and the tube was vortexed mixed. The mixture was incubated at room temperature for 15 min followed by careful dropwise addition on the monolayer of cells. Following day, the monolayer was washed and supplied with complete growth medium, OEpiCM.

Plasmids- p53-HA overexpressing plasmid, dual luciferase reporter plasmid psiCheck 2.0 were transfected using polyethyleneimine (PEI) transfection reagent. Briefly, cells were grown in a monolayer in a complete growth medium. The monolayer was washed once with 1 X PBS and supplied with transfection medium, Opti-MEM (Thermo scientific) (400 µl per 1 well of 12 well plate) at least 1 h before transfection. Plasmids (50 ng for p53-HA and 1 µg for PsiCheck 2.0) and

3 µl of PEI were diluted separately in 100 µl of Opti-MEM. Subsequently, the two dilutions were mixed by vortexing followed by incubation at room temperature for 20 min. The mixture was carefully dropped on the monolayer. Following day, the monolayer was washed and supplied with complete growth medium, OEpiCM.

3.2.8 RNA isolation and cDNA synthesis

RNA isolation for microRNA fraction was carried out using miRNeasy kit (Qiagen) following manufacturer's instructions. 700 µl of phenol containing lysis buffer was directly added on the top of the monolayer of cells in a 12 well plate after removing the medium. The cells were scrapped out and lysed using a filter tip within the well plate. The lysate was collected in an Eppendorf tube and incubated at room temperature for 10 min before proceeding with the manufacturer's RNA isolation protocol. Finally, RNA was eluted in 50 µl RNase free water and was further used for cDNA synthesis.

Post purification, DNA impurities in the RNA fraction were removed using Turbo DNase kit (Ambion) following manufacturer's protocols. 1/10 volume of 10X Buffer and 1 µl of the TurboDNase enzyme was used every 2 µg of RNA and incubated at room temperature for 20-30 min. Following incubation, 1/10th volume of the TurboDNase isolating beads from the kit were added to the tube and incubated further for 5 min at room temperature. After incubation, the tube was centrifuged at 18000 g for 15 min and the DNA free RNA supernatant was collected in a fresh tube and further used for cDNA synthesis reaction.

cDNA synthesis for miR-499 was carried out using miRCURY LNA Universal RT microRNA PCR kit (Exiqon). The reaction components were added in an Eppendorf tube and incubated at 42 °C for 1 h followed by termination of the reaction at 95 °C for 5 min. The resultant cDNA was used directly for quantitative PCR analysis or stored at -80 °C.

3.2.9 Quantitative Real time PCR

Quantitative PCR for relative HHV-6 viral copy number analysis was performed using the Applied Biosystems (ABI) platform and PerfeCTa qPCR master-mix (Quanta biosciences). Quantitative PCR reaction was set up as following:

2 X PerfeCTa qPCR master-mix	10 µl
Primer mix (5 µM forward + 5 µM reverse primers)	5 µl
Genomic DNA or cDNA (at least 100 ng)	5 µl
Total	20 µl

The cycling conditions for PCR reaction were set up as follows:

95 °C	15 min	
95 °C	15 sec	
60 °C	30 sec	40 cycles
72 °C	30 sec	
4 °C	∞	

Quantitative PCR for microRNA miR-499 was performed using commercially synthesized primers and master-mix from miRCURY LNA Universal RT microRNA PCR kit (Exiqon) and analysis was performed using the Applied Biosystems (ABI) platform. Quantitative PCR reaction was set up as following:

PCR master-mix	5 µl
PCR Primer set	1 µl
Dilute cDNA (at least 100 ng)	4 µl
Total	10 µl

The cycling conditions for PCR reaction were set up as follows:

95 °C	10 min
95 °C	10 sec ⎤
60 °C	60 sec ⎦ 45 cycles
4 °C	∞

All quantitative PCR analysis was performed on the StepOne Plus version 2.0 software (Applied Biosystems).

3.2.10 SDS-PAGE and Immunoblotting

Lysates- Protein lysates were made from the cells using Laemmli buffer. Laemmli buffer was directly added on the cell monolayer after removing the medium. The cells were scrapped with the buffer and the resultant lysate was collected in an Eppendorf tube and subsequently boiled at 95 °C for 5 min. The lysates were cooled after boiling prior to loading on the SDS-gel. The lysates were further stored in -20 °C for long term storage. In a denaturing polyacrylamide gel, the reducing agent (in Laemmli buffer) like dithiothreitol (DTT) or beta mercaptoethanol destroys the tertiary structures of protein and make it linearized. In an SDS-gel, the detergent sodium dodecyl sulfate (SDS) binds uniformly confers a negative charge on the linearized protein and therefore, the negatively charged protein migrates towards the positive electrode (anode) when an electric field is applied.

SDS gel- For SDS-gel preparation, a discontinuous gel running system (i.e., the buffer in the gel and the running buffer were different) was utilized. The running buffer comprises of Tris-Cl and glycine. Glycine can be positively or negatively charged or can be neutral depending on the pH. The pH of the stacking gel is 6.8 and has a lower concentration of the acrylamide whereas the

resolving gel has higher concentration of acrylamide and pH of 8.8. The glycine ions in the buffer are forced to enter the stacking gel under an electric field. Here, the glycine migrates slower whereas the Cl⁻ ions migrate faster and the proteins are 'sandwiched' in between. This sequence continues until the resolving front, where the glycine ions gain negative charge owing to the higher pH of the resolving gel. The proteins are left behind and the glycine ions migrate ahead dragging the proteins along. Since the concentration of the acrylamide is higher in the resolving gel, the proteins migrate slower and are separated according to their molecular weight. The stacking gel was prepared using 4% acrylamide whereas the resolving gel was prepared using 10% polyacrylamide. The gels were run using commercial assembly from Life technologies at 10 V/cm of the gel.

Immunoblotting- In order to detect the proteins post separation, the proteins were transferred on a polyvinylidene fluoride (PVDF) membrane using a semi-dry transfer assembly and further detected by antibodies. The gel was soaked in transfer buffer after the run was complete. It was incubated there for 10 min. Post incubation, the transfer assembly was set up using Whatman filter papers, PVDF membrane and the gel. Whatman filter papers were soaked in the transfer buffer prior setting up of transfer. The order of the setting up the transfer was as follows

Cathode- 2X Whatman filter papers- PVDF membrane- Gel- 2X Whatman filter papers- Anode

After laying the soaked Whatman papers on the cathode and on the gel, any air bubbles were removed by rolling a pipette over it. Similar procedure was repeated after PVDF membrane as well. After setting up the transfer, constant current was applied across the gel at 1 mA/ cm^2 of the gel for 2 h. After transfer, the membrane was carefully marked and blocked in 10% milk for 1 h at room temperature. Post blocking, the membrane was washed in 1X TBST buffer for 3 times, 5 min each. The membrane was then incubated in the primary antibody diluted in 3% BSA overnight

at 4 °C. The membrane was washed in 1X TBST subsequently for 3 times, 10 min each and then incubated in HRP tagged secondary antibody diluted 1:5000 in 5% milk followed by 3 washes in 1 X TBST similarly. The proteins were detected using enhanced chemiluminescence (ECL) detection system (ECL, Amersham) according to manufacturer's instructions. Medical grade highly sensitive X-Ray films were used to detect luminescence in a dark room. The films were developed using developer- Citroline 2000 (Adefo) and fixer- Adefofix (Adefo) and finally washed with water and air dried.

3.2.11 Pulsed Field Gel Electrophoresis (PFGE)

Preparation of agarose molds- Genomic DNA from HHV-6 integrated cell lines were analyzed for the presence of integrated/extra-chromosomal HHV-6 genome by PFGE. For this, it is essential to maintain the integrity of the genomic DNA and handle it extremely carefully to avoid the shearing of DNA. Hence, the cells were embedded in agarose molds and these molds were then treated with proteinase K and restriction digestion enzymes to avoid shearing during DNA isolation process. CHEF Genomic DNA plug kit (Bio-Rad) was used to prepare the agarose molds. Roughly 3 million cells were trypsinized, collected in a medium with FBS and centrifuged at 800 g for 10 min. The pellet was washed with 1X PBS and resultant pellet was gently dislodged. It was further resuspended in 100 µl of 0.75% agarose solution (prepared by mixing 2% CleanCut agarose solution and Cell Suspension Buffer) equilibrated at 50 °C. It was gently but thoroughly mixed and transferred to the molds and incubated at 4 °C to allow the agarose to solidify.

Proteinase K treatment: These molds were incubated in 500 µl of working proteinase K solution (diluted 100 µl of stock solution of proteinase K in 2.5 ml of proteinase K reaction buffer) at 50 °C overnight without agitation. The molds were washed in 1X wash buffer for 1 hour each with gentle agitation for 2 times.

Restriction digestion- The plugs were then washed with 1 ml of 0.1X wash buffer (to reduce the EDTA concentration) with gentle agitation for 1 hour in a 2 ml Eppendorf tube. The wash buffer was aspirated and 1 ml of appropriate 1X restriction digestion buffer was added followed by incubation for 1 h with gentle agitation at room temperature. The buffer was removed and replaced with 300 µl of 1X restriction digestion buffer and to this 30-50 U of the enzyme was added and the plugs were incubated at 37 °C overnight. The plugs were washed once with 1ml of 1X wash buffer before loading in the well of a gel.

Electrophoresis- The agarose gel was made by boiling 1% agarose in 0.5X TBE in a total volume of 300 ml. The gel was allowed to cast at room temperature for at least 1 h. Electrophoresis was carried out in a 1.0% agarose gel at 6 V/cm for 24 h with a switch time that ramped from 1 to 6 sec. 8–48 kb CHEF DNA size standard (Cat. No. 170–3707) and yeast chromosomal marker (Cat. No. 170–3605) were used for markers. Electrophoresis was carried out in DR II apparatus (Bio-Rad).

3.2.12 Southern Blotting

After electrophoresis, the agarose gel was immersed in 0.125N HCl for 20 min with gentle rocking at room temperature. The gel was then rinsed with ddH$_2$O and further incubated in 1X DNA denaturing buffer for 30 min. The transfer apparatus was assembled during this time. For transfer, a gel casting tray (same size as that of the gel) was inverted in a plastic tray. A Whatman paper was placed on the tray such that it made contact with the base of the plastic tray on both the sides. 1X DNA denaturing buffer was poured over the Whatman paper until the plastic tray was half filled. Two pre-soaked Whatman papers cut to the size of the gel were placed on the top and a glass pipette was rolled to remove air bubbles. The gel inverted and was placed on the top of the Whatman paper carefully. Hybond-XL Nylon membrane pre-soaked in 1X DNA denaturing buffer

was placed on the gel and air bubbles were removed. Two pre-soaked Whatman papers were placed and air bubbles were removed. Dry tissue paper stacks were placed on the top and a heavy Eppendorf rack was placed on the top. Transfer occurred by capillary action overnight or at least 16 h. Post transfer, the nylon membrane was incubated in 1X DNA neutralizing buffer for 5 min followed by air drying. After drying, the membrane was exposed to UV light for 3 min for cross-linking the DNA. The membrane was then incubated in 10 ml hybridization buffer at 42 °C with slow rotating speed for 1 h. Labelled radioactive probe was then boiled at 95 °C for 5 min and added to the buffer followed by incubation at 42 °C overnight at a slow rotating speed. The membrane was washed in 2X SSC for 3 times and exposed to phosphor imager film for 24-48 h.

3.3 Statistical Analysis

All statistical analysis was performed using Graphpad Prism software. Statistical significance was calculated using Student's t test. Two-tailed t test was used to calculate the P values.

4. RESULTS

4.1 Role of Human herpesvirus 6 (HHV-6) in causing genomic instability

4.1.1 iciHHV-6 individuals display high copy number of direct repeat (DR) sequences

HHV-6 is a unique pathogen which can integrate itself in the host chromosome in the sub-telomeric regions termed ciHHV-6 and subsequent integration in the next generation termed iciHHV-6. In iciHHV-6 individuals when the viral DNA is inherited, ordinarily, every cell should have one copy of the unique region of HHV-6 and two copies of DRs integrated in the genome. This 1:2 ratio is predicted because one viral genome is flanked by two DRs, one on each side. General assumption is that the integration occurs through the perfect telomeric repeats of DR_R in the telomeric DNA of human chromosomes and that the integrated HHV-6 genome is completely stable.

Direct detection of the HHV-6 nucleic acids have been recognized as 'gold standard' for diagnostic purposes (Flamand et al., 2014). To this end, real time quantitative polymerase chain reaction (qPCR) has emerged as a quick, sensitive and reproducible technique to detect HHV-6. Specific set of primers can be used even to differentiate between the two species HHV-6A and HHV-6B (Boutolleau et al., 2006). qPCR can be employed for any type of sample ranging from blood sample to cerebrospinal fluid. It helps to quantify the number of copies of HHV-6, viral DR or host DNA in the same sample. Detection of the HHV-6 infection is very important as its infection condition (active infection/ciHHV-6/iciHHV-6) may have a huge impact on therapy. For example, ciHHV-6 will have one copy of virus per cell in a localized sample (for example, liver or heart tissue) whereas iciHHV-6 will have one (or more) copy of virus in every nucleated cell.

Although theoretically a 1:2 ratio exists between the copy number of HHV-6 DNA and copy number of DR, various hypotheses **(Introduction Figure 1.3)** have discussed the mechanisms

through which one copy of DR is often lost in the due process of reactivation (Prusty et al., 2013b). In order to investigate this 'HHV-6 DNA: DR' ratio per cell existing in natural conditions, blood samples from previously diagnosed iciHHV-6 individuals were analyzed. Peripheral blood mononuclear cells (PBMCs) were isolated from these blood samples followed by isolation of total DNA.

Establishing a standard curve for DR gene

To determine the number of DR copies per cell by qPCR, it was first essential to calculate the threshold cycle (C_t value) per copy of DR gene. For this, a full length HHV-6A DR and HHV-6B DR were cloned in TOPO PCR 2.1 vector. One copy of this recombinant plasmid now had 2 copies of DR gene. The number of copies of this recombinant plasmid was calculated using the formula below.

$$\textit{Number of copies of plasmid} = \frac{weigh \ of \ recombinant \ plasmid \ (in \ nanograms)}{molecular \ weigh \ of \ plasmid}$$

The plasmid was further serially diluted from 10^6 plasmid copies per μl to 1 plasmid copy per μl. The dilutions were analyzed by qPCR and mean C_t values from triplicates were plotted against plasmid copy number per reaction. This gave a linear graph and a slope equation which was used to calculate number of DR copies in samples based on the generated C_t values **(Figure 4.1).** Similarly, to determine the number of copies of HHV-6A and HHV-6B genome, full length ORF of U94 gene from these genomes was amplified and cloned in TOPO PCR 2.1 vector and a standard curve was generated in a previous study (Prusty et al., 2013a). In the same study, standard curve for a host gene PI15 was also plotted.
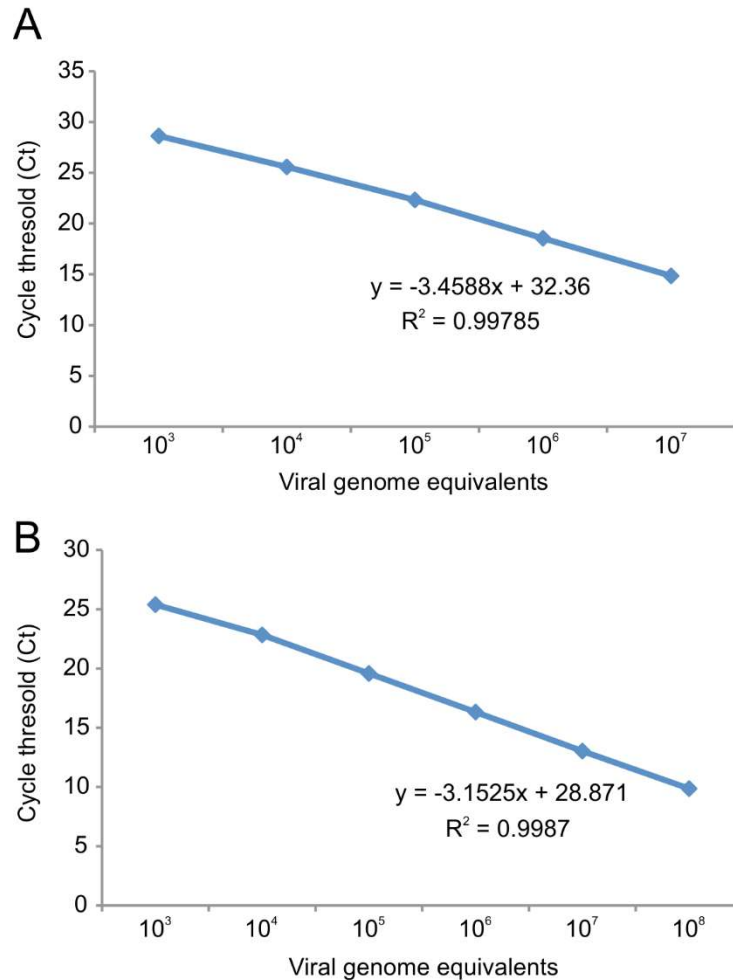
Figure 4.1. Standard curve for C_t values for different copies of HHV-6A and HHV-6B DR gene. C_t values obtained by qPCR were plotted against the respective copy number of DRs. Equation of slope was calculated using y=mx +c. Values for slope and C_t value were substituted in the equation to obtain the number of copies of DR in samples.

Total DNA was isolated from PBMCs followed by qPCR analysis using specific primers for HHV-6A, HHV-6B, HHV-6 DR and PI15. The copy numbers of HHV-6 or DR per 'one' cell was calculated using the standard curve for the host gene- PI15. Interestingly, in some samples the number of DR copies per cell were unusually high as compared to the number of viral copies. Some of the samples even showed five to six copies of DR per cell **(Figure 4.2).**
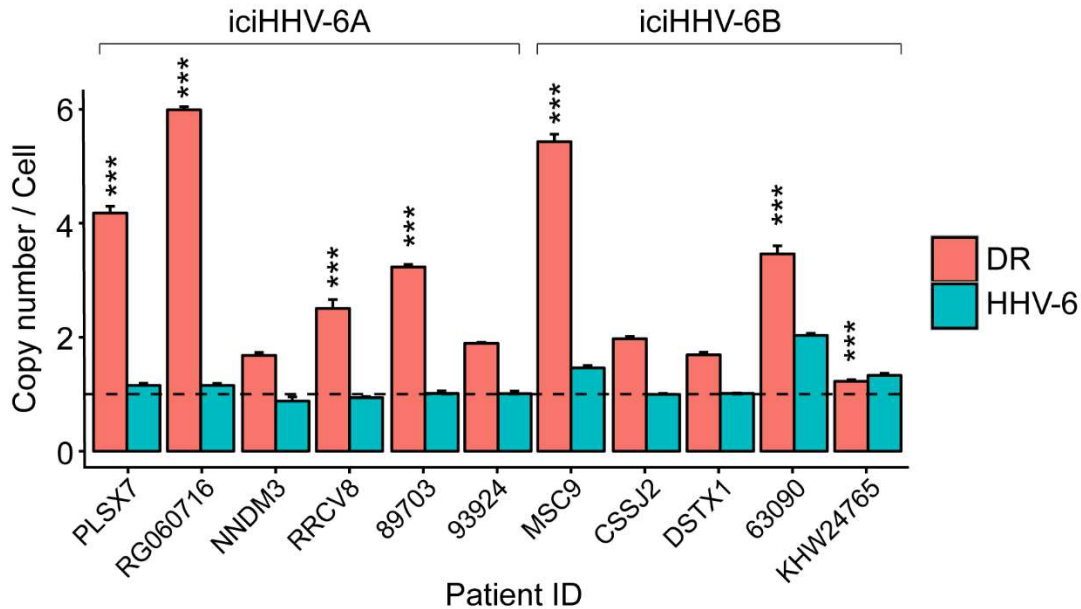
Figure 4.2. Analysis of PBMC samples for number of viral (HHV-6) and DR copies by qPCR. Patient 93924 displayed the usual 1:2 ratio and was used as a control to compare the other samples. Nearly all the samples showed one viral (HHV-6) copy but different number of DR copies. Copy number of 1 is marked as a base line. Data represents mean from three biological triplicates. P values *<0.05, **<0.01, ***<0.001.

Further, three samples CSSJ2, PLSX7 and NNMD3 were monitored over a period of three years to investigate if these unusual DR copies remain constant or vary in time. Blood samples were taken and PBMCs were isolated freshly once every year. The viral copies (HHV-6A or HHV-6B) remained constant throughout the period of three years. However, the number of DR copies varied in two out of the three individuals whereas in one of the sample it was more or less constant **(Figure 4.3).** This observation of differential behavior of DR hinted towards mechanisms enabling increased replication of DR within the host chromosomes.
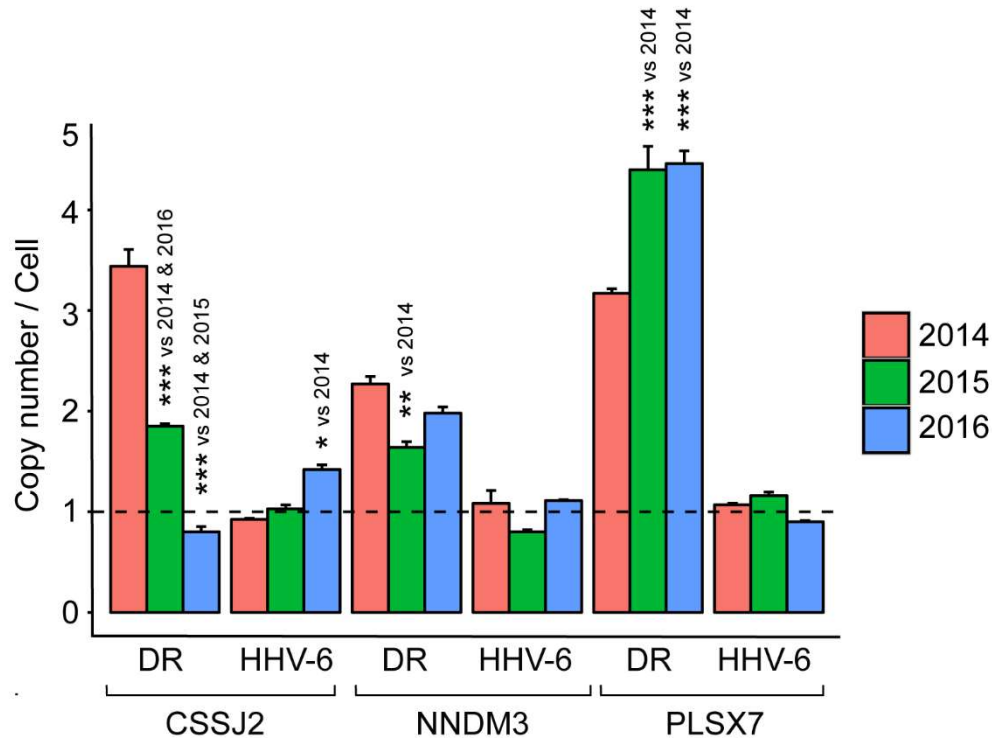
Figure 4.3. Analysis of PBMC samples for number of viral (HHV-6) and DR copies by qPCR over a three-year period. Patient CSSJ2 and PLSX7 displayed varying copy number of DR each year whereas patient NNMD3 showed more or less constant DR copy number. Nearly all the samples showed one viral (HHV-6) copy. Copy number of 1 is marked as a base line. Data represents mean from three biological triplicates. P values *<0.05, **<0.01, ***<0.001.

4.1.2. HHV-6A genome is lost but DR is retained after infection in a cell culture model of ciHHV-6

Generation of ciHHV-6 cell culture model

To confirm the unusual behavior of DR observed in iciHHV-6 patients and to understand the fate of DR after viral reactivation, an *in vitro* cell culture model was established for ciHHV-6. Different cell lines including cervical carcinoma (HeLa), ovarian epithelial (SKOV-3) and glioblastoma (U251) were employed for this purpose. Bacterial artificial chromosome (BAC) derived HHV-6A virus encoding for a green fluorescence protein (GFP) under a constitutive CMV promoter was

used for infecting these cell lines. After infection, the cells fluoresced until the virus was replicating and active. These green cells were immediately sorted and about 50 single cell clones were generated and maintained in culture conditions. The GFP expression was lost after 3-4 passages indicating that the virus was no longer active and that the viral genome was possibly integrated or lost from the cells **(Figure 4.4)**.

Figure 4.4. Schematic representation of generation ciHHV-6 cell lines. HeLa, SKOV-3 and U251 cells were infected with HHV-6A GFP viral particles followed by positive selection for green fluorescent cells and subsequent sorting and colony formation. Loss of GFP after 3-4 passages indicated integration or loss of viral genome.

Analysis of HHV-6 and DR copy numbers in the single cell clones

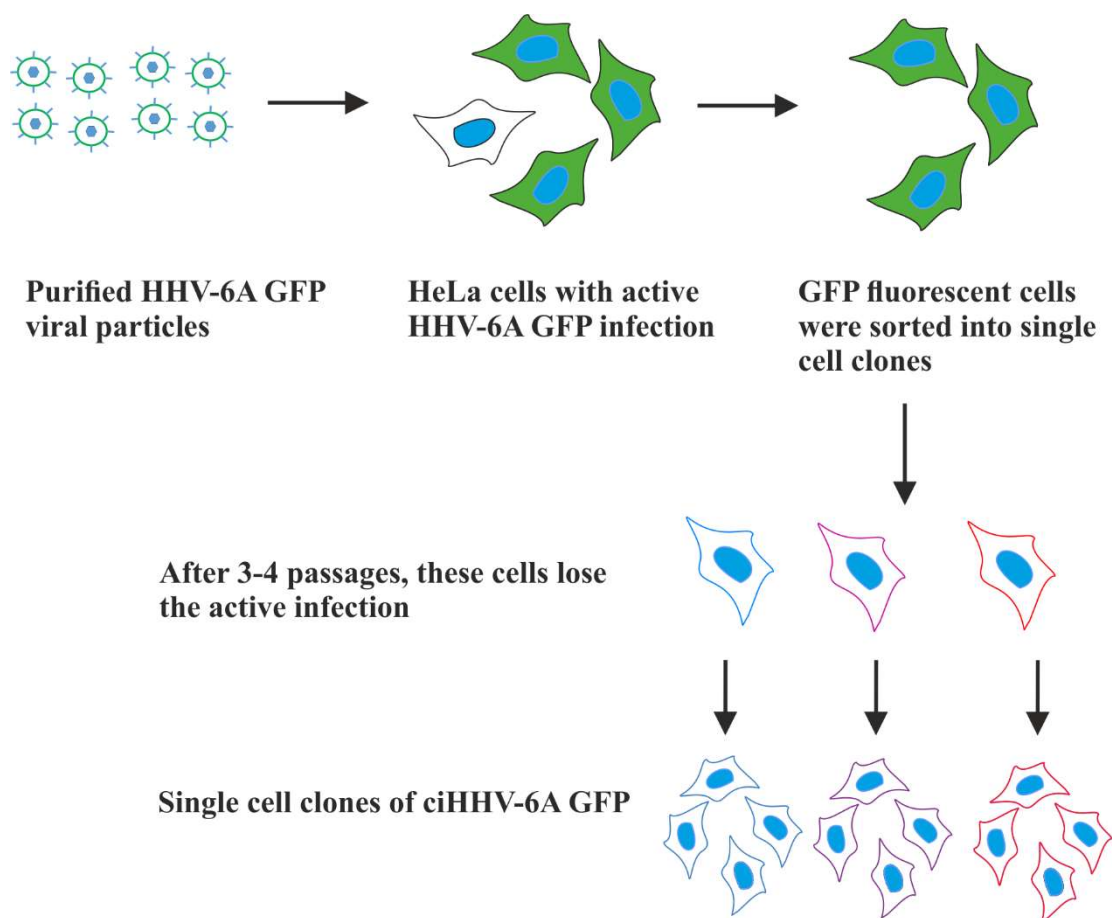In order to check the copy number of viral genome (HHV-6A) and DR in these clones, total DNA was isolated from the clones and analyzed by qPCR using specific primers. Some of the clones showed high DR copy numbers as compared to the viral genome. In some of the clones, the copy number was a high as 20 copies per cell **(Appendix Figure 6.1)**. Moreover, in many clones the viral genome was completely absent indicating a complete loss of entire viral genome. A complete analysis of the ciHHV-6 clones is presented in the **Table 4.1.**

Cell line	Number of clones analyzed	Number of clones with HHV-6A genome including DR	Number of clones with DR alone	Number of clones with neither HHV-6A genome nor DR
HeLa	35	18 (51.4%)	5 (14.2%)	12 (34.28%)
SKOV-3	50	4 (8%)	6 (12%)	40 (80%)
U251	52	2 (3.84%)	17 (32%)	33 (63.46%)

Table 4.1. qPCR analysis of different ciHHV-6 cell lines showed a different trend in the loss of HHV-6A genome and retention of DR. All three cell lines had several clones with the presence of only DR sequences but not rest of the HHV-6 genome (highlighted in red).

4.1.3 HHV-6A DR integrates in non-telomeric regions of host chromosomes

Verification of presence of viral DR without HHV-6A genome

To verify and explain the presence of viral DR copies in the absence of HHV-6A genome in some ciHHV-6 single cell clones, it was important to characterize the DR integration sites. To verify the presence of viral DR copies, a conventional PCR approach was followed. Here, ten different sets of primers specific for different regions of the HHV-6A genome were employed as shown in the **Figure 4.5 (A).** Two ciHHV-6A clones, HeLa clone 2 (HeLa c2) and HeLa clone 4 (HeLa c4)

were analyzed using this method. HeLa c2 was used as a control as it showed a normal 1:2 ratio between HHV-6A genome and DR whereas HeLa c4 showed only the presence of viral DR but not the rest of HHV-6A genome. All ten primer sets were able to amplify the DNA from HeLa c2 as observed on a 1% agarose gel. However, only the primer sets 1, 2 and 9 which were located in the DR_L region of HHV-6A genome amplified DNA from HeLa c4 **(Figure 4.5 B).** This confirmed the observation of presence of only viral DR region and the absence of the viral genome.
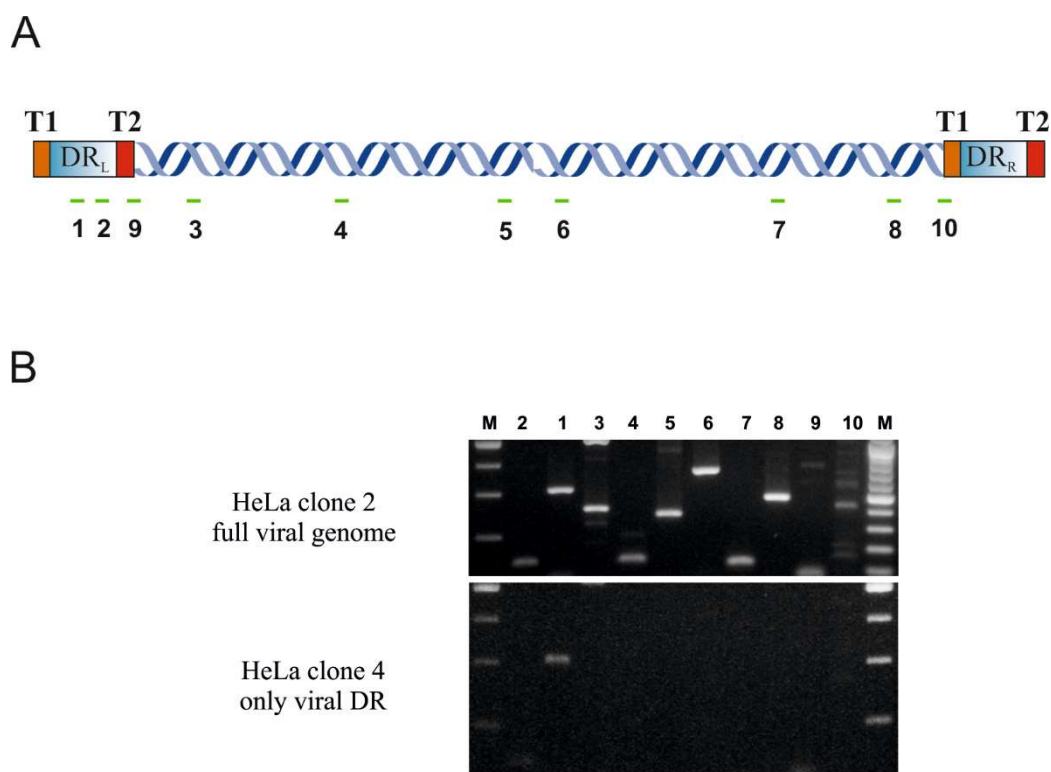
Figure 4.5. Characterization of the *in vitro* ciHHV-6 culture model by conventional PCR. (A) Schematic representation of the specific primers amplifying 10 different regions within the HHV-6A genome**. (B)** 1% Agarose gel electrophoresis of the amplified products of the two ciHHV-6 HeLa clones. HeLa clone 2 shows the presence of all the PCR products: 1-DR6, 2-DR7, 3-U33, 4-P41, 5-U42, 6-U79, 7-U83, 8-U91, 9- DR_L junction region, 10- DR_R junction region whereas clone 4 shows the presence of only 1-DR6, 2-DR7 and 9- DR_L junction region which are present in the DR_L region.

Identification of the integration status of the viral DR

After establishing the presence of only viral DR copies in HeLa c4, it was important to investigate if this viral DR was indeed integrated within the host chromosomes or if it was present in an episomal form. To identify the location of viral DR, pulsed field gel electrophoresis (PFGE) was performed. Briefly, the cells were directly embedded in agarose molds followed by treating the molds with proteinase K and were subsequently inserting in the wells of the gel. Only extrachromosomal DNA would enter the gel whereas the chromosomal DNA would remain in the gel. Sequences unique for HHV-6A and DR were used as specific detection probes in southern blotting. HeLa c2 was positive for both the HHV-6A and DR probe and the signal was localized to the wells suggesting that the entire viral genome was present in an integrated form. HeLa c4 was positive only for DR and the signal was localized to the wells as well (**Figure 4.6 A)**. This suggested that only the viral DR sequence was present in an integrated form.

This integrated viral DR was further characterized for the location of integration by fluorescence *in situ* hybridization (FISH). Metaphase chromosome spreads were prepared from both the clones- clone c2 and clone c4. FISH probes specific for viral DR were used to hybridize and visualize the integration site. In HeLa c2, the integration was at the canonical sub-telomeric regions which was confirmed by partial colocalization of telomeric probe (telomere-cy5) and viral DR probe (HHV-6 DR-cy3). However, in HeLa c4 the integration was surprisingly at non-telomeric regions **(Figure 4.6 C)**. Previous studies have shown that full genome of HHV-6 usually integrates in the telomeric regions of host chromosomes and can integrate virtually in any chromosome (Arbuckle et al., 2010, Arbuckle et al., 2013). However, this observation of only the DR region of viral genome integrating in non-telomeric region of host chromosome is completely novel.
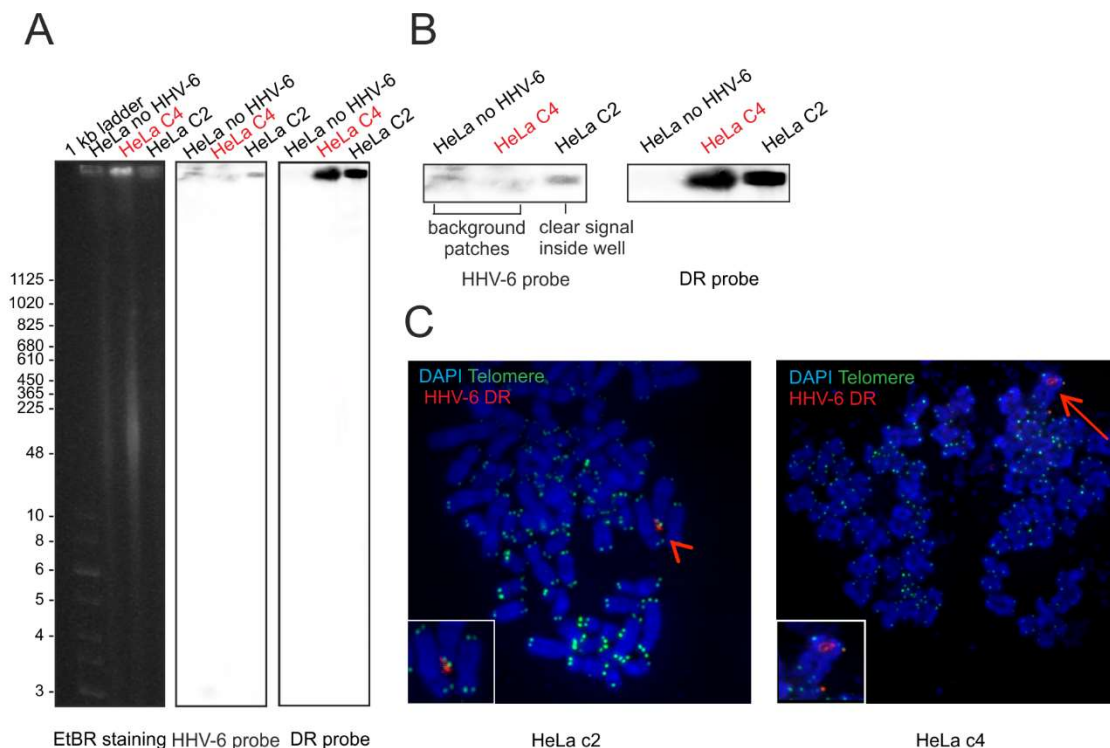
Figure 4.6. Characterization of integration sites of virus in the *in vitro* ciHHV-6 culture model by PFGE and FISH. (A) PFGE shows that HeLa c2 has a full length viral genome integrated in the chromosome while HeLa c4 has only DR integrated in the chromosome. Hybridization signal localized to the well indicates chromosomal integrated form as episomal DNA would enter the gel during electrophoresis **(B)** Enlarged section of panel (A) showing southern hybridization signal inside the wells of the gel. **(C)** FISH analysis in HeLa c2 confirms the presence of viral genome in the telomeric region while HeLa c4 shows presence of viral DR integrated in the non-telomeric regions. Arrowheads indicate integrated viral genome which is enlarged on the lower left-hand corner.

4.1.4 Identification of non-telomeric viral DR integration sites.

To identify the integration site of viral DR, an inverse PCR (iPCR) approach was followed **(Figure 4.7)**. In iPCR, 100 ng of genomic DNA was digested with a frequent cutting restriction enzyme MboI. The sites of this enzyme were already known (reference genome sequence X83413.1) and generated small fragments of genomic DNA including the fragment in the overlapping region between HHV-6 DR and human chromosome. These fragments were then self-ligated to give

circular genomes. The circular DNA were amplified with nested primers designed within the HHV-6 DR region. The amplified products were sequenced by Sanger sequencing. Sequencing data revealed non-telomeric integration sites in four of the single cell clones and one iciHHV-6 patient sample NNMD3. In some samples non-telomeric integration was found in intronic regions of *GAIP* and *AGGF1* genes **(Appendix Figure 6.2)**. The chromosome numbers with the exact location of integration sites are summarized in **Table 4.2**. The sequence analysis of SKOV-3 clone showed 100% homology to two locations due to repetitive sequences thereby making it difficult to ascertain a specific integration site.
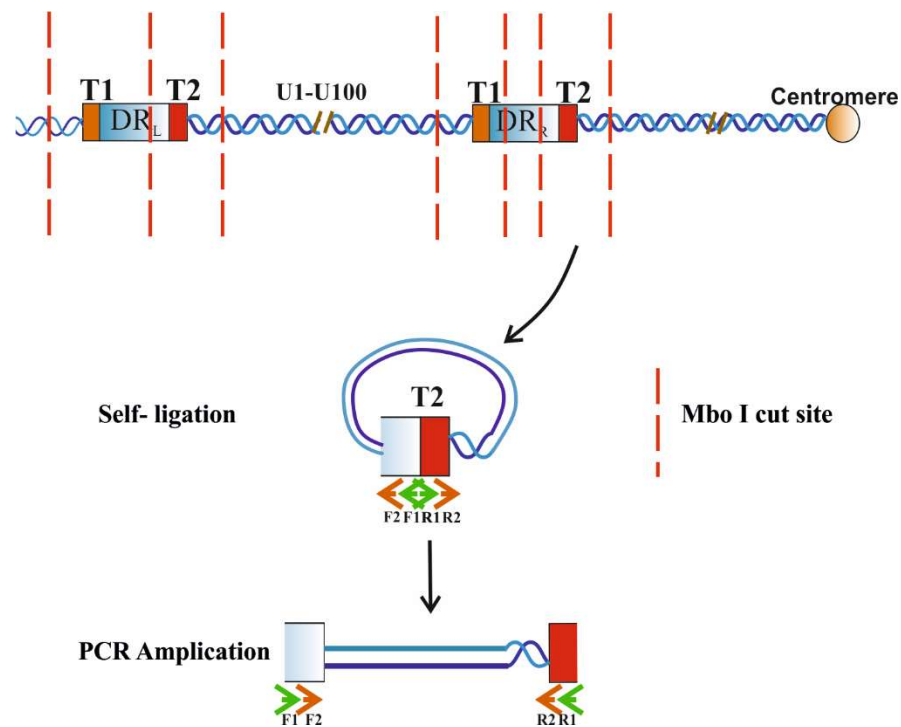
Figure 4.7. Schematic workflow of inverse PCR to amplify the junction region of HHV-6 DR and human chromosomes. The genome was digested by a frequent cutting restriction enzyme MboI. The fragments were self-ligated to generate closed circular genomes. Nested primer sets within the known sequences of DR region were employed to PCR amplify the circular DNA. The PCR products were then sequenced to identify the integration sequences.

Single cell clone	Integration site
SKOV-3 clone 33	Chr 6p25.3 or Chr 19p13.3
HeLa clone 2	Chr 13q21.33
HeLa clone 4	Chr Xq21.1
U251 clone 15	Chr 20q13.3
NNMD3	Chr 5q13.3

Table 4.2. Table showing the integration sites of HHV-6A DR in single cell clones of ciHHV-6 cell lines. Inverse PCR products were analyzed by sequencing to identify integration sites. U251 clone 15 was found to be integrated in the intronic region of human G- alpha interacting protein isoform B (GAIP) whereas the sample from ciHHV-6 individual NNMD3 showed integration at intronic region of human angiogenic factor with G-patch and FHA domains 1 (AGGF1).

These results conclude that the direct repeats (DR) of the HHV-6 genome are highly unstable in nature as they increase or decrease in number during the course of time **(Figure 4.3)**. Moreover, DR can also integrate in the non-telomeric locations in human chromosomes which may lead to abrogation or upregulation of gene expression **(Figure 4.6).** However, further studies are necessary to determine the exact mechanisms which causes the DR sequences to increase or decrease in number over a period of time. In depth analysis of mechanisms through which viral DR sequences integrate in the non-telomeric regions of host chromosome are also necessary.

4.2 Role of *C. trachomatis* in causing genomic instability

4.2.1 *C. trachomatis* infection causes oxidative DNA damage but impairs DNA repair

C. trachomatis induces ROS production which is essential for its growth and development (Abdul-Sater et al., 2010). ROS is also present in the female genital tract and also ovaries due to the normal physiology and follicular dynamics. ROS causes oxidative DNA damage which induces single-strand breaks (Yu and Anderson, 1997). Since, *C. trachomatis* causes oxidative DNA damage, an experiment was designed to quantify the oxidative DNA damage during infection. DNA damage was quantified by comet assay or single cell gel electrophoresis. However, for the comet assay purified nuclei were used instead of intact cells in order to avoid background from bacterial DNA.

The cells were infected with *C. trachomatis* for 20 h followed by treatment with H_2O_2 to induce oxidative DNA damage. Cells were then washed and were incubated in fresh medium to allow DNA repair. Nuclei were harvested before H_2O_2 treatment (basal condition), after treatment (damage) and 16 h post incubation in fresh medium (repair). After harvesting the nuclei, they were used in a comet assay and DNA damage was quantified as a function of percentage of tail DNA **(Figure 4.8 A)**.

During *C. trachomatis* infection, oxidative DNA damage was significantly increased as compared to the non-infected cells as observed by the percent tail DNA. The non-infected cells showed an increased percent tail DNA in response to H_2O_2 treatment and the percent tail DNA reduced post 16 h of incubation which indicated DNA repair. However, this repair process did not occur in the *C. trachomatis* infected cells indicated by the unchanged amount of percent tail DNA throughout the experiment **(Figure 4.8 B)**. This experiment indicated that there is high oxidative DNA damage in *C. trachomatis* infected cells but no considerable DNA repair.
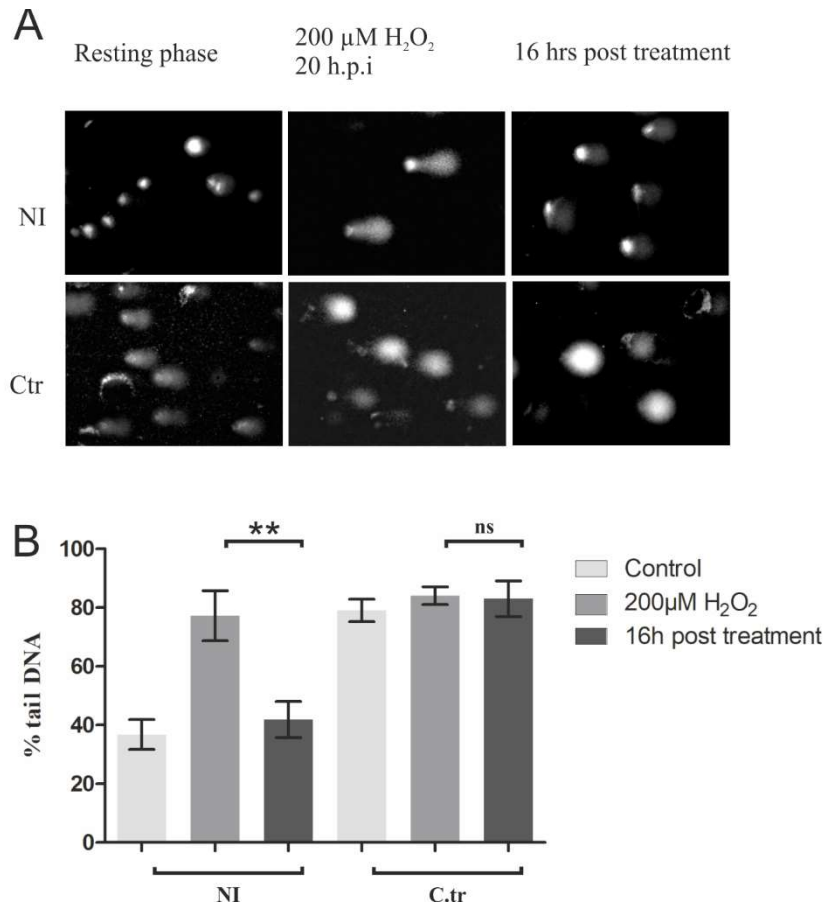
Figure 4.8. Alkaline comet assay to study oxidative DNA damage during *C. trachomatis* infection of primary HOSE cells. (A) Representative images of alkaline comet assay performed with nuclei of cells infected with *C. trachomatis* under different conditions. **(B)** Percent tail DNA quantified using 'OpenComet' macro of FIJI (Gyori et al., 2014) show a damage-repair response in non-infected cells but not in *C. trachomatis* infected cells. Error bars show mean ±SEM from three independent experiments. ** $p < 0.01$, ns not significant.

4.2.2 *C. trachomatis* downregulates polymerase β

Since *C. trachomatis* infected cells show high oxidative DNA damage but impaired repair dynamics, it was important to study the mechanisms which repair oxidative DNA damage. The oxidized DNA bases, purines and pyrimidines, are replaced by undamaged ones by base excision repair (BER) mechanism. We, therefore, studied the repair proteins of BER mechanism. *C.*

trachomatis infected primary human ovarian epithelial (HOSE) cells showed downregulated expression of polymerase β, which is the main gap-filling polymerase enzyme in the BER process.
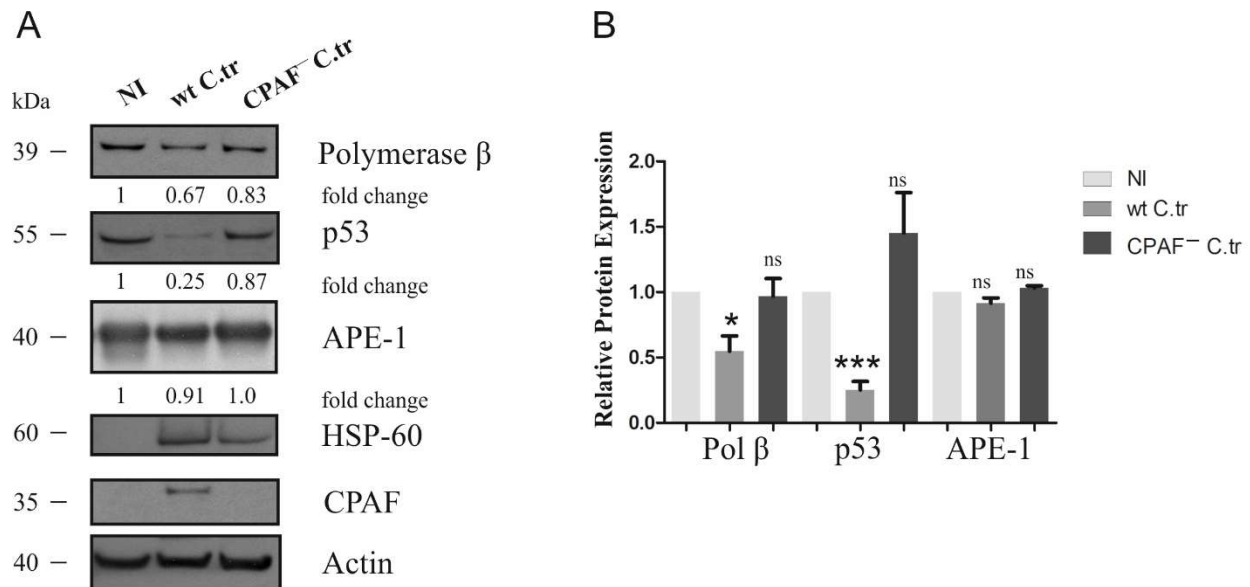
Figure 4.9. Effect of *C. trachomatis* infection on expression of polymerase β in primary HOSE cells. (A) Immunoblot analysis of primary HOSE cells infected with wild type or CPAF⁻ (RST17) *C. trachomatis* for 30 h at MOI of 1. Polymerase β, APE-1, p53, CPAF, HSP-60 were detected using specific antibodies and analyzed using actin for normalization. **(B)** Fold change for polymerase β, APE-1 and p53 was plotted. Error bars show mean ±SEM from two independent experiments. ns not significant, * $p < 0.05$, *** $p < 0.001$.

C. trachomatis secretes a protease called chlamydial protease-like activity factor (CPAF) which cleaves a defined set of chlamydial and human proteins. A mutant *C. trachomatis* strain, RST17, which had deletion in CPAF (CPAF⁻) was initially used as a control for non-specific cleavage (Snavely et al., 2014). The native nuclear lysates used in the repair assay were supplemented with clasto-lactacystin which is a specific inhibitor of CPAF activity to eliminate any post-lysis cleavage. Interestingly, CPAF⁻ *C. trachomatis* did not down regulate polymerase β **(Figure 4.9)**. Moreover, CPAF⁻ *Chlamydia* also did not downregulate tumor suppressor p53, which is a hallmark of *Chlamydia* infection **(Figure 4.9)**. Apurinic/apyrimidinic endonuclease-1 (APE-1)

another BER, was unaffected during infection suggesting that polymerase β downregulation was a specific event during *C. trachomatis* infection. **(Figure 4.9)**. These results clearly demonstrate that *C. trachomatis* specifically downregulates polymerase β in a CPAF-dependent manner.

4.2.3 Downregulation of polymerase β during *C. trachomatis* infection impairs BER

To investigate if the downregulation of polymerase β has any effect on the BER process, an *in vitro* BER assay was designed as described in the **methods section 3.2.6**. Native nuclear lysates were used in this assay to observe the repair efficiency on synthetic polymerase β substrates. The *in vitro* assay was first validated to confirm that the effect was indeed from the repair enzymes and not from the buffer components.

Designing and validating an in vitro BER assay

The oligonucleotide substrates were prepared by annealing the complementary oligonucleotides and subsequently purifying them. They were incubated in the native lysates at 30 °C and resolved on a denaturing urea gel **(Figure 4.10)**. The repair was determined by quantifying the final product. Different buffer components were eliminated from the reaction to observe the effect on repair activity and thereby determine the essential buffer components. A lysate control was involved to study if merely the buffer components were able to repair the substrate without lysate. ATP, dNTP, T4 DNA Ligase and nuclear lysate were indispensable for the repair reaction to occur. Also, repair reaction did not occur without the nuclear lysate **(Figure 4.10)**.

A

55 nts (P2)

5' TACTAGGTAGCACGAGGCACTATATCAGGTAACTTCGATTCACGACTGCAGTCTA 3'

3' ATGATCCATCGTGCTCCGTGATAT●GTCCATTGAAGCTAAGTGCTGACGTCAGAT 5'

24 nts (B)   30 nts (A)

P^{32}

B

	-	+	+	+	+	+	ATP
	+	-	+	+	+	+	dNTP
	+	+	-	+	+	+	Ligase
	+	+	+	-	+	+	PNK
	+	+	+	+	-	+	Lysate

55 mer

30 mer
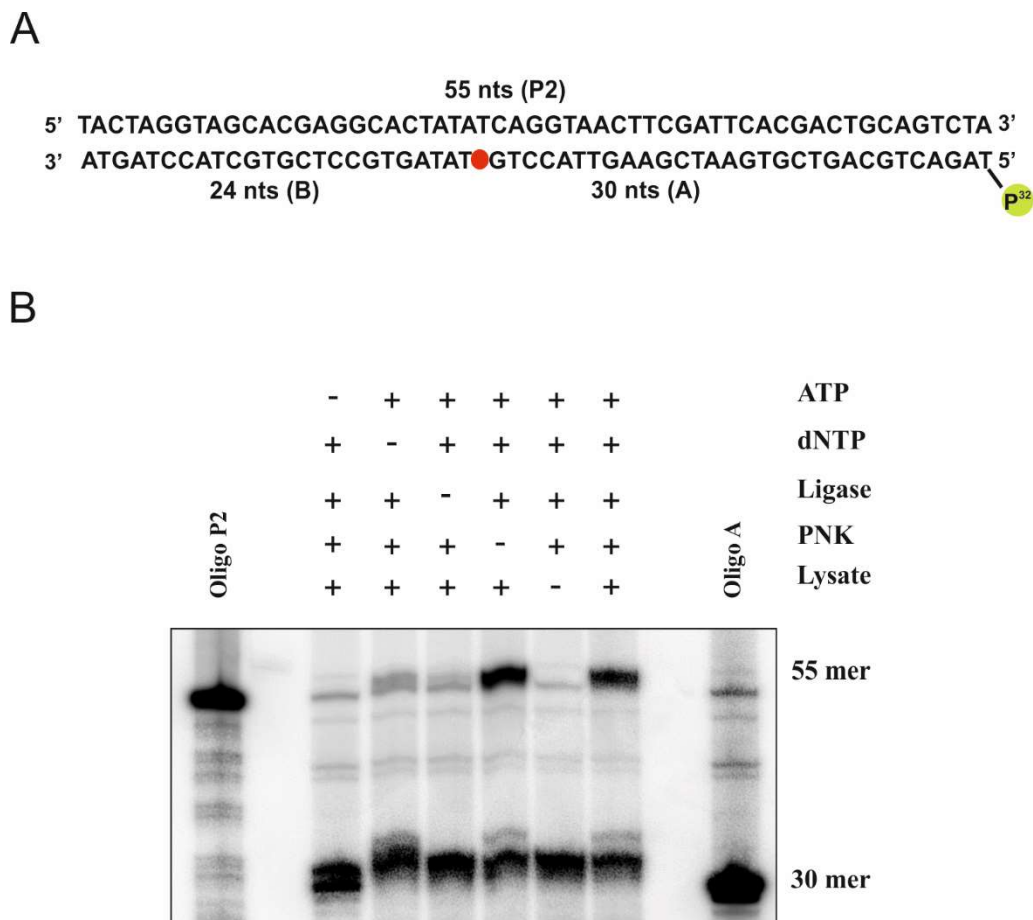
Figure 4.10. Designing and validating the *in vitro* BER assay. (A) Duplex oligonucleotide substrate prepared by annealing a parent 55 nucleotide strand with two shorter 24 nucleotide and 30 nucleotide oligonucleotides, thereby giving a single nucleotide gap. 5' end of 30 nucleotides strand was radiolabeled with radioactive P^{32}. **(B)** The repair assay was performed by incubating substrate with 10 μg of primary HOSE cell nuclear lysate. The products were resolved on a 10% polyacrylamide denaturing urea gel and visualized in a phosphor-imager. Each lane indicates the buffer components included and omitted in that reaction. Presence of a band at 55mer position indicated a working repair reaction implying that ATP, dNTP, T4 DNA Ligase and nuclear lysate were indispensable for the assay.

The specificity of the repair assay was further confirmed by performing the same repair assay using nuclear lysates after transient knock down of polymerase β in primary HOSE cells. Polymerase β was knockdown using siRNA in primary HOSE cells and the nuclear lysates were prepared and used in BER assay. Here, the oligonucleotide substrate with 3 single nucleotide gaps

was used. The substrate was prepared by annealing a 64-nucleotide parent strand with four shorter oligonucleotides. As expected, the repair decreased after siRNA mediated knockdown of polymerase β and was inversely proportional to the concentration of polymerase β siRNA **(Figure 4.11).** This confirmed that the repair activity observed in BER assay was a function of polymerase β.
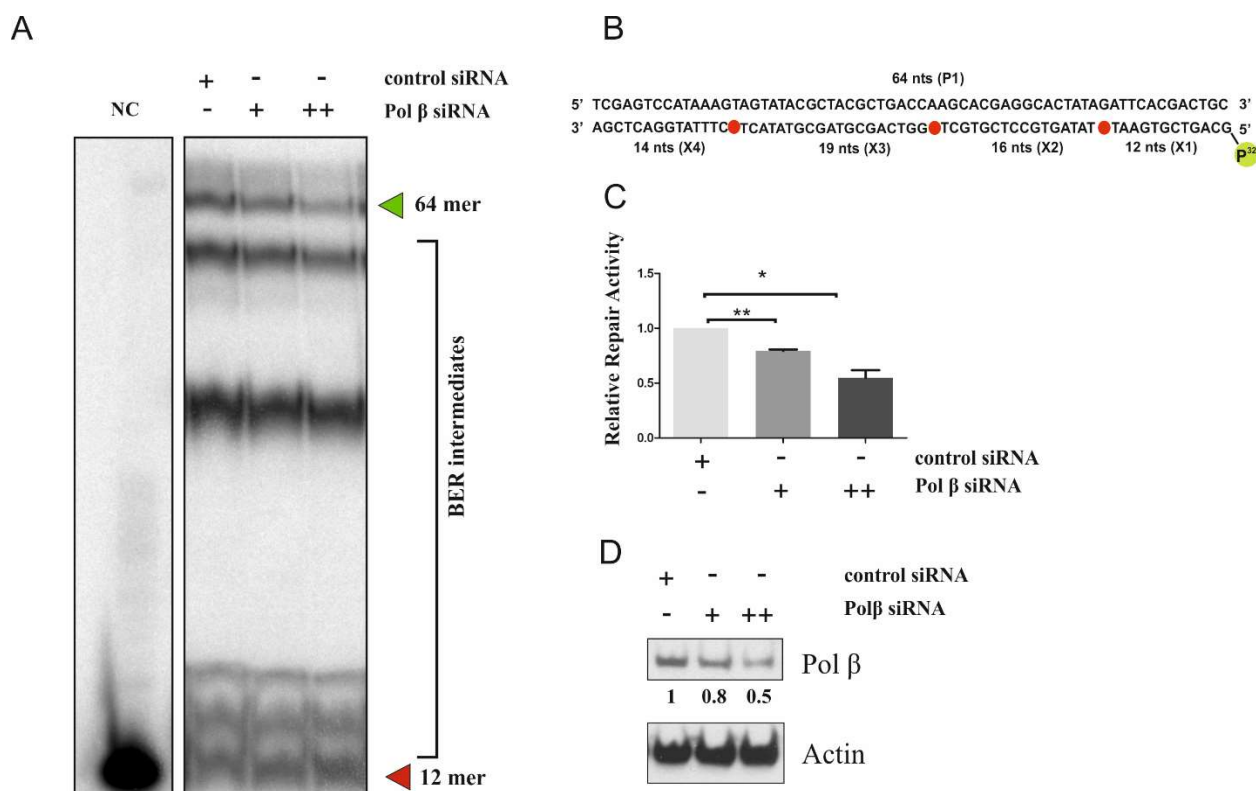
Figure 4.11. Confirmation of specificity of *in vitro* BER assay. (A) Repair assay was performed by incubating nuclear lysates of primary HOSE cells treated with two concentrations (1 nM and 5 nM) of polymerase β siRNA with oligonucleotide substrate. Red arrow corresponds to substrate and green arrow to the final product. NC is negative control wherein lysate was omitted. **(B)** Duplex oligonucleotide substrate prepared by annealing 64 nucleotide parent strand with 4 shorter oligonucleotides to generate 3 single nucleotide gaps. 5' end of short oligonucleotide (12 nucleotides) was radiolabeled with radioactive P^{32}. **(C)** Quantification of the final repair product corresponding to 64 nucleotides, marked by green arrow in panel (A) indicating repair activity in fold changes compared to control siRNA. **(D)** Immunoblot analysis for confirmation of siRNA mediated knockdown efficiency on polymerase β expression. Actin was used as normalization control.

BER during C. trachomatis infection

Using the validated *in vitro* assay, BER activity was assessed in primary HOSE cells during wild

type and CPAF⁻ *C. trachomatis* infection. Corroborating the immunoblot analysis, repair activity

was significantly reduced in wild type *C. trachomatis* but not in CPAF⁻ *C. trachomatis* infected

cells. This confirmed that *C. trachomatis* impairs BER in primary HOSE cells by downregulating

polymerase β **(Figure 4.12)**.
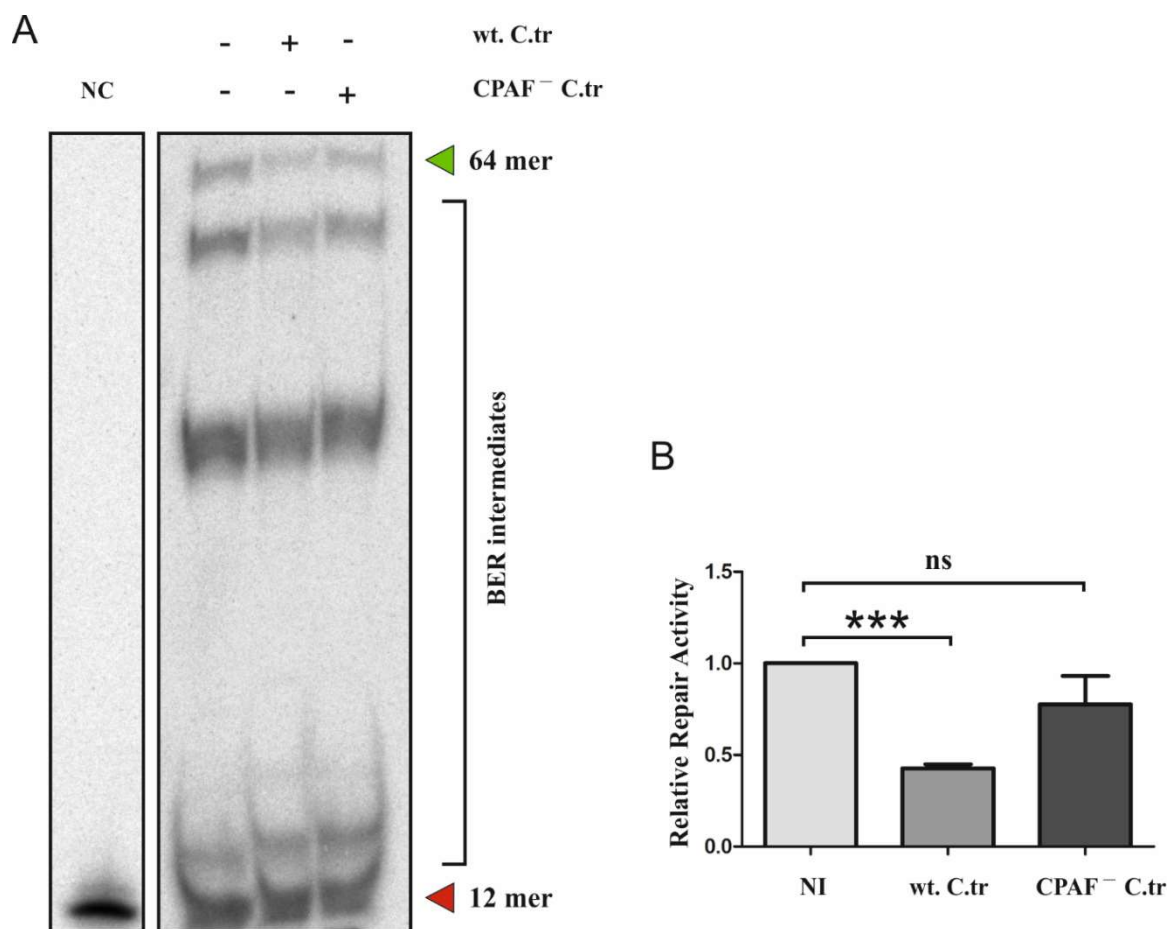
Figure 4.12. Effect of *C. trachomatis* infection on BER in primary HOSE cells. (A) Repair assay was performed using nuclear lysates of primary HOSE cells infected with wild type and CPAF⁻ *C. trachomatis* for 30 h at MOI of 1. Red arrow corresponds to substrate and green arrow to the final product. NC is negative control wherein lysate was omitted. **(B)** Quantification of the final repair product corresponding to 64 nucleotides, marked by green arrow in panel. Error bars show mean ±SEM from two independent experiments. *** $p < 0.001$, ns not significant.

Similar to the primary HOSE cells, *C. trachomatis* also downregulated base excision repair in other cell lines including transformed cervical HeLa cells, transformed ovarian epithelial SKOV-3 cells, primary human umbilical cord HUVEC cells and primary human foreskin fibroblast HFF cells **(Figure 4.13)**. These results indicate that impairment of BER during *C. trachomatis* infection is not cell type specific but occurs in many different cell types.
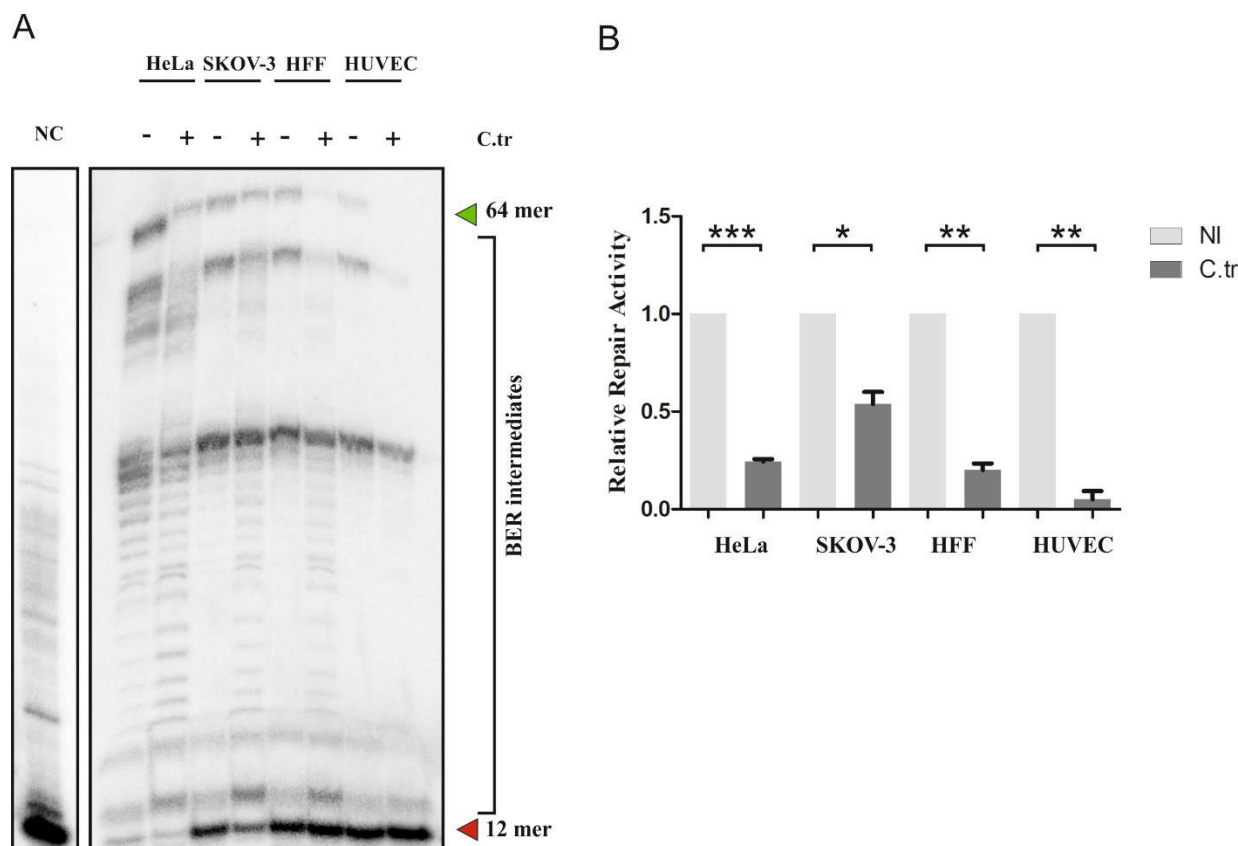
Figure 4.13. Effect of *C. trachomatis* infection on BER in different cell lines. (A) Repair assay was performed using nuclear lysates of cells infected with wild type *C. trachomatis* for 30 h at MOI of 1. Red arrow corresponds to substrate and green arrow to the final product. NC is negative control wherein lysate was omitted. **(B)** Quantification of the final repair product corresponding to 64 nucleotides, marked by green arrow in panel (A). Error bars show mean ±SEM from two independent experiments. * $p < 0.05$, ** $p < 0.01$, *** $p < 0.001$.

4.2.4 Effect of Hydrogen peroxide and progesterone on BER during *C. trachomatis* infection

Oxidative stress has been associated with all the stages of cancer including initiation, promotion and progression. Reactive oxygen species (ROS) comprises of radicals such as peroxide ($O_2\bullet^-$), hydroxyl (HO•), peroxyl (RO_2•), and alkoxyl (RO•), as well as non-radicals that can be converted to radicals or serve as oxidizing agents such as hydrogen peroxide (H_2O_2), hypochlorous acid (HOCl), ozone (O_3), and singlet oxygen ($^1O_2$). ROS not only causes mutations thereby causing genetic instability but also activates various cellular transcription factors including nuclear factor (NF)-κβ, p53 and hypoxia activating factor (HIF-1α) (Reuter et al., 2010). On the other hand progesterone, a female steroid hormone is known to have apoptotic effects on transformed ovarian epithelial cells (Syed and Ho, 2003; Yu et al., 2001).

Hence, the effects of these molecules which are prevalent in the female genital tract and in the ovarian milieu were investigated on the process of BER during *C. trachomatis* infection. Primary HOSE cells were treated H_2O_2 and progesterone followed by incubation in fresh medium and *C. trachomatis* infection at MOI of 1. Nuclear lysates were prepared after 30 h of infection and repair assay was performed.

In the duplex oligonucleotide substrate with 3 gaps, BER was impaired in *C. trachomatis* infected H_2O_2 treated cells. Interestingly, the repair was not restored in the progesterone treated cells **(Figure 4.14 A and C)**. Single gap duplex oligonucleotide substrate was also used to study the kinetics of repair during *C. trachomatis* infection. The nuclear lysates were incubated with substrates for 20 min, 40 min and 60 min, the reactions were terminated and products were resolved on a denaturing gel. Although *C. trachomatis* infected cells showed reduced repair efficiency as compared to non-infected cells, the repair increased over the period of time with a slower kinetics **(Figure 4.14 B and D).**
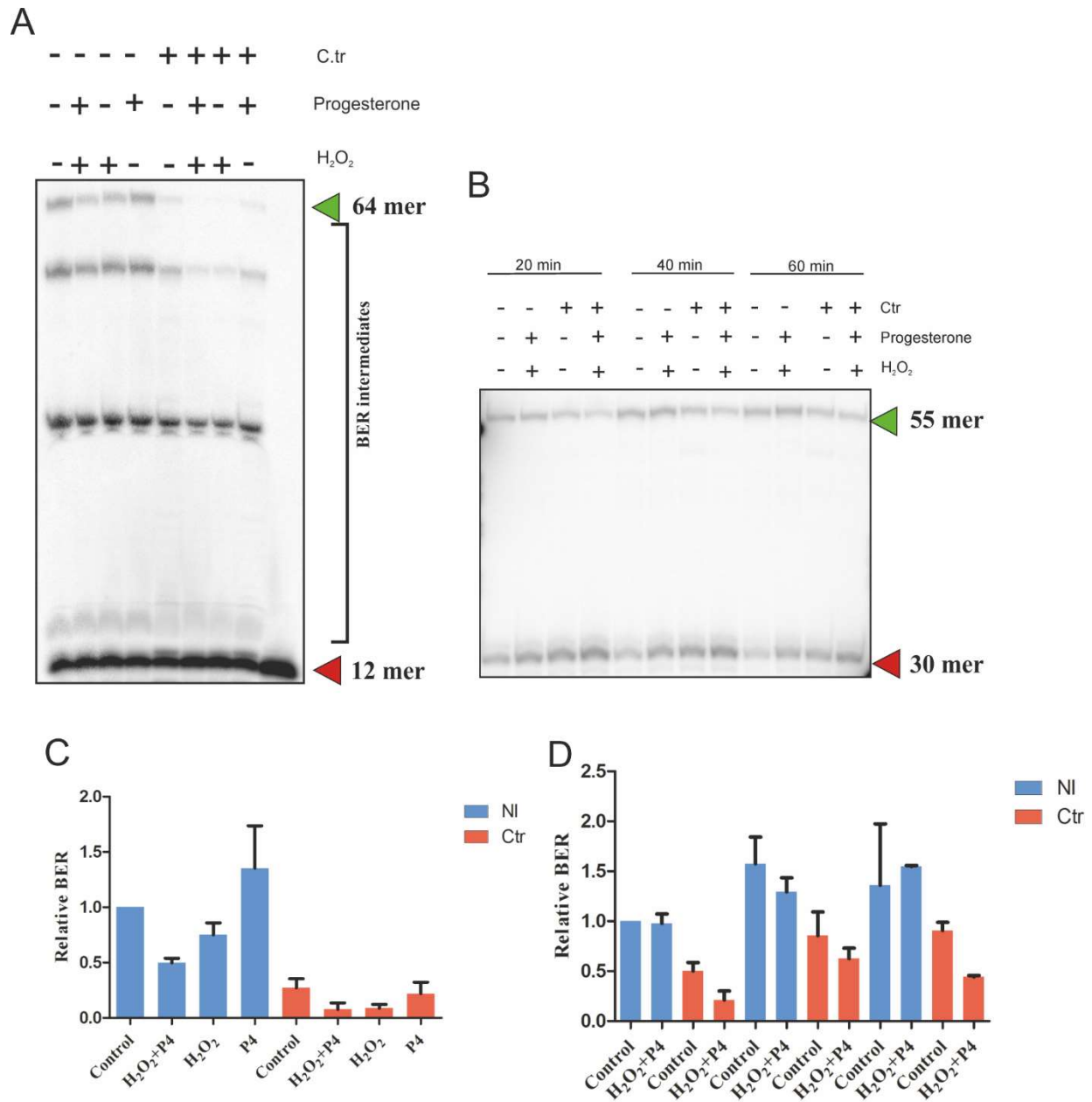
Figure 4.14. Effect of hydrogen peroxide and progesterone on BER during *C. trachomatis* infection. Primary HOSE cells were treated with 200 μM H_2O_2 for 15 min at RT and 25 ng/ml progesterone (P4) prior *C. trachomatis* infection at MOI of 1 for 30 h followed by nuclear lysate preparation and BER assay. **(A)** 3 gap duplex substrate was used to study the overall effect on BER. **(B)** 1 gap duplex substrate was used to study the kinetics of BER **(C)** Quantification of the final repair product corresponding to 64 nucleotides, marked by green arrow in panel (A) and **(D)** Quantification of the final repair product corresponding to 55 nucleotides, marked by green arrow in panel (B). Error bars show mean ±SEM from two independent experiments.

These results indicate that H_2O_2 and progesterone which are known to be present in ovarian milieu are unable to alleviate BER during *C. trachomatis* infection. Also, similar to non-infected cells, the BER efficiency increased with time in the infected cells as well. This indicated that BER is not suddenly abrogated but there is a gradual loss in the efficiency.

4.2.5 MicroRNA miR-499 is upregulated during *C. trachomatis* infection

The amount of steady state polymerase β is proportional to the magnitude of DNA damage in the cell (Parsons et al., 2008). *C. trachomatis* induces oxidative DNA damage; however, it downregulates polymerase β expression. Hence, it was important to investigate the mechanism of downregulation of polymerase β. Previous reports in mice studies have demonstrated that *C. muridarum* modulates mouse miRNA expression profile (Gupta et al., 2015; Yeruva et al., 2016). In a recent study, high throughput miRNA sequencing has shown that *C. trachomatis* induces changes in human microRNA expression profile in primary HUVECs (Chowdhury et al., 2017). Sequence based target prediction tools showed that polymerase β is also regulated by several miRNAs. Amongst these miRNAs, miR-499 displayed the highest binding score to the 3'UTR of polymerase β **(Figure 4.15 A)**. Hence, qPCR for miR-499 was performed in primary HOSE cells infected with *C. trachomatis* for 30 hours. miR-499 was indeed upregulated during *C. trachomatis* infection which corroborated with the previous study where it was shown to be upregulated in primary HUVECs. Since CPAF¯ (RST17) *C. trachomatis* did not affect the BER efficiency of the host cell, miR-499 expression during CPAF¯ *Chlamydia* was investigated. In line with the polymerase β expression and BER efficiency, CPAF¯ *C. trachomatis* did not upregulate miR-499 **(Figure 4.15 B).**
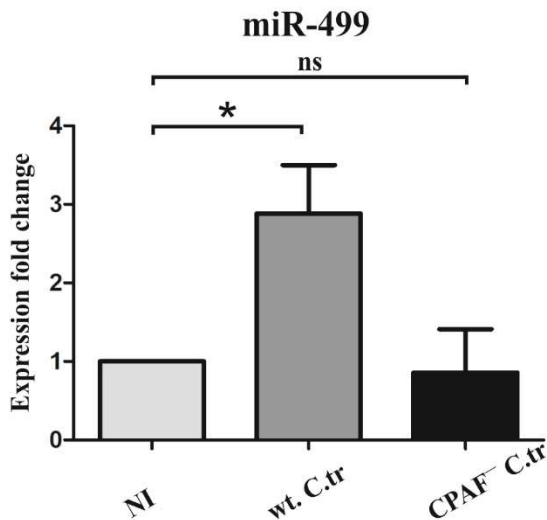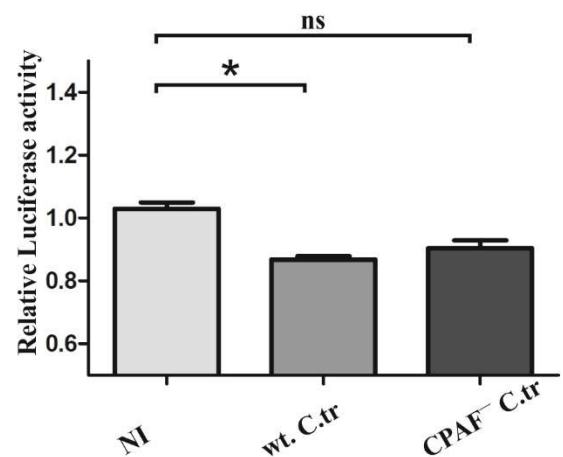
Figure 4.15. miR-499 is regulated during *C. trachomatis* infection. (A) Polymerase β 3'UTR sequence alignment with miR-499 showing the seed sequence and binding region. **(B)** qPCR analysis for miR-499 in primary HOSE cells infected with *C. trachomatis* at MOI of 1 for 30 h showed significant upregulation in wild type but not CPAF⁻ *C. trachomatis* infected cells. **(C)** Luciferase assay showing relative Renilla luciferase activity is reduced in wild type but not CPAF⁻ *C. trachomatis* infected cells. Firefly luciferase activity was used as a control to normalize the transfection efficiency. Error bars show mean ±SEM from two independent experiments. * p < 0.05, ns not significant.

To further elucidate whether the upregulation of miR-499 indeed regulates polymerase β, 3'UTR sequence from polymerase β mRNA was cloned in a dual luciferase vector- Psicheck2.0. Here, polymerase β 3'UTR was cloned downstream of Renilla luciferase gene and activity of Renilla luciferase was monitored during *C. trachomatis* infection. Another luciferase enzyme, Firefly

luciferase, was monitored and used to normalize the transfection efficiency. Renilla luciferase activity was significantly lower in wild type *C. trachomatis* infected cells but not in CPAF⁻ *C. trachomatis* infected cells suggesting that miR-499 upregulation during wild type *C. trachomatis* indeed regulates polymerase β expression by binding to its 3'UTR **(Figure 4.15 C).**

4.2.6 Polymerase β expression and BER efficiency are downregulated in *C. trachomatis* through miR-499

To confirm if the miR-499 upregulation during *C. trachomatis* infection was the cause of polymerase β downregulation, primary HOSE cells were transiently transfected with miR-499 inhibitor and miR-499 mimic for 36 h. After transfection, the cells were infected with wild type *C. trachomatis* at MOI of 1 for 30 h. Native nuclear lysates were prepared and analyzed for polymerase β expression by immunoblotting and for BER efficiency by *in vitro* repair assay **(Figure 4.16)**. After inhibiting miR-499, polymerase β expression and BER efficiency was rescued in *C. trachomatis* infected cells. Whereas after transfecting with miR-499 mimic, polymerase β expression was downregulated and BER was diminished **(Figure 4.16)**.

These experiments confirmed that during *C. trachomatis* infection, miR-499 is upregulated which downregulates polymerase β protein expression by binding to the 3'UTR of its mRNA and thereby impairs BER efficiency. Inhibiting miR-499 during *C. trachomatis* infection rescued BER efficiency.
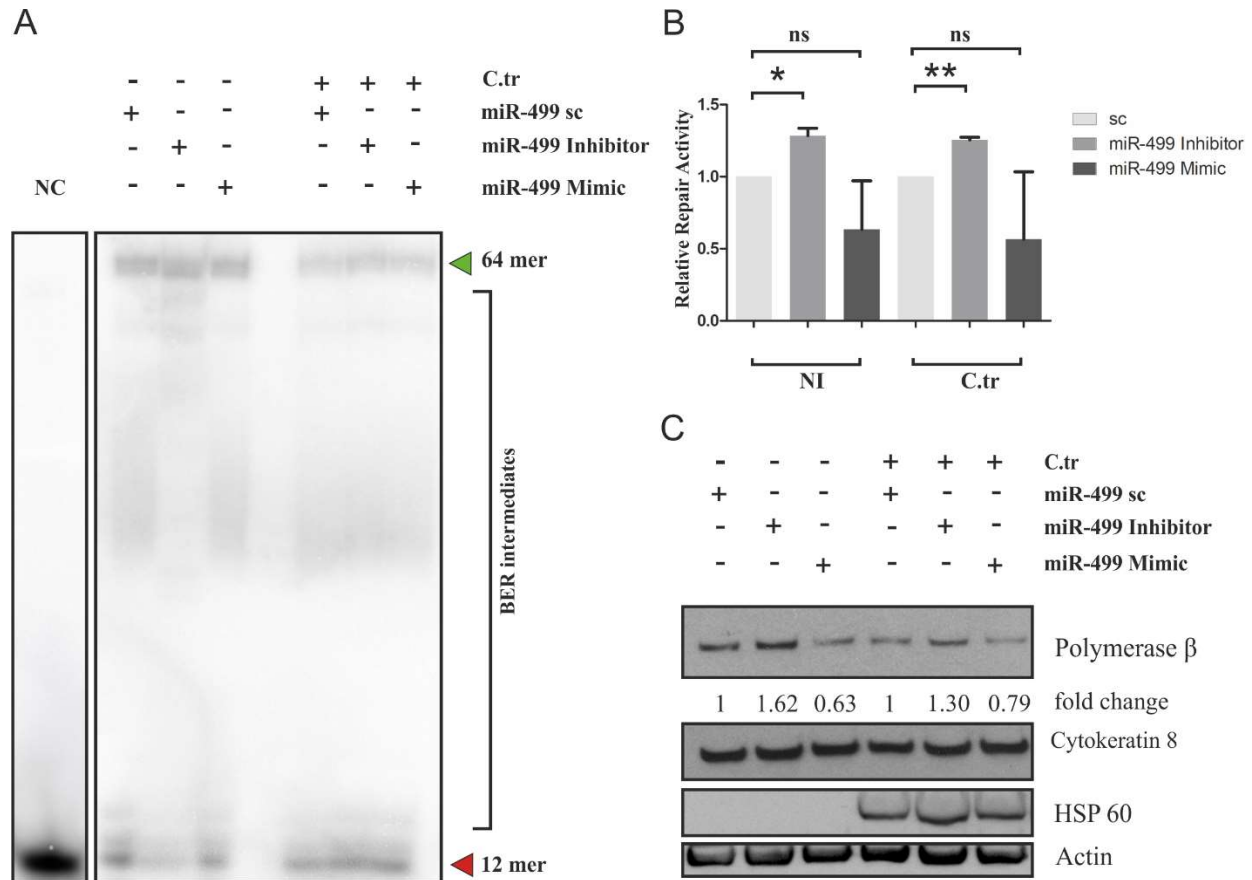
Figure 4.16. miR-499 mediated regulation of BER during *C. trachomatis* infection in primary HOSE cells. Primary HOSE cells were transfected with miR-499 inhibitor, mimic and scrambled control for 36 h followed by *C. trachomatis* infection at MOI of 1 for 30 h. **(A)** Repair assay was performed using substrate with 3 gaps and products were resolved on denaturing urea gel and scanned in phosphor-imager. Red arrow corresponds to substrate and green arrow to the final product. NC is negative control wherein lysate was omitted. **(B)** Quantification of final products of BER in panel (A) marked with green arrow. Error bars show mean ±SEM from two independent experiments. * p < 0.05, ** p < 0.01. **(C)** Immunoblot analysis of native nuclear lysates prepared after 30 h of *C. trachomatis* infection. Polymerase β was quantified, cytokeratin-8 was used as a control for bacterial protease activity. Actin was used for normalization.

4.2.7 Downregulation of p53 during *C. trachomatis* infection impairs BER efficiency.

Stabilization of p53 during *C. trachomatis* infection interferes with the growth and development of *C. trachomatis* (Siegl et al., 2014). Many intracellular bacteria, including *C. trachomatis* downregulate tumor suppressor, p53, during infection (Siegl and Rudel, 2015). Since p53 is shown to be actively involved in BER process in both *in vitro* and *in vivo* (Zhou et al., 2001; Seo et al., 2002), the effect of p53 downregulation on BER efficiency was investigated. p53 was transiently knocked down in primary HOSE cells using p53 specific siRNA. Nuclear lysates were prepared and analyzed for expression of polymerase β by immunoblotting and for BER efficiency by repair assay. In agreement with previous findings, knockdown of p53 lead to a weak albeit significant downregulation of polymerase β **(Figure 4.17 C and D)**. Transient knockdown of p53 also significantly diminished BER efficiency in the repair assay **(Figure 4.17 A and B)**. This data suggests that downregulation of p53 affects the expression of polymerase β whereas strongly reduces the BER efficiency. To further elucidate the p53 dependent mechanism of BER regulation, p53 was transiently overexpressed in primary HOSE cells by transfecting them with HA-tagged p53 plasmid. Extremely low amount of plasmid (50 ng) was used for transfection and cells were transfected after 8 h of *C. trachomatis* infection so that the growth of *Chlamydia* itself was not affected. Native nuclear lysates were prepared and analyzed for BER efficiency. Interestingly, there was no statistically significant difference in BER efficiency in p53 overexpressed cells during *C. trachomatis* infection as compared to non-infected cells **(Figure 4.18)**. This experiment indicated that p53 is essential for efficient BER and attenuation of BER during infection can be rescued by p53 upregulation.
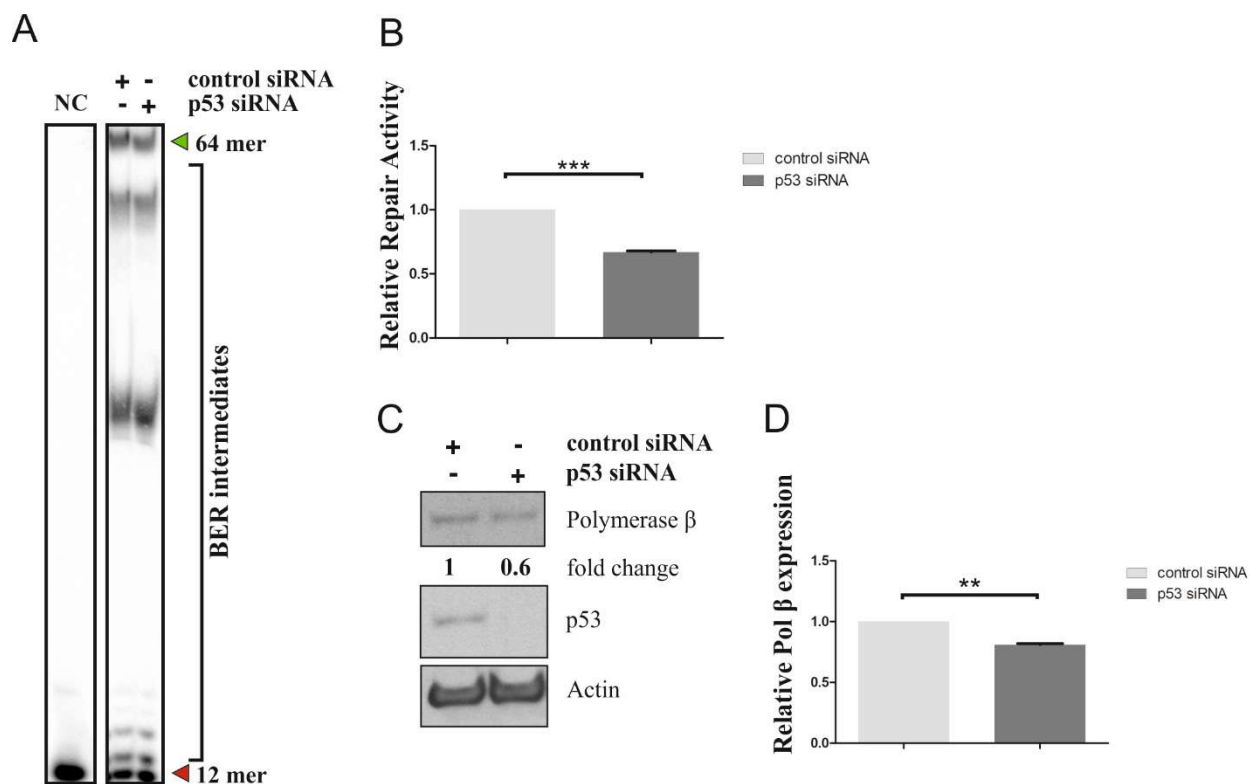
Figure 4.17. Effect of p53 knock-down on BER. Primary HOSE cells were transfected with p53 siRNA and scrambled control for 36 h. **(A)** Repair assay was performed by incubating nuclear lysates with substrate with 3 gaps and the products were resolved on denaturing urea gel and scanned in phosphor-imager. Red arrow corresponds to substrate and green arrow to the final product. NC is negative control wherein lysate was omitted. **(B)** Quantification of final products of BER in panel (A) marked with green arrow. **(C)** Immunoblot analysis of native nuclear lysates prepared after 36 h of siRNA transfection. Polymerase β and p53 were quantified, Actin was used for normalization. **(D)** Quantification of polymerase β in panel (C). Error bars show mean ±SEM from two independent experiments. ** $p < 0.01$, *** $p < 0.001$.
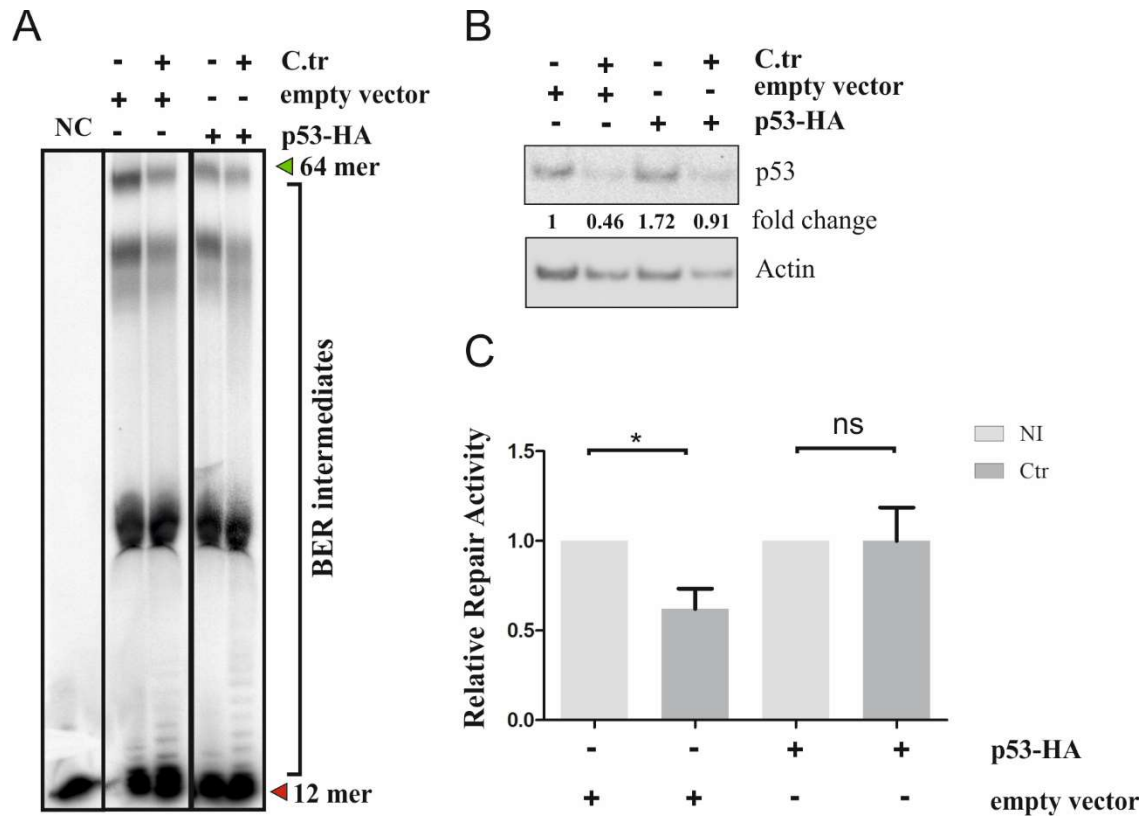
Figure 4.18. Effect of p53 overexpression on BER. Primary HOSE cells were transfected with pCDNA-p53HA plasmid and empty vector 8 h post *C. trachomatis* infection. Native nuclear lysates were prepared after 30 h of total infection. **(A)** Repair assay was performed using substrate with 3 gaps and products were resolved on denaturing urea gel and scanned in phosphor-imager. Red arrow corresponds to substrate and green arrow to the final product. NC is negative control wherein lysate was omitted. **(B)** Immunoblot analysis for p53 fold change in lysates used in repair assay in panel (A) p53 and actin specific antibodies were used for immunoblotting. **(C)** Quantification of final products of BER in panel (A) marked with green arrow. Red arrow corresponds to substrate and NC is negative control wherein lysate was omitted. Error bars show mean ±SEM from two independent experiments. * $p < 0.05$, ns not significant.

To further confirm the involvement of p53 in regulation of BER during *C. trachomatis* infection, similar repair experiments were performed in lung adenocarcinoma H1299 cells which have a homozygous deletion in the *TP53* gene. Interestingly, *C. trachomatis* infection did not have significant effect on BER efficiency in H1299 cells **(Figure 4.19)**.
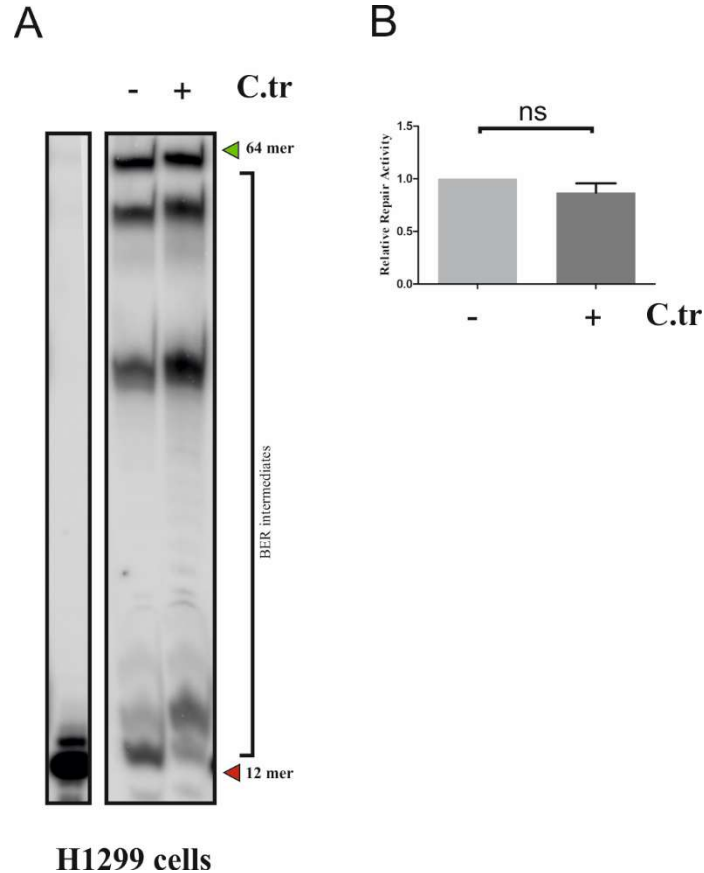
Figure 4.19. Effect of *C. trachomatis* on BER in p53^{-/-} H1299 cells. H1299 cells with a homozygous deletion in *TP53* gene were infected with *C. trachomatis* at MOI of 1 for 30 h. Native nuclear lysates were prepared after 30 h of infection. **(A)** Repair assay was performed using substrate with 3 gaps and products were resolved on denaturing urea gel and scanned in phosphor-imager. Red arrow corresponds to substrate and green arrow to the final product. NC is negative control wherein lysate was omitted. **(B)** Quantification of final products of BER in panel (A) marked with green arrow. Error bars show mean ±SEM from two independent experiments. ns not significant.

These experiments suggest that p53 is essential for BER as transient downregulation of p53 lead to downregulation of polymerase β and impaired BER **(Figure 4.17).** The efficiency of BER during *C. trachomatis* infection could be rescued by complementing infected cells with low amount of p53 **(Figure 4.18).** Moreover, *C. trachomatis*-mediated downregulation of BER is

absent in p53$^{-/-}$ H1299 cell line **(Figure 4.19).** This suggests that miR-499-mediated downregulation of polymerase β during *C. trachomatis* infection is dependent on p53. Another explanation for this result would be the differential expression of miR-499 in H1299 cells (cell-type specific miRNA expression). Hence, *C. trachomatis* could not downregulate BER in these cells as miR-499-mediated regulation of polymerase β was absent. However, further studies are required to confirm if this is a cell line specific effect or if the impaired BER efficiency during infection is mediated exclusively through p53.

5. DISCUSSION

Nearly one-sixth of the global cases of cancer are attributed to infectious agents (Plummer et al., 2016). This makes it very critical to understand the biology of microbial pathogenesis and mechanism of host cell modulations to successfully be able to avoid tumorigenesis. Although the microbes and types of cancers they cause are varied, the mechanisms of oncogenesis remain more or less conserved. Generally, oncogenic pathogens act by modulating host cell signal transduction, altering host cell physiology, inducing chronic inflammation or interacting with other microbes (Blaser, 2008). Several studies have confirmed Human herpesvirus 6 and *C. trachomatis* signatures in ovarian cancer samples. (Banerjee et al., 2017; Idahl et al., 2010; Ness et al., 2008, 2003; Shanmughapriya et al., 2012). This work attempts to identify the mechanisms through which these pathogens may induce tumorigenesis in their individual capacity and provides insight on possible ensuing changes in the host cell due to their co-infection.

5.1 Multiple HHV-6 DR copies may be present in ciHHV-6 individuals

HHV-6 integrates in the telomeric or sub-telomeric regions of the host chromosomes and integration is facilitated by telomeric sequences present in the direct repeat (DR) region of HHV-6 genome (Arbuckle et al., 2010). It was believed that almost full length genome integrates in host telomeres and studies have demonstrated genome sequences of integration sites (Tweedy et al., 2015). The integrated genome is quite unstable and prone to be released from host telomeres (Huang et al., 2014). This study shows that despite of the expected theoretical 1:2 ratio between HHV-6 genome and DR, additional DR copies per HHV-6 genome may be present both in patients and cultured cell lines. Here, three iciHHV-6 patient PBMC samples indicated that more than two copies of DR may be present per single copy of HHV-6 genome. Moreover, when these patients were followed up for a period of three years the number of DR copies fluctuated in two out of

three samples over the period of time. This unstable nature of DR suggested the existence of a mechanism by which DR sequences replicated or were lost. The extra copies of DR may not necessarily mean that multiple integrations of DR occur within the genome. Presence of extrachromosomal circular DR copies were reported in previous studies (Huang et al., 2014; Prusty et al., 2013b). These extrachromosomal DRs may replicate by rolling circle replication method using telomeric DNA as template (Schofield, 2007) and later integrate as a DR concatemer. This concatemeric DR may be detected as more than one copy by PCR analysis employing single set of primer pair. There are two possibilities of DR retention after viral reactivation. First, where simply DR may be excised **(Figure 1.3-a)** which may later replicate and re-integrate. Or second, where viral genome may be excised with one DR leaving behind the other DR integrated in the host genome **(Figure 1.3-f)** (Prusty et al., 2013b; Wood and Royle, 2017). FISH analysis in this work show that DR present in the absence of HHV-6 genome is still integrated in the genome and not necessarily present in episomal form. *In vitro* assays and patient sample analysis confirmed that extra DR copies may be present in iciHHV-6 individuals and these copies may still remain integrated in the genome.

5.2 Viral DR copies may integrate in non-telomeric regions of host chromosomes

Although it is a general understanding that HHV-6 integrates in telomeric and sub-telomeric regions of chromosome, an unusual observation of non-telomeric integration is presented in this work. In the ciHHV-6 cell culture model employed for this study many single cell clones which did not possess any HHV-6 genome but had DR copies showed the presence of DR copies in non-telomeric regions of chromosomes. Both FISH analysis and inverse PCR confirmed non-telomeric integration in both cell line models as well as patient PBMC samples. Moreover, sequencing of the non-telomeric junction regions indicated DR integrations in intronic regions of chromosomes

5q13.3 and 20q13.33 which may alter the expression of important genes like *AGGF1* and *GAIP* respectively. AGGF1 is angiogenesis factor with G patch and FHA domains 1 whereas GAIP is a G-alpha interacting protein. Integration of a viral sequence in intronic regions of genes may enhance the expression of the gene (Ikeda et al., 2007). Moreover, intronic integration may also result in viral-human fusion transcript which is also reported to increase the expression of a gene as shown during integration of HBV in hepatocarcinoma (Leary et al., 2008). GAIP is a GTPase interacting protein and is implicated in various signal transduction pathways including activation and phosphorylation of protein kinase C (De Vries et al., 1995). Thus, HHV-6 DR integration in the intronic regions of this region may alter or induce signal transduction of host cell. AGGF1 plays an important role in angiogenesis and proliferation of endothelial cells (Fan et al., 2009). Overexpression of AGGF1 would certainly point towards tumorigenesis. Furthermore, HHV-6 DR codes for DR6/7 proteins which are known to inhibit the function of tumor suppressor p53 and thereby have a potential for oncogenesis (Lacroix et al., 2010; Schleimann et al., 2014, 2009). DR region also codes for viral microRNAs which may modulate expression of host cell proteins (Tuddenham et al., 2012). Therefore, assuming that non-telomeric integration is a random event, integration of DR in an open reading frame would be definitely plausible and may lead to tumorigenesis.

Recent report has also corroborated this observation of finding viral genome in ovarian cancer samples (Banerjee et al., 2017). Here a microarray methodology was used to screen 99 ovarian cancer samples against matched and unmatched controls. Integration was identified using primers against HHV-6 U47 ORF and non-telomeric integration was found in several potential oncogenic genes.

This study, thus, reported an important observation that the presence of HHV-6 DR sequences as well high copy number of DR sequences may contribute towards tumorigenesis.

5.3 *C. trachomatis* impairs base excision repair (BER)

C. trachomatis causes oxidative DNA damage throughout the course of its infection. In alkaline comet assay, non-infected cells showed increased tail DNA indicating damage after H_2O_2 treatment whereas tail DNA retreats back to the nucleus after removal of H_2O_2 indicating DNA repair. This damage-repair response is not seen in cells infected with *C. trachomatis.* Infected cells display elevated DNA damage throughout the infection suggesting that the rate of oxidative DNA repair was not proportionate to the severity of oxidative DNA damage.

Polymerase β which is the primary polymerase enzyme involved in repairing the oxidized DNA bases through BER mechanism was downregulated during *C. trachomatis* infection. Interestingly, only wild type *C. trachomatis* could downregulate polymerase β but not CPAF⁻ *C. trachomatis.* This indicated that CPAF which is an important protease for *Chlamydia* itself, could acts as an effector protein in this mechanism of downregulation. *C. trachomatis* changes the host miRNome and one of the microRNAs upregulated during infection was miR-499 which is known to regulate polymerase β. Quantitative PCR showed that miR-499 was nearly 3-fold upregulated during infection. Corroborating with polymerase β expression levels, CPAF⁻ *Chlamydia* mutant did not upregulate miR-499. Inhibiting miR-499 rescued the polymerase β expression as well the BER activity. Also, BER activity was inhibited by using miR-499 mimic. The specificity of miR-499-polymerase β interaction was checked by cloning polymerase β 3'UTR in a dual luciferase vector. Here, polymerase β 3'UTR was cloned downstream of Renilla luciferase and Firefly luciferase was used as a transfection control. Wild type but not CPAF⁻ *Chlamydia* downregulated the Renilla luciferase activity. This confirmed that the downregulation of polymerase β was miR-499 specific.

However, the downregulation of luciferase activity during wild type *Chlamydia* infection was marginal. This could be explained by presence of a single binding site for miR-499 within the polymerase β 3'UTR.
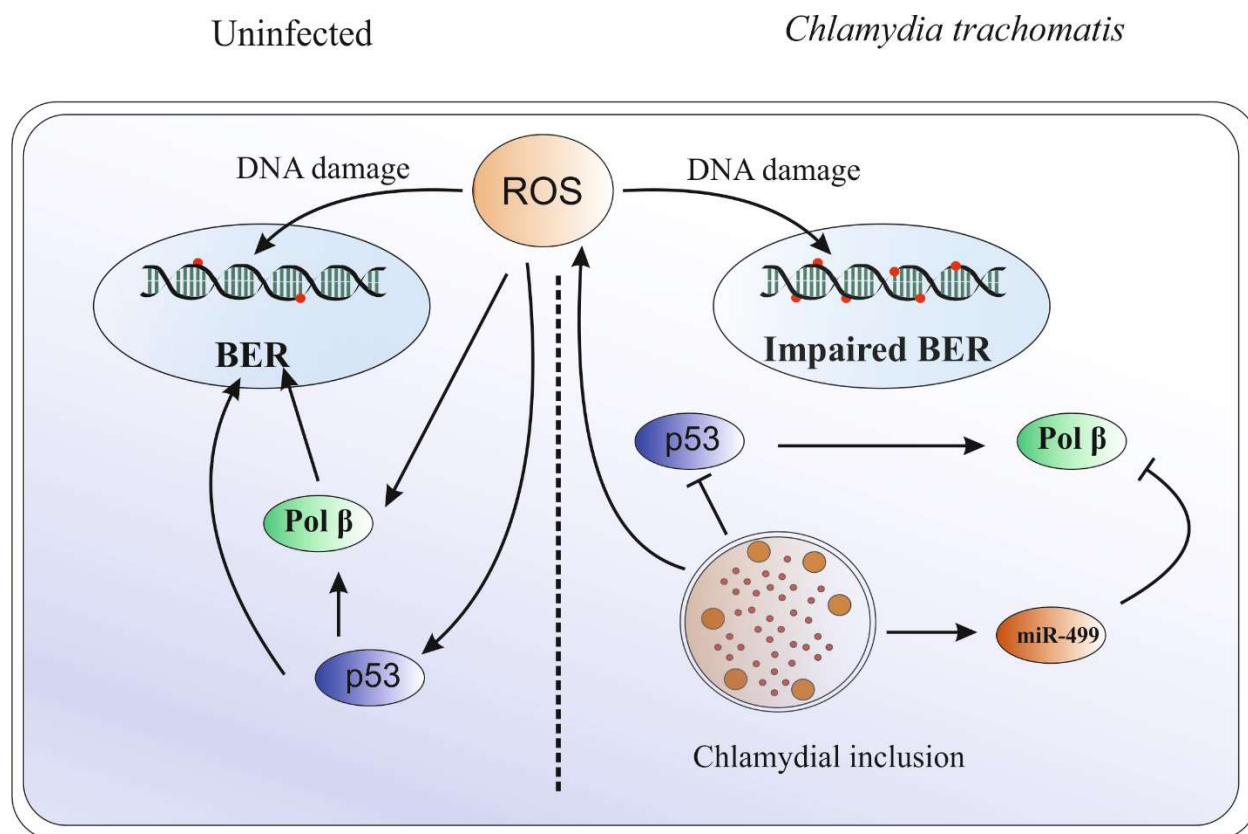
Figure 5.1. Schematic representation of *C. trachomatis* mediated impaired BER. *Chlamydia* downregulates p53 through previously studied mechanisms and polymerase β through miR-499 upregulation. Both p53 and polymerase β are involved in BER process. Thus, *C. trachomatis* impairs BER by downregulating p53 and polymerase β.

Furthermore, wild type *C. trachomatis* downregulated tumor suppressor p53 which is agreement with previous studies (González et al., 2014; Siegl et al., 2014). Interestingly however, CPAF⁻ *Chlamydia* did not downregulate p53. Tumor suppressor p53 is also known to play direct role in BER process (Seo et al., 2002). *In vitro* assays using recombinant proteins have shown that p53

binds directly to polymerase β and stabilizes its interaction with abasic DNA (Zhou et al., 2001). Transient siRNA mediated knockdown of p53 in primary human ovarian surface epithelial cells indeed displayed reduced BER efficiency. Moreover, after transient upregulation of p53 using p53-HA plasmid, there did not seem significant reduction in BER in the infected cells as compared to the non-infected control. *In vitro* BER assay also showed that there was no difference in the BER activity during *C. trachomatis* infection in p53$^{-/-}$ H1299 cells. These results indicated that impaired BER could be dependent on downregulation of p53 during infection as well.

Taken together, these results illustrate that *C. trachomatis* impairs host BER biaxially through CPAF-miR-499-polymerase β axis as well as via the CPAF-p53-polymerase β axis **(Figure 5.1)**.

5.4 *C. trachomatis* mediates alternate lengthening of telomeres (ALT) and epigenetic modifications.

Besides causing pan-genomic oxidative DNA damage, *C. trachomatis* also causes telomere specific damage of the host chromosomes. Past studies have shown that *C. trachomatis* causes transient telomere shortening i.e. telomeres are shortened during early infection and are later re-built transiently during middle stage of infection followed by complete loss in the final stage of infection. (Prusty et al., 2013b). Recently a nuclear effector protein of *Chlamydia*, NUE, which is secreted via the type III secretion system during late stages (18-24 h) of infection was identified (Pennini et al., 2010). Imaging and biochemical analysis of chromatin bound proteins suggested that NUE translocates to the nucleus during infection (Pennini et al., 2010). Experiments from our group show that NUE has telomere specific binding activity (Prusty et al., unpublished). Interestingly, the phenomenon of transient telomere shortening which is observed in wild type *Chlamydia* infected cell was absent in NUE⁻ *Chlamydia* infected cells. In the NUE⁻ *Chlamydia* infected cells, telomeres are shortened much later in infection and the typical 'rebuilding' of

chromosomes was not seen **(Figure 5.2)**. These experiments suggest that NUE may be able to elongate the telomeres. Critically shortened telomeres initiate a p53 mediated response leading the cells to senescence (Evan and d'Adda di Fagagna, 2009) or apoptosis (Vaziri et al., 1997). This rebuilding of telomeres may explain the strategy employed by *Chlamydia* to circumvent p53-mediated apoptosis or senescence.

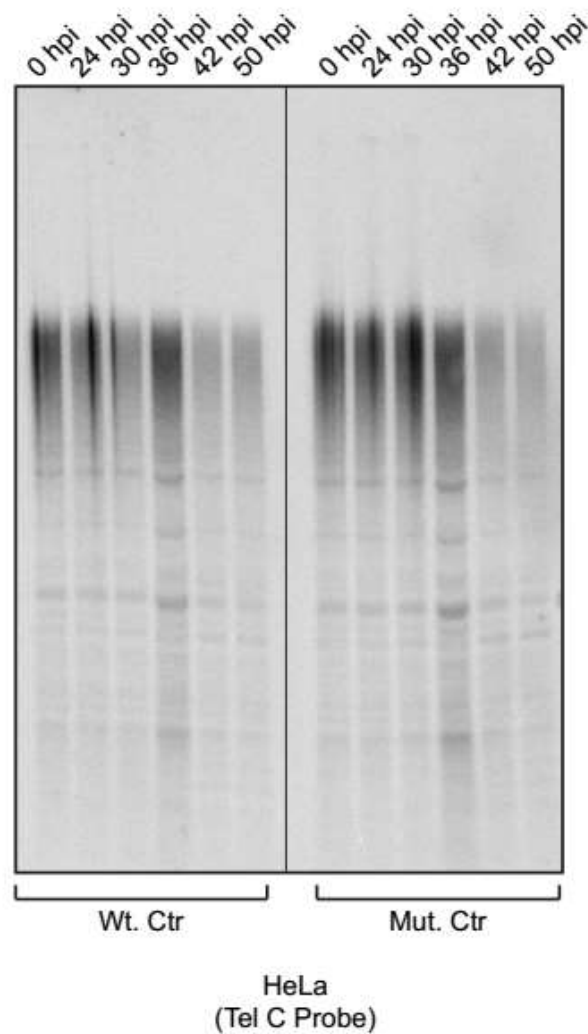**Figure 5.2.** *C. trachomatis* **infection causes alternate lengthening of telomeres.** HeLa cells were infected with wild type and NUE⁻ *Chlamydia* for different time points. During wild type *Chlamydia* infection telomeres are shortened from 24-30 h but are transiently elongated after 30 h. During NUE⁻ *Chlamydia,* however, a consistent loss of telomeres is observed till the end of infection cycle.

NUE protein also has histone methyltransferase activity and is able to methylate H2A, H3 and H4 histones (Pennini et al., 2010). Intracellular pathogens are known to induce epigenetic modifications to support their survival (Hamon and Cossart, 2008). It has also been suggested that *C. trachomatis* induces hypermethylation of the genome to create heterochromatin and thereby limit DNA damage and related apoptotic response (Chumduri et al., 2013). Preliminary data from our group shows that *C. trachomatis* induced changes in the epigenetic makeup of host genome. Immunoblot analysis of acetylation and methylation markers of histones H3 and H4 showed differences in wild type and NUE⁻ *Chlamydia* infections **(Figure 5.3)**. Trimethylation of lysine 4 residue (H3K4me3) and trimethylation of lysine 27 (H3K27me3) residue of histone H3 were nearly unchanged in wild type *Chlamydia* infected cells but reduced NUE⁻ *Chlamydia* infected cells **(Figure 5.3)**. However, there was a noticeable difference in the methylation pattern of lysine 9 residue of histone H3 (H3K9me3) which was nearly 3 times upregulated in both wild type and NUE⁻ *Chlamydia* infected cells **(Figure 5.3)**. The pan-acetylation of histone H4 (H4ac) and that of lysine 27 residue of histone 3 (H3K27ac) was decreased in the NUE⁻ as compared to the wild type *Chlamydia* infection **(Figure 5.3).**

These results suggest that during *C. trachomatis* infection, there is telomere shortening which is transiently repaired in wild type chlamydia but not in NUE⁻ *Chlamydia* infected cells. This is indicative of NUE protein being responsible for the transient repairing of telomeres. Also, these results show that trimethylation of histone 3 at lysine 9 (H3K9me3) is highly upregulated in *C. trachomatis* infected cells which is an indicator of heterochromatin formation. Surprisingly, acetylation at lysine 27 residue of H3 and pan-acetylation of H4 are markedly reduced in NUE⁻ *C. trachomatis*. Since NUE is a histone methyl transferase, it is unlikely to be involved directly in

acetylation of histone residues. The low acetylation signal in NUE^{-} *Chlamydia* infected cells may

be due to an indirect mechanism which needs to be further investigated.
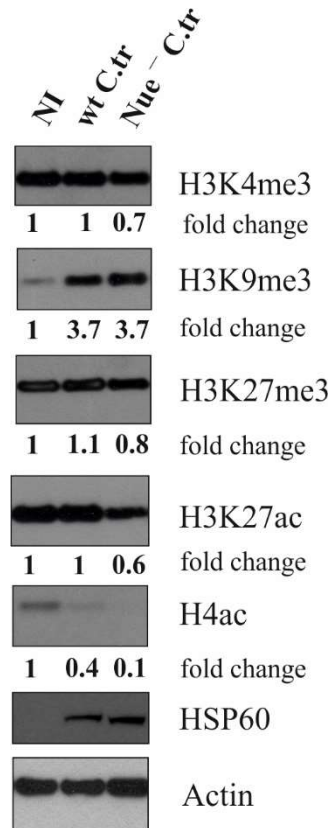
Figure 5.3. *C. trachomatis* **infection causes epigenetic modification of the host genome.** Primary HOSE cells were infected with wild type and NUE^{-} mutant *C. trachomatis* at MOI of 1 for 24 h. Post-translational modifications of histones H3 and H4 were analyzed by western blotting using respective specific antibodies.

5.5 *C. trachomatis* and HHV-6 in Ovarian Cancer- Hypothesis and Perspective

Physicist Thomas Kuhn defined paradigms as the best ways of explaining progress in science

(Kuhn, 1970). As opposed to the popular belief that progress is accumulation of corpus of scientific

knowledge, he believed that progress is in fact identifying a puzzle and then providing a standard

solution for the same. The standard solution, or a *paradigm,* would ensure the scientists that a

solution exists for every puzzle. But when puzzles repeatedly resist the paradigm, a crisis of

confidence occurs which may result in rejecting the paradigm and replacing it in turn with a new one. And thus, begins a *paradigm-shift* or scientific revolution.

The current functional paradigm of ovarian cancer being caused by infectious agents involves identifying an isolated pathogen in the ovarian tissue and then using *in vitro* methodologies to provide evidence of the oncogenic potential of the pathogen in question. Several studies have shown that infection of a cell with certain pathogens such as HPV, KSHV or EBV may lead to tumorigenesis which are well within the scope of the existing paradigm (White et al., 2014). This approach has however failed in the field of *C. trachomatis* or HHV-6 to come to a consensus concerning the mechanism through which they might cause the transformation. *C. trachomatis* with its 48 hours life cycle and HHV-6 with its benign nature do not form tangible examples of the current paradigm. Therefore, infection of a cell with these pathogens simply is very unlikely to induce oncogenesis.

Many theories have been put forward to explain the epidemiological relevance of *C. trachomatis* infection in ovarian cancer. One of the theory argues that *Chlamydia* infects the fimbrial cells which are further transplanted in the ovary where it develops into cancer (Carvalho and Carvalho, 2008). Although this work mentioned anatomical proximity of the ovary to fimbria as one of the reasons, it does not elaborate on the molecular mechanism. Another study explains an interesting take on paracrine signaling in *C. trachomatis* infected epithelial cells through Wnt signaling followed by subsequent regulation of transcription (Kessler et al., 2012). This theory would explain the absence of pathogen in ovarian tissue wherein only few cells are *infected* but many in the vicinity are *affected*.

This work focuses on the genomic instability which *C. trachomatis* infection may cause in epithelial cells, how this instability in turn may interact with a latent ciHHV-6 and how these

changes may cumulatively prove detrimental. This study has shown that *C. trachomatis* impairs the BER capacity in primary ovarian epithelial cells. BER primarily repairs SSBs which if left unrepaired leads to mutations. For instance, if oxidized guanine or 8-oxo-guanine is left unrepaired, the replication machinery may mis-insert adenine in place of guanine and in the subsequent replication cycles there will be a G:C to A:T mismatch mutation (Cheng et al., 1992). This study also focuses on epigenetic manipulations of *C. trachomatis* where the genome is rather condensed due to hypermethylation. In HHV-6 co-infection or *C. trachomatis* mediated ciHHV-6 reactivation scenario, the viral genome would not have access to most of the host genome as it is already in a heterochromatin form. However, *C. trachomatis* upregulates certain genes which would be still active or in euchromatin state and accessible for the virus to integrate. This would highly increase the chances of viral integration in those genes which are upregulated by *Chlamydia*. This study explains an unusual finding of DR sequences being integrated in non-telomeric regions of human chromosomes (Gulve et al., 2017). Another study has even found HHV-6 ORF at non-telomeric regions and thus disrupting crucial genes or upregulating certain oncogenes (Banerjee et al., 2017). Future high throughput studies which employ bioinformatic approach are therefore necessary to analyze upregulated genes during *Chlamydia* infection. The upregulated target genes from such an 'omics-data' should be then be analyzed for HHV-6 integration efficiency at these genes.

Treatment of infection induced ovarian cancer would certainly be benefitted from early diagnosis. Studies have shown that ovarian cancer can remain undetected for a long time even during annual CA-125 antigen testing and transvaginal ultrasound and then can be suddenly presented at late stages (Partridge et al., 2009). This makes it very important to detect the infection and address it immediately. It is time to upgrade the Hippocratic dyad which suggests the importance of man-

environment relationship with a third factor- the etiological agent. This would prove to be highly useful in combating the infectious disease induced cancer. Preventive medicine for infection induced cancer can be categorized into three stages- Primary prevention which addresses the apparently healthy individual to prevent the occurrence of disease. Secondary prevention which addresses the infection and prevent progression of disease and tertiary prevention which treats the metastasis and prevents relapse (de Flora and Bonanni, 2011). Treating HHV-6 and *Chlamydia* infections promptly would indeed be the secondary prevention strategy, primary being developing vaccines or general preventive strategies.

Understanding the molecular mechanisms of infection induced cancer also would aid in choosing the right therapy. For instance, since PI3 kinase is upregulated in *C. trachomatis* infection which is also the case in 70% of ovarian cancer patients, PI3 kinase inhibitors would surely be of importance apart from antibiotics against infection. This study underlines the role of p53 in genome stability which is also downregulated during *C. trachomatis* infection. Therefore, harnessing the role of small molecules such as nutlins which stabilize p53 by inhibiting its proteasomal degradation would serve as a key to minimize the burden of *C. trachomatis* and HHV-6 infection induced ovarian cancer.
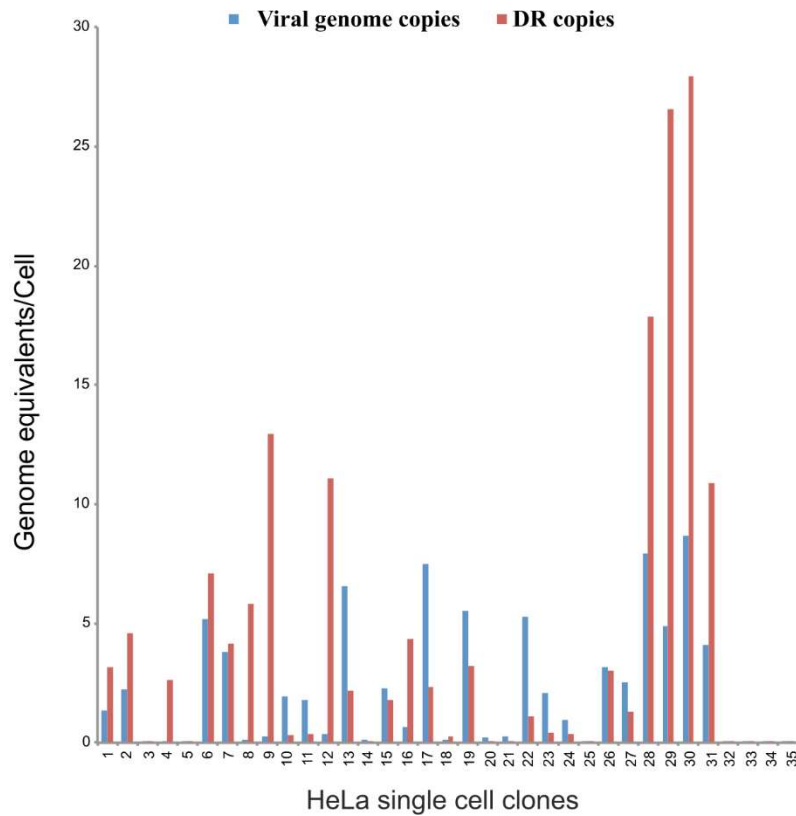
6. APPENDIX

Figure 6.1. Analysis of ciHHV-6 HeLa single cell clones for number of viral (HHV-6) and DR copies by qPCR. ciHHV-6 HeLa single cell clones demonstrate a variable number of DR per viral (HHV-6) genome. Clone numbers 29 and 30 show presence of more than 20 copies of DR. (Gulve et al., 2017)

A

```
U-251        --------------------------------TCTGGGACCCACAGACAGACCTGGACTCT
AH010108.2   CAGGTCTAGCCTGCTGCCCCTGGCTGAGACCTCTGGGACCCACAGACAGACCTGGACTCT
                                             ****************************

U-251        TGGTGGGAAGCCACTCTGCCCACTCCCCACCCCAGACACCCTAGAAGCCAGTCTGGCCAC
AH010108.2   TGGTGGGAAGCCACTCTGCCCACTCCCCACCCCAGACACCCTAGAAGCCAGTCTGGCCAC
             ************************************************************

U-251        CACCCGCACGCACCAGTTGGTAGCCCCAGACTCTCGGGGCCCCTTTGGGAGGGGCTGGGA
AH010108.2   CACCCGCACGCACCAGTTGGTAGCCCCAGACTCTCGGGGCCCCTTTGGGAGGGGCTGGGA
             ************************************************************

U-251        GCCGGAAACCAAGAAAGAGGAACCCAGGCTTCCGGCTTCCCAGGGAGTGAGCGGATGGGG
AH010108.2   GCCGGAAACCAAGAAAGAGGAACCCAGGCTTCCGGCTTCCCAGGGAGTGAGCGGATGGGG
             ************************************************************

U-251        GTGTCTCGGAACCTCCAGTGGGGGCCTCATCTGGGGCCCAGCCTGGGAGGAGGGGCCAGA
AH010108.2   GTGTCTCGGAACCTCCAGTGGGGGCCTCATCTGGGGCCCAGCCTGGGAGGAGGGGCCAGA
             ************************************************************

U-251        AGCTGCTGCAGCTCCCTCCTCAATGATC--------------------------------
AH010108.2   AGCTGCTGCAGCTCCCTCCTCAATGATCCTGGACCCCCTCCCAGCCCTGCTGTAAGCTTG
             ****************************
```

B

```
NNDM3        ------------------------------------------GCAGCTGCCCACTCTGAGAA
NG_027822.1  GCAACCACCCCGTCTGAGAAGTGAGGAGCCCCTCCGCCCGGCAGCTGCCCACTCTGAGAA
                                                       *******************

NNDM3        GTGAGGAGCCTCTCCGCCCGGCAGCCACCCCATCTGGGAAGTGAGGAGCGTCTCCGCCCG
NG_027822.1  GTGAGGAGCCTCTCCGCCCGGCAGCCACCCCATCTGGGAAGTGAGGAGCGTCTCCGCCCG
             ************************************************************

NNDM3        GCAGCCACCCCGTCCGGGAGGGAGGTGGGGG-----------------------------
NG_027822.1  GCAGCCACCCCGTCCGGGAGGGAGGTGGGGGGGATCAGCCCCCCGCCCGGCCAGCCGCCC
             ******************************
```

Figure 6.2. Sequence alignment of viral DR non-telomeric integration sites. (A) U251 clone 15 non-telomeric integration at Chr 20q13.3 aligned with human G-alpha interacting protein isoform B (GAIP) (Accession number AH010108.2). **(B)** iciHHV-6 patient NNMD3 non-telomeric integration at Chr 5q13.3 aligned with human angiogenic factor with G patch and FHA domains 1 (AGGF1) (Accession number NG_0.27822.1). (Gulve et al., 2017)

7. REFERENCES

Abdul-Sater, A.A., Saïd-Sadier, N., Lam, V.M., Singh, B., Pettengill, M.A., Soares, F., Tattoli, I., Lipinski, S., Girardin, S.E., Rosenstiel, P., Ojcius, D.M., 2010. Enhancement of reactive oxygen species production and chlamydial infection by the mitochondrial Nod-like family member NLRX1. J. Biol. Chem. 285, 41637–41645.

Ablashi, D., Agut, H., Berneman, Z., Campadelli-Fiume, G., Carrigan, D., Ceccerini-Nelli, L., Chandran, B., Chou, S., Collandre, H., Cone, R., Dambaugh, T., Dewhurst, S., DiLuca, D., Foa-Tomasi, L., Fleckenstein, B., Frenkel, N., Gallo, R., Gompels, U., Hall, C., Jones, M., Lawrence, G., Martin, M., Montagnier, L., Neipel, F., Nicholas, J., Pellett, P., Razzaque, A., Torrelli, G., Thomson, B., Salahuddin, S., Wyatt, L., Yamanishi, K., 1993. Human herpesvirus-6 strain groups: a nomenclature. Arch. Virol. 129, 363–366.

Agut, H., Bonnafous, P., Gautheret-Dejean, A., 2015. Laboratory and Clinical Aspects of Human Herpesvirus 6 Infections. Clin. Microbiol. Rev. 28, 313–335.

Akbari, M., Otterlei, M., Diaz-Peña, J., Aas, P.A., Kavli, B., Liabakk, N.B., Hagen, L., Imai, K., Durandy, A., Slupphaug, G., Krokan, H.E., 2004. Repair of U/G and U/A in DNA by UNG2-associated repair complexes takes place predominantly by short-patch repair both in proliferating and growth-arrested cells. Nucleic Acids Res. 32, 5486–5498. Aleman, L.M., Doench, J., Sharp, P.A., 2007. Comparison of siRNA-induced off-target RNA and protein effects. Rna 13, 385–395. https://doi.org/10.1261/rna.352507

Anglesio, M.S., Bashashati, A., Wang, Y.K., Senz, J., Ha, G., Yang, W., Aniba, M.R., Prentice, L.M., Farahani, H., Li Chang, H., Karnezis, A.N., Marra, M.A., Yong, P.J., Hirst, M., Gilks, B., Shah, S.P., Huntsman, D.G., 2015. Multifocal endometriotic lesions associated with cancer are clonal and carry a high mutation burden. J. Pathol. 236, 201–209.

Anglesio, M.S., Wang, Y.K., Maassen, M., Horlings, H.M., Bashashati, A., Senz, J., Mackenzie, R., Grewal, D.S., Li-Chang, H., Karnezis, A.N., Sheffield, B.S., McConechy, M.K., Kommoss, F., Taran, F.A., Staebler, A., Shah, S.P., Wallwiener, D., Brucker, S., Gilks, C.B., Kommoss, S., Huntsman, D.G., 2016. Synchronous Endometrial and Ovarian Carcinomas: Evidence of Clonality. J. Natl. Cancer Inst. 108, 1–5.

Arbuckle, J.H., Medveczky, M.M., Luka, J., Hadley, S.H., Luegmayr, a., Ablashi, D., Lund, T.C., Tolar, J., De Meirleir, K., Montoya, J.G., Komaroff, a. L., Ambros, P.F., Medveczky, P.G., 2010. The latent human herpesvirus-6A genome specifically integrates in telomeres of human chromosomes in vivo and in vitro. Proc. Natl. Acad. Sci. 107, 5563–5568.

Arbuckle, J.H., Pantry, S.N., Medveczky, M.M., Prichett, J., Loomis, S., Ablashi, D., Medveczky, P.G., 2013. Mapping the telomere integrated genome of human herpesvirus 6A and 6B. Virology 442, 3–11.

Bachmann, N.L., Polkinghorne, A., Timms, P., 2014. Chlamydia genomics: Providing novel insights into chlamydial biology. Trends Microbiol. 22, 464–472.

Bagga, S., Bracht, J., Hunter, S., Massirer, K., Holtz, J., Eachus, R., Pasquinelli, A.E., 2005. Regulation by let-7 and lin-4 miRNAs results in target mRNA degradation. Cell 122, 553–

563.

Banerjee, S., Tian, T., Wei, Z., Shih, N., Feldman, M.D., Coukos, G., Alwine, J.C., Robertson, E.S., 2017. The ovarian cancer oncobiome. Oncotarget 8, 36225–36245.

Bartel, D.P., 2004. MicroRNAs: Genomics, Biogenesis, Mechanism, and Function. Cell 116, 281–297.

Bartkova, J., Hořejší, Z., Koed, K., Krämer, A., Tort, F., Zleger, K., Guldberg, P., Sehested, M., Nesland, J.M., Lukas, C., Orntoft, T., Lukas, J., Bartek, J., 2005. DNA damage response as a candidate anti-cancer barrier in early human tumorigenesis. Nature 434, 864–870.

Bast, R.C., Hennessy, B., Mills, G.B., 2009. The biology of ovarian cancer: new opportunities for translation. Nat. Rev. Cancer 9, 415–28.

Bastidas, R.J., Elwell, C.A., Engel, J.N., Valdivia, R.H., 2013. Chlamydial intracellular survival strategies. Cold Spring Harb. Perspect. Med. 3, 1–20.

Behm-Ansmant, I., Rehwinkel, J., Doerks, T., Stark, A., Bork, P., Izaurralde, E., 2006. mRNA degradation by miRNAs and GW182 requires both CCR4 : NOT deadenylase and DCP1 : DCP2 decapping complexes. Genes Dev. 20, 1885–1898 ST–MRNA degradation by miRNAs and GW1.

Berchuck, A., Kohler, M.F., Marks, J.R., Wiseman, R., Boyd, J., Bast, R.C., 1994. The p53 tumor suppressor gene frequently is altered in gynecologic cancers. Am. J. Obstet. Gynecol. 170, 246–252.

Berek, J.S., Friedlander, M.L., Hacker, N.F., 2015. Epithelial Ovarian, Fallopian Tubes, and Peritoneal Cancer, Berek&Hacker's Gynecologic Oncology.

Biberfeld, P., Kramarsky, B., Salahuddin, S.Z., Gallo, R.C., 1987. Ultrastructural characterization of a new human B lymphotropic DNA virus (human herpesvirus 6) isolated from patients with lymphoproliferative disease. J. Natl. Cancer Inst. 79, 933–41.

Blaser, M.J., 2008. Understanding microbe-induced cancers. Cancer Prev. Res. 1, 15–20.CAPR-08-0024

Böhme, L., Albrecht, M., Riede, O., Rudel, T., 2010. Chlamydia trachomatis-infected host cells resist dsRNA-induced apoptosis. Cell. Microbiol. 12, 1340–1351.

Bohr, V.A., 2002. Repair of oxidative DNA damage in nuclear and mitochondrial DNA, and some changes with aging in mammalian cells1,2. Free Radic. Biol. Med. 32, 804–812.

Boiteux, S., Radicella, J.P., 2000. The Human OGG1 Gene: Structure, Functions, and Its Implication in the Process of Carcinogenesis. Arch. Biochem. Biophys. 377, 1–8.

Bookman, M.A., Darcy, K.M., Clarke-Pearson, D., Boothby, R.A., Horowitz, I.R., 2003. Evaluation of monoclonal humanized anti-HER2 antibody, trastuzumab, in patients with recurrent or refractory ovarian or primary peritoneal carcinoma with overexpression of HER2: A phase II trial of the Gynecologic Oncology Group. J. Clin. Oncol. 21, 283–290.

Borchert, G.M., Lanier, W., Davidson, B.L., 2006. RNA polymerase III transcribes human microRNAs. Nat. Struct. Mol. Biol. 13, 1097–1101.

Boutolleau, D., Duros, C., Bonnafous, P., Caïola, D., Karras, A., Castro, N. De, Ouachée, M., Narcy, P., Gueudin, M., Agut, H., Gautheret-Dejean, A., 2006. Identification of human herpesvirus 6 variants A and B by primer-specific real-time PCR may help to revisit their respective role in pathology. J. Clin. Virol. 35, 257–63.

Braun, D.K., Dominguez, G., Pellett, P.E., 1997. Human herpesvirus 6. Clin. Microbiol. Rev. 10, 521–67.

Cabelof, D.C., 2012. Haploinsufficiency in mouse models of DNA repair deficiency: Modifiers of penetrance. Cell. Mol. Life Sci. 69, 727–740.

Caldecott, K.W., 2003. Protein-protein interactions during mammalian DNA single-strand break repair. Biochem. Soc. Trans. 31, 247–51.

Carbone, I., Lazzarotto, T., Ianni, M., Porcellini, E., Forti, P., Masliah, E., Gabrielli, L., Licastro, F., 2014. Herpes virus in alzheimer's disease: Relation to progression of the disease. Neurobiol. Aging 35, 122–129.

Carthew, R.W., Sontheimer, E.J., 2009. Origins and Mechanisms of miRNAs and siRNAs. Cell 136, 642–655.

Carvalho, J.P., Carvalho, F.M., 2008. Is Chlamydia-infected tubal fimbria the origin of ovarian cancer. Med. Hypotheses 71, 690–693.

Chen, D., Kon, N., Li, M., Zhang, W., Qin, J., Gu, W., 2005. ARF-BP1/mule is a critical mediator of the ARF tumor suppressor. Cell 121, 1071–1083.

Cheng, K.C., Cahill, D.S., Kasai, H., Nishimura, S., Loeb, L. a, 1992. 8-Hydroxyguanine, an abundant form of oxidative DNA damage, causes G----T and A----C substitutions. J. Biol. Chem. 267, 166–172.

Chowdhury, S.R., Reimer, A., Sharan, M., Kozjak-Pavlovic, V., Eulalio, A., Prusty, B.K., Fraunholz, M., Karunakaran, K., Rudel, T., 2017. *Chlamydia* preserves the mitochondrial network necessary for replication via microRNA-dependent inhibition of fission. J. Cell Biol. jcb.201608063.

Chumduri, C., Gurumurthy, R.K., Zadora, P.K., Mi, Y., Meyer, T.F., 2013. Chlamydia infection promotes host DNA damage and proliferation but impairs the DNA damage response. Cell Host Microbe 13, 746–758.

Collin, V., Flamand, L., 2017. HHV-6A/B integration and the pathogenesis associated with the reactivation of chromosomally integrated HHV-6A/B. Viruses 9.

Daibata, M., Taguchi, T., Nemoto, Y., Taguchi, H., Miyoshi, I., 1999. Inheritance of chromosomally integrated human herpesvirus 6 DNA. Blood 94, 1545–9.

Das, B.B., Rakheja, D., Lacelle, C., Sedlak, R.H., Gulve, N., Chowdhury, S.R., Prusty, B.K., 2016. Possible progesterone-induced gestational activation of chromosomally integrated human herpesvirus 6B and transplacental transmission of activated human herpesvirus 6B. J. Hear. Lung Transplant. 1–4.

Davidson, B., Nesland, J.M., Goldberg, I., Kopolovic, J., Gotlieb, W.H., Bryne, M., Ben-Baruch,

G., Berner, A., Reich, R., 2001. Expression of angiogenesis-related genes in ovarian carcinoma – A clinicopathologic study. Clin. Exp. Metastasis 18, 501–507.

De Bolle, L., Naesens, L., De Clercq, E., 2005. Update on human herpesvirus 6 biology, clinical features, and therapy. Clin. Microbiol. Rev. 18, 217–45.

de Flora, S., Bonanni, P., 2011. The prevention of infection-associated cancers. Carcinogenesis 32, 787–795.

De Vries, L., Mousli, M., Wurmser, A., Farquhar, M.G., 1995. GAIP, a protein that specifically interacts with the trimeric G protein G alpha i3, is a member of a protein family with a highly conserved core domain. Proc. Natl. Acad. Sci. 92, 11916–11920.

Denli, A.., Tops, B.B.., Plasterk, R.H.., Ketting, R.., Hannon, G.J., 2004. Processing of pri- mary microRNAs by the microprocessor complex. Nature 432, 231–235.

Dianov, G., Lindahl, T., 1994. Reconstitution of the DNA base excision-repair pathway. Curr. Biol. 4, 1069–1076.

Dianov, G.L., Hübscher, U., 2013. Mammalian base excision repair: The forgotten archangel. Nucleic Acids Res. 41, 3483–3490.

Dianov, G.L., Thybo, T., Dianova, I.I., Lipinski, L.J., Bohr, V.A., 2000. Single nucleotide patch base excision repair is the major pathway for removal of thymine glycol from DNA in human cell extracts. J. Biol. Chem. 275, 11809–11813.

Drago, F., Broccolo, F., Javor, S., Drago, F., Rebora, A., Parodi, A., 2014. Evidence of human herpesvirus-6 and -7 reactivation in miscarrying women with pityriasis rosea. J. Am. Dermatology 71, 198–199.

Duval, M., Cossart, P., Lebreton, A., 2017. Mammalian microRNAs and long noncoding RNAs in the host-bacterial pathogen crosstalk. Semin. Cell Dev. Biol. 65, 11–19.

Elwell, C.A., Engel, J.N., 2012. Lipid acquisition by intracellular Chlamydiae. Cell. Microbiol. 14, 1010–1018.

Elwell, C., Mirrashidi, K., Engel, J., 2016. Chlamydia cell biology and pathogenesis. Nat. Rev. Microbiol. 14, 385–400.

Ensminger, M., Iloff, L., Ebel, C., Nikolova, T., Kaina, B., & Löbrich, M. 2014. DNA breaks and chromosomal aberrations arise when replication meets base excision repair. The Journal of Cell Biology, 206(1), 29–43.

Eulalio, A., Huntzinger, E., Izaurralde, E., 2008. GW182 interaction with Argonaute is essential for miRNA-mediated translational repression and mRNA decay. Nat. Struct. Mol. Biol. 15, 346–353.

Evan, G.I., d'Adda di Fagagna, F., 2009. Cellular senescence: hot or what? Curr. Opin. Genet. Dev. 19, 25–31.

Fan, C., Ouyang, P., Timur, A.A., He, P., You, S.A., Hu, Y., Ke, T., Driscoll, D.J., Chen, Q., Wang, Q.K., 2009. Novel roles of GATA1 in regulation of angiogenic factor AGGF1 and endothelial cell function. J. Biol. Chem. 284, 23331–23343.

Fathalla, M.F., 2013. Incessant ovulation and ovarian cancer - a hypothesis re-visited. Facts, views Vis. ObGyn 5, 292–7.

Feeley, K.M., Wells, M., Histopathology, D., Hospital, R.H., Feeley, K.M., Wells, M., 2001. Precursor Lesions of Ovarian Epithelial Malignancy - Journals - NCBI 87–95.

Flamand, L., Lautenschlager, I., Krueger, G.R.F., Ablashi, D. V., Gautheret-Dejean, A., Agut, H., 2014. Chapter 2 – Practical Diagnostic Procedures for HHV-6A, HHV-6B, and HHV-7, in: Human Herpesviruses HHV-6A, HHV-6B & HHV-7. pp. 9–34.

Frenkel, N., Schirmer, E.., Wyatt, L.., Katsafanas, G., Roffman, E., Danovich, R., June, C., 1990. Isolation of a new herpesvirus from human CD4+ T cells. Proc. Natl. Acad. Sci. U. S. A. 748–752.

Friedberg, E.C., 2003. DNA damage and repair. Nature 421, 436–440.

Friedman, R.C., Farh, K.K.H., Burge, C.B., Bartel, D.P., 2009. Most mammalian mRNAs are conserved targets of microRNAs. Genome Res. 19, 92–105.

Gao, Y., Katyal, S., Lee, Y., Zhao, J., Rehg, J.E., Russell, H.R., McKinnon, P.J., 2011. DNA ligase III is critical for mtDNA integrity but not Xrcc1-mediated nuclear DNA repair. Nature 471, 240–246.

Goff, B. a, Mandel, L., Muntz, H.G., Melancon, C.H., 2000. Ovarian carcinoma diagnosis. Cancer 89, 2068–2075.

Gompels, U.A., Nicholas, J., Lawrence, G., Jones, M., Thomson, B.J., Martin, M.E.D., Efstathiou, S., Craxton, M., Macaulay, H.A., 1995. The DNA Sequence of Human Herpesvirus-6: Structure, Coding Content, and Genome Evolution. Virology 209, 29–51.

González, E., Rother, M., Kerr, M.C., Al-Zeer, M. a, Abu-Lubad, M., Kessler, M., Brinkmann, V., Loewer, A., Meyer, T.F., 2014. Chlamydia infection depends on a functional MDM2-p53 axis. Nat. Commun. 5, 5201.

Gordon, A.N., Finkler, N., Edwards, R.P., Garcia, a a, Crozier, M., Irwin, D.H., Barrett, E., 2005. Efficacy and safety of erlotinib HCl, an epidermal growth factor receptor (HER1/EGFR) tyrosine kinase inhibitor, in patients with advanced ovarian carcinoma: results from a phase II multicenter study. Int. J. Gynecol. cancer 15, 785–92.

Gravel, A., Dubuc, I., Morissette, G., Sedlak, R.H., Jerome, K.R., Flamand, L., 2015. Inherited chromosomally integrated human herpesvirus 6 as a predisposing risk factor for the development of angina pectoris. Proc. Natl. Acad. Sci. U. S. A. 112, 8058–63.

Gulve, N., Frank, C., Klepsch, M., Prusty, B.K., 2017. Chromosomal integration of HHV-6A during non-productive viral infection. Sci. Rep. 7, 512.

Gupta, R., Arkatkar, T., Yu, J.J., Wali, S., Haskins, W.E., Chambers, J.P., Murthy, A.K., Bakar, S.A., Guentzel, M.N., Arulanandam, B.P., 2015. Chlamydia muridarum infection associated host microRNAs in the murine genital tract and contribution to generation of host immune response. Am. J. Reprod. Immunol. 73, 126–140.

Gyori, B.M., Venkatachalam, G., Thiagarajan, P.S., Hsu, D., Clement, M.V., 2014. OpenComet:

An automated tool for comet assay image analysis. Redox Biol. 2, 457–465.

Hackstadt, T., 2012. Initial Interactions of Chlamydiae with the Host Cell, in: Bavoil, P., Tan, M. (Eds.), Intracellular Pathogens I: Chlamydiales. American Society of Microbiology, pp. 126–148.

Hall, C.B., Caserta, M.T., Schnabel, K., Shelley, L.M., Marino, A.S., Carnahan, J.A., Yoo, C., Lofthus, G.K., Mcdermott, M.P., 2017. Chromosomal Integration of Human Herpesvirus 6 Is the Major Mode of Congenital Human Herpesvirus 6 Infection 122.

Hall, C.B., Caserta, M.T., Schnabel, K., Shelley, L.M., Marino, A.S., Carnahan, J.A., Yoo, C., Lofthus, G.K., McDermott, M.P., 2008. Chromosomal integration of human herpesvirus 6 is the major mode of congenital human herpesvirus 6 infection. Pediatrics 122, 513–20.

Hamon, M.A., Cossart, P., 2008. Histone modifications and chromatin remodeling during bacterial infections. Cell Host Microbe 4, 100–109.

Hanahan, D., Weinberg, R.A., 2011. Hallmarks of cancer: The next generation. Cell 144, 646–674.

Havrilesky, L., Darcy, K.M., Hamdan, H., Priore, R.L., Leon, J., Bell, J., Berchuck, A., 2003. Prognostic significance of p53 mutation and p53 overexpression in advanced epithelial ovarian cancer: A Gynecologic Oncology Group Study. J. Clin. Oncol. 21, 3814–3825.

Hegre, S.A., Sætrom, P., Aas, P.A., Pettersen, H.S., Otterlei, M., Krokan, H.E., 2013. Multiple microRNAs may regulate the DNA repair enzyme uracil-DNA glycosylase. DNA Repair (Amst). 12, 80–86.

Huang, Y., Hidalgo-Bravo, A., Zhang, E., Cotton, V.E., Mendez-Bermudez, A., Wig, G., Medina-Calzada, Z., Neumann, R., Jeffreys, A.J., Winney, B., Wilson, J.F., Clark, D.A., Dyer, M.J., Royle, N.J., 2014. Human telomeres that carry an integrated copy of human herpesvirus 6 are often short and unstable, facilitating release of the viral genome from the chromosome. Nucleic Acids Res. 42, 315–327.

Humphreys, D.T., Westman, B.J., Martin, D.I.K., Preiss, T., 2005. MicroRNAs control translation initiation by inhibiting eukaryotic initiation factor 4E/cap and poly(A) tail function. Proc. Natl. Acad. Sci. 102, 16961–16966.

Hunn J, Rodriguez GC., 2012. Ovarian cancer: etiology, risk factors, and epidemiology. [Review]. Clin. Obstet. Gynecol. 55, 3–23.

Hybiske, K., Stephens, R.S., 2007. Mechanisms of host cell exit by the intracellular bacterium Chlamydia. Proc. Natl. Acad. Sci. 104, 11430–11435.

Idahl, A., Lundin, E., Elgh, F., Jurstrand, M., Møller, J.K., Marklund, I., Lindgren, P., Ottander, U., 2010. Chlamydia trachomatis, Mycoplasma genitalium, Neisseria gonorrhoeae, human papillomavirus, and polyomavirus are not detectable in human tissue with epithelial ovarian cancer, borderline tumor, or benign conditions. Am. J. Obstet. Gynecol. 202, 71.e1-71.e6.

Ikeda, T., Shibata, J., Yoshimura, K., Koito, A., Matsushita, S., 2007. Recurrent HIV-1 Integration at the *BACH2* Locus in Resting CD4 [+] T Cell Populations during Effective Highly Active Antiretroviral Therapy. J. Infect. Dis. 195, 716–725.

Kessler, M., Zielecki, J., Thieck, O., Mollenkopf, H.J., Fotopoulou, C., Meyer, T.F., 2012. Chlamydia trachomatis disturbs epithelial tissue homeostasis in fallopian tubes via paracrine Wnt signaling. Am. J. Pathol. 180, 186–198.

Khan, S., Guevara, C., Fujii, G., Parry, D., 2004. p14ARF is a component of the p53 response following ionizing irradiation of normal human fibroblasts. Oncogene 23, 6040–6046.

Kim, J.H., Jiang, S., Elwell, C.A., Engel, J.N., 2011. Chlamydia trachomatis co-opts the FGF2 signaling pathway to enhance infection. PLoS Pathog. 7.

Kim, V.N., 2005. MicroRNA biogenesis: Coordinated cropping and dicing. Nat. Rev. Mol. Cell Biol. 6, 376–385.

Kühl, U., Lassner, D., Wallaschek, N., Gross, U.M., Krueger, G.R.F., Seeberg, B., Kaufer, B.B., Escher, F., Poller, W., Schultheiss, H.P., 2015. Chromosomally integrated human herpesvirus 6 in heart failure: Prevalence and treatment. Eur. J. Heart Fail. 17, 9–19.

Kuhn, T.S., 1970. The Structure of Scientific Revolutions, Philosophical Review.

Kurman, R.J., Shih, I.-M., 2010. The Origin and Pathogenesis of Epithelial Ovarian Cancer- a Proposed Unifying Theory. Am. J. Surg. Pathol. 34, 433–443.

Kurman, R.J., Shih, I.M., 2011. Molecular pathogenesis and extraovarian origin of epithelial ovarian cancer - Shifting the paradigm. Hum. Pathol. 42, 918–931.

Kuzminov, A., 2001. Single-strand interruptions in replicating chromosomes cause double-strand breaks. Proc. Natl. Acad. Sci. 98, 8241–8246.

Lacroix, A., Collot-Teixeira, S., Mardivirin, L., Jaccard, A., Petit, B., Piguet, C., Sturtz, F., Preux, P.M., Bordessoule, D., Ranger-Rogez, S., 2010. Involvement of human herpesvirus-6 variant B in classic Hodgkin's lymphoma via DR7 oncoprotein. Clin. Cancer Res. 16, 4711–4721.

Lan, L., Nakajima, S., Oohata, Y., Takao, M., Okano, S., Masutani, M., Wilson, S.H., Yasui, A., 2004. In situ analysis of repair processes for oxidative DNA damage in mammalian cells. Proc. Natl. Acad. Sci. U. S. A. 101, 13738–43.

Lancaster, J.M., Wooster, R., Mangion, J., Phelan, C.M., Cochran, C., Gumbs, C., Seal, S., Barfoot, R., Collins, N., Bignell, G., Patel, S., Hamoudi, R., Larsson, C., Wiseman, R.W., Berchuck, a, Iglehart, J.D., Marks, J.R., Ashworth, a, Stratton, M.R., Futreal, P. a, 1996. BRCA2 mutations in primary breast and ovarian cancers. Nat. Genet. 13, 238–240.

Laxmi Yeruva, Dakota L. Pouncey, M.R.E., Sudeepa Bhattacharya, A., Chunqiao Luo, a, c E.W.W., Ojcius, D.M., Roger G. Ranka, B., 2016. MicroRNAs Modulate Pathogenesis Resulting from Chlamydial Infection in Mice. Infect. Immun. 85, 1–14.

Leary, R.J., Lin, J.C., Cummins, J., Boca, S., Wood, L.D., Parsons, D.W., Jones, S., Sjöblom, T., Park, B.-H., Parsons, R., Willis, J., Dawson, D., Willson, J.K. V, Nikolskaya, T., Nikolsky, Y., Kopelovich, L., Papadopoulos, N., Pennacchio, L.A., Wang, T.-L., Markowitz, S.D., Parmigiani, G., Kinzler, K.W., Vogelstein, B., Velculescu, V.E., 2008. Integrated analysis of homozygous deletions, focal amplifications, and sequence alterations in breast and colorectal cancers. Proc. Natl. Acad. Sci. U. S. A. 105, 16224–9.

Ledesma, F.C., El Khamisy, S.F., Zuma, M.C., Osborn, K., Caldecott, K.W., 2009. A human 5'-tyrosyl DNA phosphodiesterase that repairs topoisomerase-mediated DNA damage. Nature 461, 674–678.

Lee, Y., Kim, M., Han, J., Yeom, K.-H., Lee, S., Baek, S.H., Kim, V.N., 2004. MicroRNA genes are transcribed by RNA polymerase II. EMBO J. 23, 4051–4060.

Liang, P., Rosas-Lemus, M., Patel, D., Fang, X., Tuz, K., Juárez, O., 2018. Dynamic energy dependency of Chlamydia trachomatis on host cell metabolism during intracellular growth: Role of sodium-based energetics in chlamydial ATP generation. J. Biol. Chem. 293, 510–522.

Lindahl, T., 1993. Instability and decay of the primary structure of DNA. Lett. to Nat. 366, 461–464.

Lindahl, T., 1979. DNA Glycosylases, Endonucleases for Apurinic/Apyrimidinic Sites, and Base Excision-Repair. Prog. Nucleic Acid Res. Mol. Biol. 22, 135–192.

Liu, J., Rivas, F. V., Wohlschlegel, J., Yates, J.R., Parker, R., Hannon, G.J., 2005. A role for the P-body component GW182 in microRNA function. Nat. Cell Biol. 7, 1161–1166.

Lombard, D.B., Chua, K.F., Mostoslavsky, R., Franco, S., Gostissa, M., Alt, F.W., 2005. DNA repair, genome stability, and aging. Cell 120, 497–512.

MacRae, I.J., Zhou, K., Li, F., Repic, A., Brooks, A.N., Cande, W.Z., Adam, P.D., Doudna, J.A., 2006. Structural Basis for Double-Stranded RNA Processing by Dicer. Science (80-.). 311, 195–198.

Malhotra, M., Sood, S., Mukherjee, A., Muralidhar, S., Bala, M., 2013. Genital Chlamydia trachomatis: an update. Indian J. Med. Res. 138, 303–16.

Markkanen, E., Fischer, R., Ledentcova, M., Kessler, B.M., Dianov, G.L., 2015. Cells deficient in base-excision repair reveal cancer hallmarks originating from adjustments to genetic instability. Nucleic Acids Res. 43, 3667–3679.

Maroney, P.A., Yu, Y., Fisher, J., Nilsen, T.W., 2006. Evidence that microRNAs are associated with translating messenger RNAs in human cells. Nat. Struct. Mol. Biol. 13, 1102–1107.

Matsumoto, Y., Kim, K., 1995. Excision of deoxyribose phosphate residues by DNA polymerase beta during DNA repair. Science (80-.). 269, 699–702.

Maudet, C., Mano, M., Sunkavalli, U., Sharan, M., Giacca, M., Förstner, K.U., Eulalio, A., 2014. Functional high-throughput screening identifies the miR-15 microRNA family as cellular restriction factors for Salmonella infection. Nat. Commun. 5.

Mehlitz, A., Rudel, T., 2013. Modulation of host signaling and cellular responses by Chlamydia. Cell Commun. Signal. 11, 1–11.

Meister, G., Landthaler, M., Peters, L., Chen, P.Y., Urlaub, H., Lührmann, R., Tuschl, T., 2005. Identification of novel argonaute-associated proteins. Curr. Biol. 15, 2149–2155.

Meister, G., Tuschi, T., 2004. Mechanisms of gene silencing by double-stranded RNA. Nature 431, 343–349.

Mital, J., Lutter, E.I., Barger, A.C., Dooley, C.A., Hackstadt, T., 2015. Chlamydia trachomatis inclusion membrane protein CT850 interacts with the dynein light chain DYNLT1 (Tctex1). Biochem. Biophys. Res. Commun. 462, 165–170.

Morissette, G., Flamand, L., 2010. Herpesviruses and Chromosomal Integration. J. Virol. 84, 12100–12109.

Ness, R.B., Cottreau, C., 1999. Possible role of ovarian epithelial inflammation in ovarian cancer. J. Natl. Cancer Inst. 91, 1459–1467.

Ness, R.B., Goodman, M.T., Shen, C., Brunham, R.C., 2003. Serologic evidence of past infection with Chlamydia trachomatis, in relation to ovarian cancer. J. Infect. Dis. 187, 1147–1152.

Ness, R.B., Shen, C., Bass, D., Jackson, C., Moysich, K., Edwards, R., Brunham, R.C., 2008. Chlamydia trachomatis serology in women with and without ovarian cancer. Infect. Dis. Obstet. Gynecol. 2008, 5–10.

Offer, H., Wolkowicz, R., Matas, D., Blumenstein, S., Livneh, Z., Rotter, V., 1999. Direct involvement of p53 in the base excision repair pathway of the DNA repair machinery. FEBS Lett. 450, 197–204.

Ogata, M., Fukuda, T., Teshima, T., 2015. Human herpesvirus-6 encephalitis after allogeneic hematopoietic cell transplantation : What we do and do not know 50, 1030–1036.

Ogata, M., Satou, T., Kadota, J., Saito, N., Yoshida, T., Okumura, H., Ueki, T., Nagafuji, K., Kako, S., Uoshima, N., Tsudo, M., Itamura, H., 2017. Human Herpesvirus 6 (HHV-6) Reactivation and HHV-6 Encephalitis After Allogeneic Hematopoietic Cell Transplantation : A Multicenter , Prospective Study 6.

Ohashi, M., Yoshikawa, T., Ihira, M., Suzuki, K., Suga, S., Tada, S., Udagawa, Y., Sakui, H., Iida, K., Saito, Y., Nisiyama, Y., Asano, Y., 2002. Reactivation of Human Herpesvirus 6 and 7 in Pregnant Women 358, 354–358.

Omsland, A., Sixt, B.S., Horn, M., Hackstadt, T., 2014. Chlamydial metabolism revisited: Interspecies metabolic variability and developmental stage-specific physiologic activities. FEMS Microbiol. Rev. 38, 779–801.

Padberg, I., Jan??en, S., Meyer, T.F., 2013. Chlamydia trachomatis inhibits telomeric DNA damage signaling via transient hTERT upregulation. Int. J. Med. Microbiol. 303, 463–474.

Pantry, S.N., Medveczky, P.G., 2017. Latency, integration, and reactivation of human herpesvirus-6. Viruses 9, 1–12.

Parsons, J.L., Dianova, I.I., Boswell, E., Weinfeld, M., Dianov, G.L., 2005. End-damage-specific proteins facilitate recruitment or stability of X-ray cross-complementing protein 1 at the sites of DNA single-strand break repair. FEBS J. 272, 5753–5763.

Parsons, J.L., Tait, P.S., Finch, D., Dianova, I.I., Allinson, S.L., Dianov, G.L., 2008. CHIP-Mediated Degradation and DNA Damage-Dependent Stabilization Regulate Base Excision Repair Proteins. Mol. Cell 29, 477–487.

Partridge, E., Kreimer, A.R., Greenlee, R.T., Williams, C., Xu, J.-L., Church, T.R., Kessel, B., Johnson, C.C., Weissfeld, J.L., Isaacs, C., Andriole, G.L., Ogden, S., Ragard, L.R., Buys, S.S., 2009. Results from four rounds of ovarian cancer screening in a randomized trial. Obstet. Gynecol. 113, 775–82.

Pennini, M.E., Perrinet, S., Dautry-Varsat, A., Subtil, A., 2010. Histone methylation by NUE, a novel nuclear effector of the intracellular pathogen Chlamydia trachomatis. PLoS Pathog. 6, e1000995.

Petersen, C.P., Bordeleau, M.E., Pelletier, J., Sharp, P.A., 2006. Short RNAs repress translation after initiation in mammalian cells. Mol. Cell 21, 533–542.

Pillai, R.S., Bhattacharya, S.N., Artus, C.G., Zoller, T., Cougot, N., Basyuk, E., Bertrand, E., Filipowicz, W., 2005. Inhibition of Translational Initiation by Let-7 MicroRNA in Human Cells. Science (80-.). 309, 1573–1576.

Pinto, E.M., Chen, X., Easton, J., Finkelstein, D., Liu, Z., Pounds, S., Rodriguez-galindo, C., Lund, T.C., Mardis, E.R., Wilson, R.K., Boggs, K., Yergeau, D., Cheng, J., Mulder, H.L., Manne, J., Jenkins, J., Mastellaro, M.J., Figueiredo, B.C., Dyer, M.A., Pappo, A., Zhang, J., Downing, J.R., 2015. Genomic landscape of paediatric adrenocortical tumours. Nat. Commun. 6, 1–10.

Plummer, M., de Martel, C., Vignat, J., Ferlay, J., Bray, F., Franceschi, S., 2016. Global burden of cancers attributable to infections in 2012: a synthetic analysis. Lancet Glob. Heal. 4, e609–e616.

Poletto, M., Legrand, A.J., Fletcher, S.C., Dianov, G.L., 2016. P53 coordinates base excision repair to prevent genomic instability. Nucleic Acids Res. 44, 3165–3175.

Prusty, B.K., Krohne, G., Rudel, T., 2013a. Reactivation of chromosomally integrated human herpesvirus-6 by telomeric circle formation. PLoS Genet. 9, e1004033.

Prusty, B.K., Siegl, C., Hauck, P., Hain, J., Korhonen, S.J., Hiltunen-Back, E., Puolakkainen, M., Rudel, T., 2013b. Chlamydia trachomatis infection induces replication of latent HHV-6. PLoS One 8, e61400.

Qi, Y., Nam, K., Spong, M.C., Banerjee, a., Sung, R.-J., Zhang, M., Karplus, M., Verdine, G.L., 2012. Strandwise translocation of a DNA glycosylase on undamaged DNA. Proc. Natl. Acad. Sci. 109, 1086–1091.

Rajaram, M.V.S., Ni, B., Morris, J.D., Brooks, M.N., Carlson, T.K., Bakthavachalu, B., Schoenberg, D.R., Torrelles, J.B., Schlesinger, L.S., 2011. Mycobacterium tuberculosis lipomannan blocks TNF biosynthesis by regulating macrophage MAPK-activated protein kinase 2 (MK2) and microRNA miR-125b. Proc. Natl. Acad. Sci. 108, 17408–17413.

Reimer, D., Sadr, S., Wiedemair, A., Goebel, G., Concin, N., Hofstetter, G., Marth, C., Zeimet, A.G., 2006. Expression of the E2F family of transcription factors and its clinical relevance in ovarian cancer. Ann. N. Y. Acad. Sci. 1091, 270–281.

Reuter, S., Gupta, S.C., Chaturvedi, M.M., Aggarwal, B.B., 2010. Oxidative stress, inflammation, and cancer: How are they linked? Free Radic. Biol. Med.

Reyburn, H., 2016. WHO Guidelines for the Treatment of Chlamydia trachomatis. Who 340, c2637–c2637.

Riol, H., Jeune, B., Moskovic, A., Bathum, L., Wang, E., 1999. Optimized lymphocyte protein extraction performed simultaneously with DNA and RNA isolation: Application to the study of factors affecting DNA, RNA, and protein recovery from lymphocytes of the oldest individuals. Anal. Biochem. 275, 192–201.

Risch, H.A., Howe, G.R., 1995. Pelvic inflammatory disease and the risk of epithelial ovarian cancer. Cancer Epidemiol. Biomarkers Prev. 4, 447–51.

Saka, H.A., Thompson, J.W., Chen, Y.S., Kumar, Y., Dubois, L.G., Moseley, M.A., Valdivia, R.H., 2011. Quantitative proteomics reveals metabolic and pathogenic properties of Chlamydia trachomatis developmental forms. Mol. Microbiol. 82, 1185–1203.

Salahuddin, S.Z., Ablashi, D. V, Markhiam, P.D., Josephs, S.F., Sturzenegger, S., Kaplan, M., Halligan, G., Biberfeld, P., Wong-staal, F., Kramarsky, B., Gallo, R.C., 2000. Isolation of a New Virus , HBLV , in Patients with Lymphoproliferative Disorders 234.

Santoro, F., Kennedy, P.E., Locatelli, G., Malnati, M.S., Berger, E.A., Lusso, P., 1999. CD46 is a cellular receptor for human herpesvirus 6. Cell 99, 817–27.

Schleimann, M.H., Hoberg, S., Solhøj Hansen, A., Bundgaard, B., Witt, C.T., Kofod-Olsen, E., Höllsberg, P., 2014. The DR6 protein from human herpesvirus-6B induces p53-independent cell cycle arrest in G2/M. Virology 452–453, 254–263.

Schleimann, M.H., Møller, J.M.L., Kofod-Olsen, E., Höllsberg, P., 2009. Direct repeat 6 from human herpesvirus-6b encodes a nuclear protein that forms a complex with the viral DNA processivity factor p41. PLoS One 4, 1–8.

Schofield, L., 2007. Intravascular infiltrates and organ-specific inflammation in malaria pathogenesis. Immunol. Cell Biol. 85, 130–7.

Schuyer, M., van der Burg, M.E., Henzen-Logmans, S.C., Fieret, J.H., Klijn, J.G., Look, M.P., Foekens, J.A., Stoter, G., Berns, E.M., 2001. Reduced expression of BAX is associated with poor prognosis in patients with epithelial ovarian cancer: a multifactorial analysis of TP53, p21, BAX and BCL-2. Br. J. Cancer 85, 1359–1367.

Seo, Y.R., Fishel, M.L., Amundson, S., Kelley, M.R., Smith, M.L., 2002. Implication of p53 in base excision DNA repair: in vivo evidence. Oncogene 21, 731–737.

Shanmughapriya, S., SenthilKumar, G., Vinodhini, K., Das, B.C., Vasanthi, N., Natarajaseenivasan, K., 2012. Viral and bacterial aetiologies of epithelial ovarian cancer. Eur. J. Clin. Microbiol. Infect. Dis. 31, 2311–2317.

Siegl, C., Prusty, B.K., Karunakaran, K., Wischhusen, J., Rudel, T., 2014. Tumor suppressor p53 alters host cell metabolism to limit Chlamydia trachomatis infection. Cell Rep. 9, 918–929.

Siegl, C., Rudel, T., 2015. Modulation of p53 during bacterial infections. Nat. Rev. Microbiol.

Snavely, E.A., Kokes, M., Dunn, J.D., Saka, H.A., Nguyen, B.D., Bastidas, R.J., Mccafferty,

D.G., Valdivia, R.H., 2014. Reassessing the role of the secreted protease CPAF in Chlamydia trachomatis infection through genetic approaches. Pathog. Dis. 71, 336–351.

Sobol, R.W., Horton, J.K., K??hn, R., Gu, H., Singhal, R.K., Prasad, R., Rajewsky, K., Wilson, S.H., 1996. Requirement of mammalian DNA polymerase-β in base-excision repair.

Sood, A.K., Bhatty, R., Kamat, A.A., Landen, C.N., Han, L., Thaker, P.H., Li, Y., Gershenson, D.M., Lutgendorf, S., Cole, S.W., 2006. Stress hormone-mediated invasion of ovarian cancer cells. Clin. Cancer Res. 12, 369–375.

Stephens, R.S., Kalman, S., Lammel, C., Jun, F., Marathe, R., Aravind, L., Mitchell, W., Olinger, L., Tatusiv, R.L., Zhao, Q., Koonin, E. V., Davis, R.W., 1998. Genome Sequence of an Obligate Intracellular Pathogen of Humans: Chlamydia trachomatis. Science (80-.). 282, 754–759.

Subbarayal, P., Karunakaran, K., Winkler, A.C., Rother, M., Gonzalez, E., Meyer, T.F., Rudel, T., 2015. EphrinA2 Receptor (EphA2) Is an Invasion and Intracellular Signaling Receptor for Chlamydia trachomatis. PLoS Pathog. 11, 1–32.

Syed, V., Ho, S.-M., 2003. Progesterone-induced apoptosis in immortalized normal and malignant human ovarian surface epithelial cells involves enhanced expression of FasL. Oncogene 22, 6883–6890.

Tan, M., 2012. Temporal Gene Regulation during the Chlamydial Developmental Cycle, in: Bavoil, P., Tan, M. (Eds.), Intracellular Pathogens I: Chlamydiales. American Society of Microbiology, pp. 149–169.

Tan, M., Bavoil, P.M., 2012. Intracellular pathogens I : Chlamydiales. American Society of Microbiology

Tang, B., Li, N., Gu, J., Zhuang, Y., Li, Q., Wang, H.-G., Fang, Y., Yu, B., Zhang, J.-Y., Xie, Q.-H., Chen, L., Jiang, X.-J., Xiao, B., Zou, Q.-M., Mao, X.-H., 2012. Compromised autophagy by MIR30B benefits the intracellular survival of Helicobacter pylori . Autophagy 8, 1045–1057.

Tang, H., Serada, S., Kawabata, A., Ota, M., Hayashi, E., Naka, T., Yamanishi, K., Mori, Y., 2013. CD134 is a cellular receptor specific for human herpesvirus-6B entry. Proc. Natl. Acad. Sci. U. S. A. 110, 9096–9.

Tebbs, R.S., Thompson, L.H., Cleaver, J.E., 2003. Rescue of Xrcc1 knockout mouse embryo lethality by transgene- complementation. DNA Repair (Amst). 2, 1405–1417.

Tipples, G., Pellett, P.E., 2015. Human Herpesviruses 6, 7, and 8, in: Manual of Clinical Microbiology, 11th Edition. American Society of Microbiology, pp. 1754–1768.

Tuddenham, L., Jung, J.S., Chane-Woon-Ming, B., Dolken, L., Pfeffer, S., 2012. Small RNA Deep Sequencing Identifies MicroRNAs and Other Small Noncoding RNAs from Human Herpesvirus 6B. J. Virol. 86, 1638–1649.

Tweedy, J., Spyrou, M.A., Hubacek, P., Kuhl, U., Lassner, D., Gompels, U.A., 2015. Analyses of germline, chromosomally integrated human herpesvirus 6A and B genomes indicate emergent infection and new inflammatory mediators. J. Gen. Virol. 96, 370–389.

Vaziri, H., West, M.D., Allsopp, R.C., Davison, T.S., Wu, Y.S., Arrowsmith, C.H., Poirier, G.G., Benchimol, S., 1997. ATM-dependent telomere loss in aging human diploid fibroblasts and DNA damage lead to the post-translational activation of p53 protein involving poly(ADP-ribose) polymerase. EMBO J. 16, 6018–6033.

Verbeke, P., Welter-Stahl, L., Ying, S., Hansen, J., Häcker, G., Darville, T., Ojcius, D.M., 2006. Recruitment of BAD by the Chlamydia trachomatis vacuole correlates with host-cell survival. PLoS Pathog. 2, e45.

Vivanco, I., Sawyers, C.L., 2002. The phosphatidylinositol 3-Kinase–AKT pathway in human cancer. Nat. Rev. Cancer 2, 489–501.

Wallaschek, N., Sanyal, A., Pirzer, F., Gravel, A., Mori, Y., Flamand, L., Kaufer, B.B., 2016. The Telomeric Repeats of Human Herpesvirus 6A (HHV-6A) Are Required for Efficient Virus Integration. PLOS Pathog. 12, e1005666.

Wang, Y., Feng, J., Zang, W., Du, Y., Chen, X., Sun, Q., Dong, Z., Zhao, G., 2015. MIR-499 Enhances the Cisplatin Sensitivity of Esophageal Carcinoma Cell Lines by Targeting DNA Polymerase β. Cell. Physiol. Biochem. 36, 1587–1596.

Weström, L., Wölner-Hanssen, P., 1993. Pathogenesis of pelvic inflammatory disease. Genitourin. Med. 69, 9–17.

White, M., Pagano, J., Khalili, K., 2014. Viruses and Human Cancers: a Long Road of Discovery of Molecular Paradigms. Clin. Microbiol. Rev. vol. 27 no. 3 463-481

Wiederhold, L., Leppard, J.B., Kedar, P., Karimi-Busheri, F., Rasouli-Nia, A., Weinfeld, M., Tomkinson, A.E., Izumi, T., Prasad, R., Wilson, S.H., Mitra, S., Hazra, T.K., 2004. AP endonuclease-independent DNA base excision repair in human cells. Mol. Cell 15, 209–220.

Wilson, S.H., Kunkel, T.A., 2000. Passing the baton in base excision repair. Nat. Struct. Biol. 7, 176–178.

Wood, M., Royle, N., 2017. Chromosomally Integrated Human Herpesvirus 6: Models of Viral Genome Release from the Telomere and Impacts on Human Health. Viruses 9, 184.

Yu, S., Lee, M., Shin, S., Park, J., 2001. Apoptosis induced by progesterone in human ovarian cancer cell line SNU-840. J. Cell. Biochem. 82, 445–451.

Yu, T.-W., Anderson, D., 1997. Reactive oxygen species-induced DNA damage and its modification: A chemical investigation. Mutat. Res. Mol. Mech. Mutagen. 379, 201–210.

Zharkov, D.O., Mechetin, G. V., Nevinsky, G.A., 2010. Uracil-DNA glycosylase: Structural, thermodynamic and kinetic aspects of lesion search and recognition. Mutat. Res. - Fundam. Mol. Mech. Mutagen. 685, 11–20.

Zhou, J., Ahn, J., Wilson, S.H., Prives, C., 2001. A role for p53 in base excision repair. Embo J 20.

CURRICULUM VITAE

Department of Microbiology,
Biocenter, University of Würzburg,
97074, Germany
nitish.gulve@biozentrum.uni-wuerzburg.de

NITISH GULVE
Date of Birth- 05.10.1989
Nationality- Indian
npgulve@gmail.com

Career Summary

Degree	University	Year
PhD (Life Sciences)	University of Würzburg, Germany	2013- 2018
M.Sc. (Virology)	National Institute of Virology, (University of Pune) India	2010-2012
B.Sc. (Biotechnology)	University of Mumbai, India	2007- 2010

Research Summary

- **Role of *Chlamydia trachomatis* and Human herpesvirus-6 (HHV-6) co-infection in malignant transformation of the ovarian epithelial cells**
(March'14-2018)
Doctoral Thesis
Supervisors: Prof. Dr. Thomas Rudel, Prof. Dr. Jörg Wischhusen, Dr. Bhupesh Prusty
University of Würzburg, Germany

- **Effect of *Chlamydia trachomatis* infection on host DNA base excision repair (BER)**
Supervisors: Prof. Dr. Thomas Rudel, Dr. Bhupesh Prusty
University of Würzburg, Germany

- **Role of *Chlamydia trachomatis* nuclear effector (NUE) protein in host cell telomere damage and maintenance.**
Supervisors: Prof. Dr. Thomas Rudel, Dr. Bhupesh Prusty
University of Würzburg, Germany

- **Role of chaperone protein GP96 in host cell defence mechanism against Human herpesvirus-6 (HHV-6)**
Supervisors: Prof. Dr. Thomas Rudel, Dr. Bhupesh Prusty
University of Würzburg, Germany

- **Effect of Human herpesvirus-6 (HHV-6) and Human herpesvirus-7 (HHV-7) integration on the host genome integrity**
  Supervisor: Dr. Bhupesh Prusty
  University of Würzburg, Germany
- **Dynamics of anti-N-ORF2, anti-ORF2 and anti-NE antibodies in Hepatitis E virus infection** (Dec'11-Jun'12)
  Masters' Thesis
  Supervisor: Dr. V.A. Arankalle
  National Institute of Virology, India.

Awards and Fellowship

- **Career Development Fellowship** from the Graduate School of Life Sciences (GSLS), University of Würzburg, Germany in 2018
- Awarded **'Best Abstract/Invited talk'** award at the International Conference on Human herpesvirus-6 & 7 held at Harvard Medical School, Boston, USA in 2015.
- Awarded 1st prize **(Gold medal)** in chemistry project organized by the Department of Chemistry at the V. G. Vaze college, Mumbai, India in 2008.

References

Prof. Dr. Thomas Rudel	**Dr. Bhupesh Prusty**	**Prof. Dr. Jörg Wischhusen**
Department of Microbiology Biozentrum, Am Hubland 97074, Würzburg, Germany Phone: +49 (0)931-31 84401 Email: thomas.rudel@biozentrum.uni-wuerzburg.de	Department of Microbiology, Biozentrum, Am Hubland 97074, Würzburg, Germany Phone: +49 (0)931-31 88067 Email: bhupesh.prusty@biozentrum.uni-wuerzburg.de	Department of Gynaecology and Obstetrics Josef-Schneider-Str. 4 D-97080 Würzburg, Germany Phone: +49 (0)931 20125291 Email: Wischhusen_J@ukw.de

Würzburg,

Nitish Gulve

135

LIST OF PUBLICATIONS

- **Gulve, N**., Frank, C., Klepsch, M., & Prusty, B. K. (2017). Chromosomal integration of HHV-6A during non-productive viral infection. *Scientific Reports*.

- Prusty, B. K., **Gulve, N**., Rasa, S., Murovska, M., Hernandez, P. C., & Ablashi, D. V. (2017). Possible chromosomal and germline integration of human herpesvirus 7. *Journal of General Virology*.

- Das, B. B., Rakheja, D., Lacelle, C., Sedlak, R. H., **Gulve, N**., Chowdhury, S. R., & Prusty, B. K. (2016). Possible progesterone-induced gestational activation of chromosomally integrated human herpesvirus 6B and transplacental transmission of activated human herpesvirus 6B. *The Journal of Heart and Lung Transplantation*.

- **Gulve, N**., Kimmerling, K., Johnston, A. D., Krueger, G. R., Ablashi, D. V., & Prusty, B. K. (2016). Anti-herpesviral effects of a novel broad range anti-microbial quaternary ammonium silane, K21. *Antiviral Research*.

- Prusty, B. K., Siegl, C., **Gulve, N**., Mori, Y & Rudel, T. (2014). GP96 Interacts with HHV-6 during Viral Entry and Directs It for Cellular Degradation. *PLoS ONE*.